

# Oxidation and Reduction of Copper in Steam Generator Deposits

Under Shutdown, Layup, and Startup Conditions

*Technical Report*

---



# **Oxidation and Reduction of Copper in Steam Generator Deposits**

Under Shutdown, Layup and Startup Conditions

**1001204**

Final Report, September 2001

EPRI Project Manager  
A. McIlree

## **DISCLAIMER OF WARRANTIES AND LIMITATION OF LIABILITIES**

THIS DOCUMENT WAS PREPARED BY THE ORGANIZATION(S) NAMED BELOW AS AN ACCOUNT OF WORK SPONSORED OR COSPONSORED BY THE ELECTRIC POWER RESEARCH INSTITUTE, INC. (EPRI). NEITHER EPRI, ANY MEMBER OF EPRI, ANY COSPONSOR, THE ORGANIZATION(S) BELOW, NOR ANY PERSON ACTING ON BEHALF OF ANY OF THEM:

(A) MAKES ANY WARRANTY OR REPRESENTATION WHATSOEVER, EXPRESS OR IMPLIED, (I) WITH RESPECT TO THE USE OF ANY INFORMATION, APPARATUS, METHOD, PROCESS, OR SIMILAR ITEM DISCLOSED IN THIS DOCUMENT, INCLUDING MERCHANTABILITY AND FITNESS FOR A PARTICULAR PURPOSE, OR (II) THAT SUCH USE DOES NOT INFRINGE ON OR INTERFERE WITH PRIVATELY OWNED RIGHTS, INCLUDING ANY PARTY'S INTELLECTUAL PROPERTY, OR (III) THAT THIS DOCUMENT IS SUITABLE TO ANY PARTICULAR USER'S CIRCUMSTANCE; OR

(B) ASSUMES RESPONSIBILITY FOR ANY DAMAGES OR OTHER LIABILITY WHATSOEVER (INCLUDING ANY CONSEQUENTIAL DAMAGES, EVEN IF EPRI OR ANY EPRI REPRESENTATIVE HAS BEEN ADVISED OF THE POSSIBILITY OF SUCH DAMAGES) RESULTING FROM YOUR SELECTION OR USE OF THIS DOCUMENT OR ANY INFORMATION, APPARATUS, METHOD, PROCESS, OR SIMILAR ITEM DISCLOSED IN THIS DOCUMENT.

ORGANIZATION(S) THAT PREPARED THIS DOCUMENT

**Dominion Engineering, Inc.**

## **ORDERING INFORMATION**

Requests for copies of this report should be directed to the EPRI Distribution Center, 1355 Willow Way, Suite 2478, Concord, CA 94520, (800) 313-3774, press 2.

Electric Power Research Institute and EPRI are registered service marks of the Electric Power Research Institute, Inc. EPRI. ELECTRIFY THE WORLD is a service mark of the Electric Power Research Institute, Inc.

Copyright © 2001 Electric Power Research Institute, Inc. All rights reserved.

# CITATIONS

---

This report was prepared by

Dominion Engineering, Inc.  
6862 Elm Street  
McLean, VA 22101

Principal Investigators

C. Marks  
R. Varrin, Jr.

This report describes research sponsored by EPRI.

The report is a corporate document that should be cited in the literature in the following manner:

*Oxidation and Reduction of Copper in Steam Generator Deposits: Under Shutdown, Layup and Startup Conditions*, EPRI, Palo Alto, CA: 2000. 1001204



# REPORT SUMMARY

---

This project was initiated to address recent experience suggesting that the oxidation of secondary-side tube scale during shutdown, layup and startup (SLS) is a major factor in the corrosion degradation of pressurized water reactor (PWR) steam generators (SGs). The objective of this project was to evaluate the potential for oxidation and reduction of SG deposits under prototypical SLS conditions. Steam generator deposits contain a variety of compounds or metals that could potentially be oxidized or reduced during plant operations. The project involved three parts: a detailed literature search, analytical modeling to investigate the effect of oxygen diffusion through the tube scale and a series of oxidation and reduction experiments under aqueous and atmospheric conditions.

## Background

Experience including laboratory data and recent anecdotal plant data has indicated that the oxidation and reduction of secondary-side deposits have a strong influence on the occurrence of intergranular attack and stress corrosion cracking (IGA/SCC) of Alloy 600 SG tubes. For example, at South Korea's Kori 1 significant corrosion of steam generator materials was observed in conjunction with an unusually high degree of copper in the steam generator deposits (approximating 50%). When tighter control of oxygen ingress and reduction of oxidized deposits during startup were imposed, the corrosion of the steam generator tubes decreased significantly. Additional evidence of an SLS link to accelerated corrosion was found in a Belgian study that found that corrosion corresponded more closely with the number of cycles than with the duration of operation. Likewise, it has been observed that in Swedish plants, which exercise stringent control over SLS oxygen ingress, there is very low IGA/SCC.

## Objectives

The objective of this project was to determine the effects of SLS conditions on the rate of oxide conversion of secondary-side SG deposits. An additional objective was to determine whether the deposit layer may act as a significant barrier to the oxidation of metallic copper particles located deep in the deposit layer.

## Approach

The focus of the present evaluation is on copper in the deposits, although limited studies of the oxidation of iron oxide species are also included. The results of this study will be used in the development of an oxidation-reduction model, which can hopefully form a scientific basis for guidelines for shutdown, layup and startup oxidant control. In the aqueous oxidation and reduction experiments, temperature, pH and initial hydrazine concentration were controlled, the oxidation-reduction potential (ORP) was recorded, and oxide conversion was measured using X-ray diffraction (XRD). In the atmospheric copper oxidation experiments, temperature and

humidity were controlled, and oxide conversion was measured using thermogravimetric analysis (TGA). A one-dimensional, steady-state oxidation-diffusion model was developed as the principal tool for investigating the effect of diffusion through the deposit layer on the overall copper oxidation rate.

## **Results**

The analytical modeling indicated that the diffusional resistance of the scale does not significantly reduce the rate of oxidation of metallic copper particles located deep within the deposit. This conclusion depends on the existence of at least a small level of porosity (e.g., 1%) deep within the deposit, which is believed to be the case for the vast majority of plants. Major specific results from the experimental tests were as follows. No conversion of magnetite ( $\text{Fe}_3\text{O}_4$ ) to hematite ( $\text{Fe}_2\text{O}_3$ ) was observed under low-temperature, wet-layup conditions. The conversion of metallic copper to cuprite ( $\text{Cu}_2\text{O}$ ) under simulated wet-layup conditions was found to be influenced strongly by the temperature and the pH. At high pH (10) and low temperature ( $30^\circ\text{C}$ ), an oxide film formed on the copper particles that grew linearly at about 0.08 nm/day, while at low pH (7) and  $30^\circ\text{C}$ , the oxide film grew linearly at a rate of 0.8 nm/day. At a higher temperature ( $60^\circ\text{C}$ ), the film grew at about 1.2 nm/day regardless of pH. The conversion of metallic copper to cuprite under atmospheric conditions was found to increase greatly with increasing temperature. At room temperature, increasing humidity was found to moderately increase the conversion rate, while at  $60^\circ\text{C}$ , no such effect was observed. Finally, it was determined that cuprite films on copper particles could be reduced to copper metal by treatment with hydrazine solutions.

## **EPRI Perspective**

The work presented in this report is part of EPRI's ongoing efforts to develop practical recommendations to extend steam generator life and reduce inspection and maintenance costs. Specifically, this report is expected to aid in the development and revision of EPRI guidelines regarding the control of oxides during layup and startup. The information in this report will aid utility personnel in assessing the impact of various layup and startup procedures on the oxidation of SG deposits.

**1001204**

## **Keywords**

Sludge

Steam generators

Corrosion products

Layup

Oxidation and reduction



# ABSTRACT

---

The objective of this project was to evaluate the potential for oxidation and reduction of pressurized water reactor (PWR) steam generator (SG) deposits under prototypical shutdown, layup and startup conditions. Recent experience has indicated that the oxidation and reduction of secondary-side deposits have a strong influence on the occurrence of intergranular attack and stress corrosion cracking (IGA/SCC) of Alloy 600 SG tubes. Steam generator deposits contain a variety of compounds or metals that could potentially be oxidized or reduced during plant operations. The focus of the present evaluation is on copper in the deposits, although limited studies of the oxidation of iron oxide species are also included. The results of this study will be used in the development of an oxidation-reduction model, which can hopefully form a scientific basis for guidelines for shutdown, layup and startup oxidant control.

The present study consisted of (1) a literature review, (2) development of a deposit oxidation-diffusion model and (3) an experimental test program. The literature search and previous work by the authors revealed that deposits, although consisting mainly of magnetite (a form of iron oxide), also contain metallic copper. When the copper is oxidized, it may significantly contribute to the degradation of steam generator tubes. Many sources describing the kinetics of oxidation and reduction were found. However, in general, the literature data regarding oxidation were not applicable to aqueous layup environments. In addition, the data that were available often were in terms of copper dissolution rates rather than oxide conversion rates. Furthermore, the literature data regarding atmospheric oxidation generally did not address the effect of humidity, consistently control for different starting conditions (pretreatments), nor take advantage of the accuracy of thermogravimetric analysis (TGA). The experimental test program initiated for this study specifically addresses these weaknesses.

The deposit oxidation model used three related evaluations to determine if diffusion through deposits could limit the rate of oxidation of embedded copper. A steady-state diffusion model, an efficiency factor evaluation and a comparison of time scales all indicated that diffusion was not a limiting factor. Therefore, the diffusional resistance of the magnetite scale is shown not to prevent undesirable amounts of oxidation of copper particles embedded in tube scale. Note that this conclusion depends on the existence of at least a small level of porosity (e.g., 1%) in any consolidated scale layer, which is believed to be the case for the vast majority of plants.

The experimental test program investigated the influence of environmental conditions on the oxidation rates of copper and magnetite. No conversion of magnetite ( $\text{Fe}_3\text{O}_4$ ) to hematite ( $\text{Fe}_2\text{O}_3$ ) was observed under low-temperature, wet-layup conditions. The conversion of metallic copper to cuprite ( $\text{Cu}_2\text{O}$ ) under simulated wet-layup conditions was found to be influenced strongly by the temperature and the pH. At high pH (10) and low temperature ( $30^\circ\text{C}$ ), an oxide film formed on the copper particles that grew linearly at about 0.08 nm/day, while at low pH (7) and  $30^\circ\text{C}$ , the oxide film grew linearly at a rate of 0.8 nm/day. At a higher temperature ( $60^\circ\text{C}$ ), the film grew at

---

about 1.2 nm/day regardless of pH. The conversion of metallic copper to cuprite under atmospheric conditions was found to increase greatly with increasing temperature. At room temperature, increasing humidity was found to moderately increase the conversion rate, while at 60°C, no such effect was observed. Finally, it was determined that cuprite films on copper particles could be reduced to copper metal by treatment with hydrazine solutions.

# CONTENTS

---

<b>1 SUMMARY AND CONCLUSIONS.....</b>	<b>1-1</b>
Objective and Scope .....	1-1
Summary.....	1-1
Literature Review .....	1-3
Deposit Characterization.....	1-3
Effects of Copper Deposits on Steam Generators.....	1-3
Oxidation Reaction Rates .....	1-4
Reduction Reaction Rates .....	1-4
Deposit Oxidation-Diffusion Model.....	1-4
Experimental Test Program.....	1-5
Characterization of SG Deposit Copper Inclusions .....	1-5
Oxidation of Copper under Wet-Layup Conditions .....	1-6
Overall Susceptibility of Copper in Steam Generator Deposits to Oxidation .....	1-6
Role of Hydrazine.....	1-6
Role of the Oxidation-Reduction Potential (ORP) .....	1-7
Oxidation of Magnetite under Wet-Layup Conditions .....	1-8
Overall Susceptibility of Magnetite to Oxidation.....	1-8
Hydrazine Decomposition .....	1-8
Comparison of Steam Generator Deposits to Synthetic Powders.....	1-9
Oxidation of Copper under Atmospheric Conditions.....	1-9
General Susceptibility of Copper to Oxidation .....	1-9
Quantitative Description of Oxidation Rates .....	1-9
Reduction of Copper under Startup Conditions.....	1-10
Reduction of Copper Oxides .....	1-10
Low Oxygen Oxidation Reaction .....	1-11
Film Thickness Versus Oxide Fraction .....	1-11
<b>2 INTRODUCTION .....</b>	<b>2-1</b>

---

Purpose and Working Hypothesis .....	2-1
Report Organization .....	2-2
Literature Review .....	2-3
Deposit Oxidation-Diffusion Model .....	2-3
Experimental Test Program .....	2-3
Characterization of SG Deposit Copper Inclusions .....	2-4
Oxidation of Copper under Wet-Layup Conditions .....	2-4
Oxidation of Magnetite under Wet-Layup Conditions .....	2-4
Atmospheric Oxidation Experiments .....	2-5
Reduction Experiments for Copper under Startup Conditions .....	2-5
<b>3 LITERATURE REVIEW .....</b>	<b>3-1</b>
Summary .....	3-1
Deposit Characterization .....	3-1
Chemical Characterization .....	3-2
Physical Characterization .....	3-2
Effects of Copper Deposits on Steam Generators .....	3-3
Plant Observations .....	3-3
Laboratory Data .....	3-3
Relating Laboratory Data to Plant Operations .....	3-4
Oxidation Reaction Rates .....	3-5
Types of Reactions .....	3-5
Models of Atmospheric Oxidation .....	3-5
Very Thin Film Oxidation .....	3-6
Thin Film Oxidation .....	3-7
Thick Film Oxidation .....	3-8
Linear Oxidation Models .....	3-8
Empirical Oxidation Models .....	3-9
Aqueous Oxidation .....	3-9
Type of Oxide Formed .....	3-9
Reduction Reaction Rates .....	3-10
Release of Oxygen to Another Metal .....	3-11
Release of Oxygen to Solution or Scavenger .....	3-11
<b>4 DEPOSIT OXIDATION-DIFFUSION MODEL .....</b>	<b>4-1</b>

---

Introduction .....	4-1
Steady-State Reaction/Diffusion Model .....	4-2
Determination of Physical and Chemical Parameters .....	4-2
Scale Parameters.....	4-3
Diffusion Parameters.....	4-4
Reaction Parameters .....	4-6
Determination of the Diffusion Characteristic Time Scale.....	4-6
Derivation of the Steady-State Model.....	4-7
Evaluation of the Model and Parameter Effects .....	4-10
Effectiveness Factor .....	4-11
Comparison of Characteristic Times.....	4-13
<b>5 EXPERIMENTAL TEST PROGRAM .....</b>	<b>5-1</b>
Introduction .....	5-1
Analytical Techniques.....	5-1
Electron Microprobe Analysis.....	5-2
Thermogravimetric Analysis (TGA) .....	5-2
X-Ray Diffraction.....	5-4
Oxidation-Reduction Potential (ORP) Measurement .....	5-6
The Theoretical Electrochemical Potential (ECP) .....	5-6
Oxide Surface Layers and the ORP .....	5-7
ORP Measurement Technique .....	5-8
pH Measurement .....	5-8
Oxygen and Hydrazine Detection .....	5-8
BET Specific Surface Area Analysis .....	5-8
Characterization of SG Deposit Copper Inclusions .....	5-9
Aqueous Oxidation Experiments .....	5-11
Aqueous Oxidation Experimental Technique .....	5-11
Experimental Results for Oxidation of Copper under Wet-Layup Conditions.....	5-12
Hydrazine Decomposition .....	5-12
pH and ORP Data .....	5-13
Degree of Oxidation .....	5-13
Effect of Hydrazine .....	5-14
Effect of Temperature.....	5-17
Effect of pH.....	5-17

---

Experimental Results for Oxidation of Magnetite under Wet-Layup Conditions .....	5-17
Hydrazine Decomposition .....	5-17
pH and ORP Data .....	5-19
Degree of Oxidation .....	5-22
Atmospheric Oxidation Experiments.....	5-22
Thermogravimetric Analysis (TGA) Experimental Technique .....	5-22
Pretreatment Step .....	5-23
Control of Relative Humidity .....	5-23
Measurement Step .....	5-23
TGA Results for Atmospheric Oxidation of Copper .....	5-26
Thermal Dependence of the Reaction Rate Constants.....	5-27
Parameter A .....	5-27
Parameter B .....	5-29
Humidity Dependence of the Reaction Rate Constants.....	5-29
Reduction Experiments for Copper under Startup Conditions.....	5-31
Reduction Experimental Technique .....	5-31
Reduction Experimental Results .....	5-32
Stoichiometric Shortage of Hydrazine with Respect to Cuprite .....	5-32
Oxygen Stoichiometry .....	5-33
Possibility of Anaerobic Oxidation .....	5-33
Stoichiometric Excess of Hydrazine with Respect to Cuprite .....	5-34
Implications .....	5-34
Materials Used .....	5-36
<b>6 REFERENCES .....</b>	<b>6-1</b>
<b>A SUMMARIES OF THE LITERATURE REVIEWED .....</b>	<b>A-1</b>
<b>B FILM THICKNESS AS A FUNCTION OF FRACTION OF OXIDE.....</b>	<b>B-1</b>
Purpose.....	B-1
Summary of Results .....	B-1
Calculation Input Requirements.....	B-1
References.....	B-1
Assumptions.....	B-1
Analysis.....	B-2

---

Calculation of the Area-Weighted Average Radius .....	B-2
Spherical Approximation .....	B-2
Planar Approximation .....	B-3
Nomenclature.....	B-4
<b>C X-RAY DIFFRACTION (XRD) PENETRATION DEPTH .....</b>	<b>C-1</b>
Purpose.....	C-1
Summary of Results .....	C-1
Calculation Input Requirements.....	C-1
References.....	C-1
Assumptions.....	C-2
Analysis.....	C-2
Calculation of the Area-Weighted Average Radius .....	C-2
Determination of Penetration Depth.....	C-3





# LIST OF FIGURES

---

Figure 1-1 Aqueous Copper Oxidation Rates as a Function of Temperature and pH .....	1-7
Figure 1-2 Aqueous Copper Oxidation Rates as a Function of Temperature and pH .....	1-10
Figure 2-1 Schematic of the Working Hypothesis.....	2-2
Figure 3-1 Literature Data for Copper Oxide Thin Film Growth .....	3-7
Figure 3-2 The Dissociation Pressures of Copper Oxides [10] .....	3-10
Figure 4-1 Typical Dense Tube Scale: SEM Microphotograph (top) and Copper Map (bottom).....	4-1
Figure 4-2 Schematic of the Diffusion Model.....	4-3
Figure 4-3 The Effectiveness Factor as a Function of the Thiele Modulus.....	4-12
Figure 5-1 Thermogravimetric Analysis (TGA) Schematic.....	5-3
Figure 5-2 XRD Calibration Curve for Mixture of Cuprite ( $\text{Cu}_2\text{O}$ ) and Copper Powders .....	5-5
Figure 5-3 XRD Calibration Curve for Mixture of Tenorite ( $\text{CuO}$ ) and Copper Powders.....	5-5
Figure 5-4 XRD Calibration Curve for Mixture of Hematite ( $\text{Fe}_2\text{O}_3$ ) and Magnetite ( $\text{Fe}_3\text{O}_4$ ) Powders .....	5-6
Figure 5-5 Schematic of Oxidation-Reduction Potential (ORP) Configuration .....	5-7
Figure 5-6 Copper Inclusions Examined by Electron Microprobe .....	5-10
Figure 5-7 Aqueous Oxidation Experimental Setup.....	5-11
Figure 5-8 ORP of Aqueous Solutions with Copper Powder as a Function of pH .....	5-14
Figure 5-9 Degree of Copper Oxidation, 30°C, Low pH Solutions .....	5-15
Figure 5-10 Degree of Copper Oxidation, 30°C, High pH Solutions.....	5-15
Figure 5-11 Degree of Copper Oxidation, 60°C, Low pH Solutions .....	5-16
Figure 5-12 Degree of Copper Oxidation, 60°C, High pH Solutions.....	5-16
Figure 5-13 Hydrazine Decomposition (Powder–Temperature (°C)–Solution #) .....	5-19
Figure 5-14 ORP of Aqueous Solutions with Magnetite Powder.....	5-20
Figure 5-15 ORP of Aqueous Solutions with Steam Generator (SG) Deposits .....	5-20
Figure 5-16 Student T-test for ORP ( $9 < \text{pH} < 10$ ).....	5-21
Figure 5-17 ORP of Various Powder Types (with no hydrazine and at 30°C and 60°C) .....	5-21
Figure 5-18 Schematic of Relative Humidity Control Process.....	5-24
Figure 5-19 Psychrometric Chart [43, Perry, R.H. and D.W. Green, <i>Perry's Chemical Engineering Handbook</i> , Sixth Edition, McGraw-Hill Companies, New York, 1984. Reproduced with permission of The McGraw-Hill Companies.] .....	5-25
Figure 5-20 Copper Oxidation in Dry Air at 30°C.....	5-26

---

Figure 5-21 Thermal Dependence of Rate Constant <i>A</i> for Atmospheric Copper Oxidation.....	5-28
Figure 5-22 Thermal Dependence of Rate Constant <i>B</i> for Atmospheric Copper Oxidation.....	5-28
Figure 5-23 Humidity Dependence of Rate Constant <i>A</i> for Atmospheric Copper Oxidation .....	5-30
Figure 5-24 Humidity Dependence of Rate Constant <i>B</i> for Atmospheric Copper Oxidation .....	5-30
Figure 5-25 High Temperature Oxidation of Copper Powder at 0.4 ppm Oxygen and 400 ppm Hydrazine .....	5-32
Figure 5-26 Reaction of Copper Powder with 2× Stoichiometric Hydrazine with Respect to Cuprite.....	5-35
Figure 5-27 Reaction of Copper Powder with 10× Stoichiometric Hydrazine with Respect to Cuprite.....	5-35
Figure C-1 Penetration of X-Rays into a Copper Sample .....	C-3

## LIST OF TABLES

---

Table 3-1 Kinetic Parameter Dependence on the Partial Pressure of Oxygen.....	3-6
Table 4-1 Scale Parameter Values for Base and Conservative Cases .....	4-4
Table 4-2 Comparison of Diffusivities in Solids and Fluids .....	4-5
Table 4-3 Experimental Reaction Rate Constants for Copper Oxidation .....	4-6
Table 4-4 Model Results for Base and Conservative Cases .....	4-11
Table 4-5 Effectiveness Factor Calculation .....	4-13
Table 5-1 Specific Surface Areas of Experimental Materials .....	5-9
Table 5-2 Elemental Composition of Copper Inclusions .....	5-10
Table 5-3 Aqueous Solutions Used .....	5-12
Table 5-4 Detection of Hydrazine Decomposition Time, Copper Powder Experiments (1 ppm detection limit) .....	5-13
Table 5-5 Detection of Hydrazine Decomposition Time, Magnetite and SG Deposit Experiments .....	5-18
Table 5-6 Experimental Materials.....	5-36
Table 5-7 Elemental Makeup of the Steam Generator Deposit Used (Plant C) .....	5-36



# 1

## SUMMARY AND CONCLUSIONS

---

### Objective and Scope

The objective of this project was to evaluate the potential for oxidation and reduction of pressurized water reactor (PWR) steam generator (SG) deposits under prototypical shutdown, layup and startup conditions. The impetus for this evaluation is that it is considered plausible that the oxidation and reduction of secondary-side deposits have a strong influence on the occurrence of intergranular attack and stress corrosion cracking (IGA/SCC) of Alloy 600 steam generator tubes. The degradation of SG tubes is of considerable importance because these tubes form the boundary between the primary coolant and the secondary cycle. The results of this study will be used in the development of an oxidation-reduction model (see Figure 2-1 on page 2-2), which can hopefully form a scientific basis for guidelines for shutdown, layup and startup oxidant control.

Steam generator deposits contain a variety of compounds or metals that could potentially be oxidized or reduced during plant operations. The focus of the present evaluation is on copper in the deposits, although limited studies of the oxidation of iron oxide species are also included. Laboratory investigations have demonstrated that oxidized copper species can greatly increase the occurrence of IGA/SCC of Alloy 600 tube materials. For example, it has been found that as little as 0.045 weight percent CuO (on a liquid mass basis) can significantly raise the corrosion potential of Alloy 600 in the presence of other deposit species in a caustic environment [1]. Other tests have shown that increasing the potential by this amount dramatically increases the rate of IGA/SCC [1]. Furthermore, even at nominally “copper-free” plants, PWR steam generator deposits contain some copper due to the presence of copper as a tramp element in numerous secondary circuit components.

### Summary

The present work consisted of three parts:

- Literature Review
- Deposit Oxidation-Diffusion Model
- Experimental Test Program

The literature review consisted of a search of several commercial databases for information on the oxidation-reduction behavior of deposit constituents and covered journal articles, workshop and conference presentations, EPRI reports and reference books. The deposit oxidation-diffusion model used three different analyses to determine whether the diffusion of oxygen through a

porous deposit would slow the rate of oxidation of copper particles embedded within the deposit. The experimental test program investigated the rates of oxidation and reduction of copper and magnetite under several conditions.

The literature search and previous work by the authors revealed that deposits, although consisting mainly of magnetite, also contain metallic copper. When this copper is oxidized, it may significantly contribute to the degradation of steam generator tubes. Many sources describing the kinetics of oxidation and reduction were found. However, in general, the literature data regarding oxidation were not applicable to aqueous layup environments. In addition, the data that were available often were in terms of copper dissolution rates rather than oxide conversion rates. Furthermore, the literature data regarding atmospheric oxidation generally did not address the effect of humidity, consistently control for different starting conditions (pretreatments), nor take advantage of the accuracy of thermogravimetric analysis (TGA). The experimental test program initiated for this study specifically addresses these weaknesses.

The deposit oxidation model used three related evaluations (a steady-state diffusion model, an efficiency factor evaluation and a comparison of time scales) to determine if diffusion through deposits could limit the rate of oxidation of embedded copper. All three of these analyses indicated that diffusion was not a limiting factor. Therefore, the diffusional resistance of the magnetite scale is shown not to prevent undesirable amounts of oxidation of copper particles embedded in tube scale. Note that this conclusion depends on the existence of at least a small level of porosity (e.g., 1%) in any consolidated scale layer, which is believed to be the case for the vast majority of plants.

The experimental test program investigated the influence of environmental conditions on the oxidation rates of copper and magnetite. No conversion of magnetite ( $\text{Fe}_3\text{O}_4$ ) to hematite ( $\text{Fe}_2\text{O}_3$ ) was observed under low-temperature, wet-layup conditions. The conversion of metallic copper to cuprite ( $\text{Cu}_2\text{O}$ ) under simulated wet-layup conditions was found to be influenced strongly by the temperature and the pH. At high pH (10) and low temperature ( $30^\circ\text{C}$ ), an oxide film formed on the copper particles which grew linearly at about 0.08 nm/day, while at low pH (7) and  $30^\circ\text{C}$ , the oxide film grew linearly at a rate of 0.8 nm/day. At a higher temperature ( $60^\circ\text{C}$ ), the film grew at about 1.2 nm/day regardless of pH (see Figure 1-1, below). The conversion of metallic copper to cuprite under atmospheric conditions was found to increase greatly with increasing temperature (see Figure 1-2, below). See Table 4-3 on page 4-6 for reaction rates typical of copper oxidation under atmospheric and wet-layup conditions. At room temperature, increasing humidity was found to moderately increase the conversion rate, while at  $60^\circ\text{C}$ , no such effect was observed. Finally, it was determined that cuprite films on copper particles could be reduced to copper metal by treatment with hydrazine solutions.

The detailed conclusions of the three parts of the investigation are presented below.

## Literature Review

The literature review was conducted by searching several commercial databases for references to copper oxidation and reduction and the influence of copper and iron oxides on the degradation of PWR steam generator tubes. The literature search focused on four main topics:

- Deposit Characterization
- Effects of Copper Deposits on Steam Generators
- Oxidation Reaction Rates
- Reduction Reaction Rates

### ***Deposit Characterization***

Although SG deposits typically consist mostly of iron oxide (generally magnetite,  $\text{Fe}_3\text{O}_4$ ), metallic copper is often a significant constituent species.

- Deposits are typically >85% by weight magnetite [2].
- Deposits are typically ~5% by weight metallic copper [2].
- Even in nominally “copper-free” plants, copper can account for ~0.3% by weight of the deposits [2].
- Copper can account for as much as 50% by weight of the deposits in some PWR steam generators [3].
- Copper in deposits is generally found as copper metal, but minor amounts of cuprite ( $\text{Cu}_2\text{O}$ ) and tenorite ( $\text{CuO}$ ) have also been found [4].

### ***Effects of Copper Deposits on Steam Generators***

There are numerous anecdotal data showing that SG deposit oxides can accelerate the degradation of SG tubes. There is also considerable laboratory evidence showing that copper oxides can accelerate IGA/SCC in nickel-alloy tubes. It is most likely that the degree of acceleration is a function of size of the copper area in contact with the secondary fluid. However, all of the data present in the literature are reported in terms of the concentration of copper oxides in the liquid solution contacting the nickel-alloy samples.

- Copper oxides significantly raise the corrosion potential of Alloy 600 in caustic environments [1,5].
- Copper can accelerate corrosion of Alloy 690 without raising the corrosion potential [6].
- Levels of copper oxide as low as 0.045% (as a percent of the liquid solution mass) can significantly accelerate stress corrosion cracking [1].

### **Oxidation Reaction Rates**

The data available in the literature are mostly for the oxidation of copper in air. However, a few controversial papers discuss the oxidation of copper in low oxygen water.

- Mathematical models for describing copper oxidation in air are based on the diffusion of oxygen through a semi-protective oxide layer [7].
- Depending on the temperature and the thickness of the oxide film, oxidation may proceed according to a linear, parabolic or logarithmic rate law [7].
- A thin film of copper oxide at room temperature or slightly higher (less than 75°C) will generally form according to a logarithmic rate law where the thickness of the film ( $x$ ) is given as a function of time,  $t$ , as  $x = A \ln(Bt+1)$ , where  $A$  and  $B$  are constants which are known from theory only to an order of magnitude [8].
- Copper generally forms a two layer oxide film with a layer of tenorite ( $\text{CuO}$ ) at the oxide-air interface and a layer of cuprite ( $\text{Cu}_2\text{O}$ ) between the tenorite and the metal [9–11].
- Some experiments indicate that copper can oxidize in aqueous solutions in the absence of oxygen by dissociating water molecules to produce hydrogen [12], while other investigations indicate that this is not the case [13].

### **Reduction Reaction Rates**

The literature contains data which indicate that copper oxides can be reduced to copper metals. Three mechanisms are described.

- At extremely high temperatures ( $>1000^\circ\text{C}$ ) oxygen will spontaneously dissociate from the copper oxide forming copper metal and oxygen gas [14].
- At moderate temperatures, an oxygen scavenger (such as hydrazine or hydrogen gas) will strip the oxygen from copper oxide leaving copper metal [15].
- At moderate temperatures, other metals, such as iron, will strip copper oxides of oxygen leaving copper metal and forming oxides of the second metal [16].

### **Deposit Oxidation-Diffusion Model**

Copper in PWR steam generator deposits is generally located in copper inclusions within the scale. These inclusions are often found close to the tube. Thus, oxygen necessary for the oxidation of the copper must first diffuse through much of the tube scale before reaching the copper. It is conceivable that diffusion through the tube scale is so slow that oxygen does not reach the imbedded copper in quantities sufficient to cause significant oxidation of the copper metal. To determine whether diffusion limits the oxidation of imbedded copper, a mathematical model was constructed to investigate the relative importance of diffusion in determining the rate of oxidation. Two dimensional analyses were also performed to supplement the results of the diffusion model.



Typically, copper in tube scales contacts the fluid on the secondary side of the steam generator through an interconnected network of pores. In this study, diffusion of oxygen through the pores present in SG tube scales was not found to retard significantly the rate of oxidation of embedded copper. This is based on the following:

- A steady-state diffusion model indicated that the ratio of the concentration of oxygen at the surface of an embedded copper particle to the concentration in the bulk layup environment was near unity (0.982 for most conservative case).
- The effectiveness factor (the ratio of the reaction rate with diffusion to the reaction rate without diffusion) was found to be nearly equal to unity (0.9995 for a conservative case), indicating that diffusion does not slow the oxidation reaction.
- An evaluation of characteristic time scales indicated that diffusion generally took place over the course of a few seconds, while the characteristic time for the reaction was estimated to be one hour, even in the most aggressive environment. This indicates that diffusion will not limit the oxidation reaction rate.

## **Experimental Test Program**

The third part of this investigation consisted of laboratory investigations into the oxidation and reduction of steam generator deposits. The experimental program can be divided into five different investigations:

- Characterization of SG Deposit Copper Inclusions
- Oxidation of Copper under Wet-Layup Conditions
- Oxidation of Magnetite under Wet-Layup Conditions
- Oxidation of Copper under Atmospheric Conditions
- Reduction Experiments

### ***Characterization of SG Deposit Copper Inclusions***

Deposit samples from PWR steam generators at two plants were examined. Electron microprobe analysis was performed on copper inclusions from these samples to determine the elemental makeup of the copper inclusions. Deposits from one plant had a high overall zinc content in its deposits (8%).

- No zinc (<0.01%) was found in the copper inclusions examined.
- Copper inclusions in steam generator deposits can be modeled as pure copper.
- Pure copper powders can be used to experimentally predict the behavior of copper inclusions in deposits.

### ***Oxidation of Copper under Wet-Layup Conditions***

The results of the experiments that focused on the oxidation of copper in steam generator deposits during wet-layup fall into three general categories:

- Overall Susceptibility of Copper in Steam Generator Deposits to Oxidation
- Role of Hydrazine
- Role of the Oxidation-Reduction Potential (ORP)

#### **Overall Susceptibility of Copper in Steam Generator Deposits to Oxidation**

Copper with a morphology, size and purity typical of that found in steam generator deposits will oxidize under prototypical wet-layup conditions. The present experiments have revealed the following:

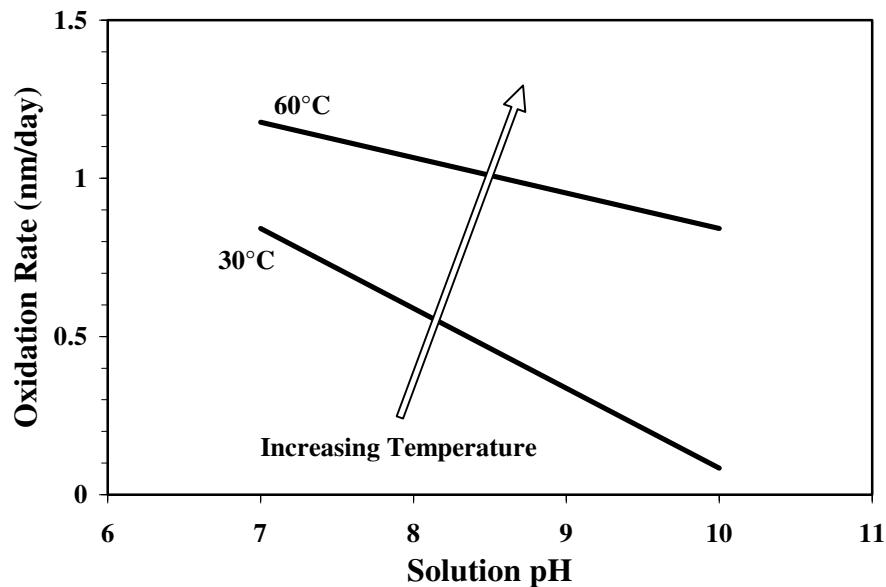
- The oxide formed is primarily cuprite ( $\text{Cu}_2\text{O}$ ) with no traces of tenorite ( $\text{CuO}$ ).
- Copper particles representative of copper in steam generator deposits oxidize heterogeneously, i.e., a copper oxide corrosion layer forms over the surface of the copper particle or inclusion.
- The reaction rate for the formation of copper oxide at the surface of the particle is roughly constant with time. Thus, longer periods of exposure to wet-layup conditions lead to correspondingly thicker oxide layers.
- Under neutral-pH, wet-layup conditions ( $30^\circ\text{C}$ ,  $\text{pH}\sim 7$ , hydrazine at  $\sim 400$  ppm), the oxidation rate is on the order of 0.8 nm/day. For a particle with a radius of 310 nm this corresponds to about 2.5% conversion of Cu to  $\text{Cu}_2\text{O}$  in five days. The particles used in this project were about 310 nm in radius. Although this is smaller than the typical copper inclusion in steam generator deposits, the extent of oxidation in terms of the thickness of the  $\text{Cu}_2\text{O}$  layer formed will not change due to the size of the particle. However, the fractional conversion will be smaller for larger particles (see “Film Thickness Versus Oxide Fraction” on page 1-11).
- Under higher pH conditions ( $30^\circ\text{C}$ ,  $\text{pH}=10$ ), the rate of oxidation decreases by a factor of ten to 0.08 nm/day (or for a 310 nm particle, 0.25% conversion to  $\text{Cu}_2\text{O}$  in five days).
- In simulated startup conditions ( $200^\circ\text{C}$ ), oxidation can still take place even in the nominal absence of oxygen (see “Low Oxygen Oxidation Reaction” on page 1-11).

Figure 1-1 shows the general trends in the rate of oxidation in simulated layup conditions with dissolved oxygen at its saturation level as a function of temperature and pH (assuming no hydrazine).

#### **Role of Hydrazine**

Hydrazine is known to change the surface of iron to impart a protective film. Therefore, experiments were performed to determine if hydrazine has a similar effect on copper.

- Despite past experience with iron in steam generator environments, in this work hydrazine did not cause the formation of an oxide layer on the copper surface which protected the copper from further oxidation.
- When hydrazine is present, it initially retards oxidation. However, copper quickly decomposes hydrazine. After hydrazine has been decomposed, the copper proceeds to oxidize at a rate equivalent to that seen in hydrazine-free environments. This shows that the benefit of hydrazine addition did not occur through passivation of the copper surface.



**Figure 1-1**  
**Aqueous Copper Oxidation Rates as a Function of Temperature and pH**

### Role of the Oxidation-Reduction Potential (ORP)

The oxidation-reduction potential (ORP) measures the polarization of a platinum electrode immersed in a solution, giving a measurement of the corrosive tendency of that solution. An increase in the ORP indicates a lower energy barrier to dissolution, leading to a greater tendency for metal ions to dissolve into the contact solution. A decrease in the ORP indicates a lower tendency for metal ions to dissolve into the solution. The ORP of the layup simulating solutions containing the test powders was measured during these experiments.

- The ORP in simulated wet-layup conditions was found to be a function of pH but was not dependent on the degree of copper oxidation.
- Some reduction of the ORP was observed when hydrazine was present (a decrease of about 300 mV).
- An increase in ORP measured at room temperature occurred in the presence of copper powder or actual steam generator deposits on the order of +60 mV. The increase in ORP in the presence of the copper powder is believed to be associated with the presence of a thin layer of copper oxide on the copper particles. At operating SG temperatures (~275°C

(530°F)), an increase in ORP of +210 to +250 mV has been associated with a significant increase in the rate of Alloy 600 corrosion [1], and other tests have indicated that lower potentials also increase the rate of corrosion. Elevated potential is of particular concern for corrosion during power operation (few percent power or greater) when impurities are concentrated within the scale matrix.

### ***Oxidation of Magnetite under Wet-Layup Conditions***

Experimental data on the conversion of magnetite (from synthetic sources and from real plant deposits) were collected under simulated wet-layup conditions. The results of experiments investigating the oxidation of magnetite suggest conclusions which fall into three general categories:

- Overall Susceptibility of Magnetite to Oxidation
- Hydrazine Decomposition
- Comparison of Steam Generator Deposits to Synthetic Powders

#### **Overall Susceptibility of Magnetite to Oxidation**

A fine magnetite powder (~100 nm average radius) was used to accentuate any oxidation because smaller particles have higher and more easily detected conversions for the same oxide film thickness. Plant deposit powder with a slightly larger average radius (~420 nm) was also tested in parallel experiments.

- No oxidation of magnetite to hematite was observed in either synthetic magnetite or real steam generator deposit powder under simulated wet-layup conditions.
- The harshest condition studied was one month at pH=7, 60°C, no hydrazine and high (saturated ~7 ppm) dissolved oxygen levels.
- Hematite, if formed at all, was below the XRD level of detection (1% conversion of magnetite to hematite) in all of the oxidation tests performed.

#### **Hydrazine Decomposition**

Hydrazine decomposition is known to be catalyzed by copper. In order to determine the effect of magnetite on hydrazine decomposition, the concentration of hydrazine was measured during the synthetic magnetite and plant deposit oxidation experiments.

- Lower levels of hydrazine decomposition were observed with synthetic magnetite powders compared to either copper powders or real steam generator powders.
- Hydrazine was present in solutions exposed to synthetic magnetite even after 30 days at 30°C or 10 days at 60°C. In contrast, in solutions exposed to either copper powder or real steam generator deposits, hydrazine is decomposed within five days at either 30°C or 60°C. Consequently, hydrazine maintained a lower ORP for a longer period of time in tests with synthetic magnetite powder.

## Comparison of Steam Generator Deposits to Synthetic Powders

While copper powder was found to accelerate the decomposition of hydrazine and commercial magnetite powder had a minimal effect, real steam generator deposits behaved more like copper powder than magnetite powder.

- ORP elevations due to the presence of real steam generator deposits were equivalent to those for copper powder (+60 mV) and much greater than those for magnetite powder (+20 mV).
- Hydrazine was decomposed quickly (in a few days) by deposits and copper powder. Hydrazine was not measurably decomposed over the course of a month by magnetite powder alone.

## ***Oxidation of Copper under Atmospheric Conditions***

The key results of the experiments measuring the oxidation of copper in steam generator deposits exposed to atmospheric environments fall into two categories:

- General Susceptibility of Copper to Oxidation
- Quantitative Description of Oxidation Rates

### General Susceptibility of Copper to Oxidation

The oxidation of copper in air was studied using thermogravimetric analysis (TGA) which measures the weight gain of a sample exposed to air. The weight gain is due to the addition of oxygen molecules to the sample through the oxidation of copper. The following results were obtained:

- Upon exposure to dry or moist air, copper oxidizes at an initially rapid rate. An oxide film about 1 nm thick forms in about an hour.
- Subsequent to the initial film formation, the rate of oxidation slows, so that the film will not grow more than a few nanometers thick over the course of several weeks (about 1% conversion of Cu to Cu<sub>2</sub>O for a 310 nm particle).
- The oxide formed was primarily cuprite (Cu<sub>2</sub>O) with no traces of tenorite (CuO).

### Quantitative Description of Oxidation Rates

The data obtained from the studies of copper oxidation in air were analyzed to determine which theoretical model of oxidation fit the data best.

- The formation of a copper oxide film is described well by a logarithmic rate law. Specifically, the equation  $x = A \ln(Bt+1)$ , where  $x$  is the oxide film thickness,  $t$  is the exposure time and  $A$  and  $B$  are fitted parameters, describes the oxidation of copper quite well over a broad range of atmospheric conditions.
- The rate constants  $A$  and  $B$  are temperature dependent with an activation energy of 24 kcal/mol, which agrees well with the literature value of 25 kcal/mol [7].

- The reaction rate constants are a linear function of humidity, even at relative humidity levels as low as 30%.

Figure 1-2 shows the oxide film thickness as a function of exposure time for several temperatures. As can be seen, higher temperatures lead to thicker oxide films.

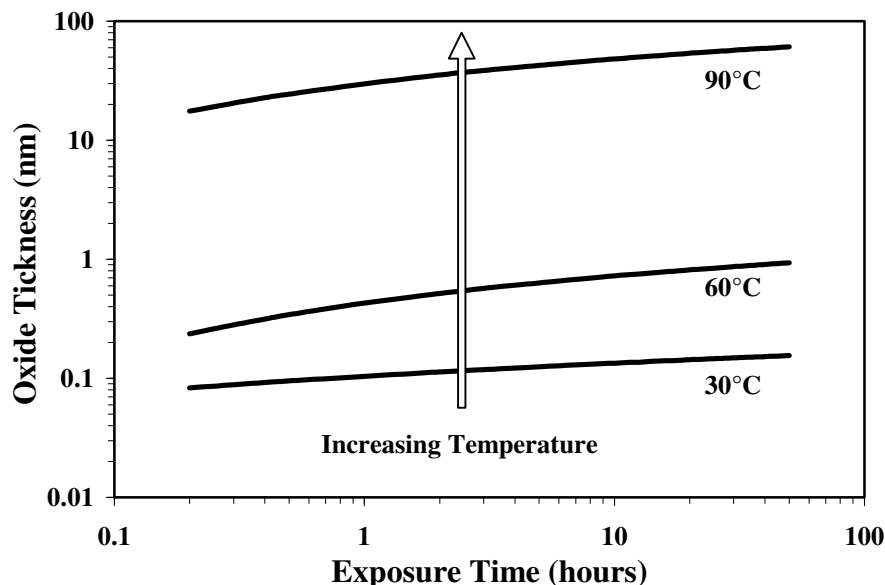


**Figure 1-2**  
**Aqueous Copper Oxidation Rates as a Function of Temperature and pH**

### ***Reduction of Copper under Startup Conditions***

The preliminary investigation into deposit oxide reduction under simulated startup conditions (100°C to 200°C, low dissolved oxygen) led to conclusions in two general categories:

- Reduction of Copper Oxides
- Low Oxygen Oxidation Reaction

The conclusions reached from this investigation are given below. Future work is expected to result in more specific recommendations regarding the best conditions to perform a reduction step during steam generator startup, including suggested hydrazine levels and temperatures.

#### **Reduction of Copper Oxides**

Cuprite ( $\text{Cu}_2\text{O}$ ) films, formed on copper particles under aqueous conditions in other parts of this study, were subjected to reducing conditions. Cuprite was found to be reducible back to metallic copper.

- Copper can be fully reduced from  $\text{Cu}_2\text{O}$  to Cu at moderate temperatures (100°C to 200°C) by excess hydrazine.

- Increased hydrazine levels lead to both faster and more complete reduction to copper metal.
- If hydrazine is not in stoichiometric excess of the oxide, no reduction occurs.
- Reduction was faster and more complete at 100°C than 200°C, possibly due to temperature acceleration of the decomposition of hydrazine or an oxidation reaction (see below).

### Low Oxygen Oxidation Reaction

During the reduction experiments, some experiments led to an increase in the fraction of cuprite, instead of the expected reduction.

- Some oxidation of Cu to  $\text{Cu}_2\text{O}$  takes place even in the nominal absence of oxygen (i.e., in solutions with enough hydrazine to completely consume all of the oxygen present). This is consistent with the literature, which indicates that there is a water/metal reaction to produce oxides [12].
- In water at moderately high temperatures (100°C to 200°C), more  $\text{Cu}_2\text{O}$  forms than could be accounted for by dissolved oxygen levels equivalent to atmospheric saturation (~7 ppm).
- The water-only oxidation reaction is accelerated at higher temperatures.

### Film Thickness Versus Oxide Fraction

Oxide film thickness and the area of the copper exposed to the secondary-side fluid are the parameters that govern the effects of copper on SG tube degradation. However, literature studies use the weight percentage of copper oxide relative to the secondary-side water mass as the relevant parameter [1, 5, 6, 17, 18]. To compare the literature data with actual steam generator conditions, it is therefore necessary to be able to convert between film thicknesses and fractional conversion to oxide (or oxide weight fraction).

- Conversion to percentages requires knowledge of the particle or inclusion size.
- For the powders used in this study, a 1 nm oxide film corresponds to about 0.6% conversion to oxide.
- For typical steam generator copper inclusion sizes, a 1 nm oxide film corresponds to about 0.04% conversion of Cu to  $\text{Cu}_2\text{O}$ .





# 2

## INTRODUCTION

---

### **Purpose and Working Hypothesis**

Despite the fact that essentially all western style PWR plants adhere to the strict requirements of EPRI's Secondary Water Chemistry Guidelines, many plants continue to experience significant secondary-side corrosion of the steam generator (SG) tubes. SG tubes form the boundary between the primary side and the secondary side of the steam generator. Thus, tube degradation is important for nuclear safety as well as for plant performance.

One area in which chemistry control has not been consistent from plant to plant is the environment to which the SG is exposed during shutdown, layup and startup (SLS). The hypothesis that SLS conditions lead to an increase in corrosion is supported by considerable anecdotal evidence. However, to support development of guidelines for stricter SLS chemistry control, a strong theoretical basis must be developed to explain the anecdotal evidence and predict the effects of tighter controls.

Toward this end a qualitative working hypothesis of the effects of SLS on SG chemistry has been developed. The hypothesis postulates four steps:

1. During normal operation, some corrosion in the secondary water loop occurs, introducing dissolved metal into the feedwater in minute quantities.
2. Normal operation of the SG concentrates these metal ions, forcing precipitation of metal and oxides in the SG.
3. During SLS, the deposits in the SG are oxidized and serve as an oxygen reservoir, and oxides are also formed in other parts of the secondary system.
4. During the initial phases of operation, these oxides—together with oxides introduced from the secondary plant by the feedwater—are reduced, either by directly oxidizing the metal of the SG tubes or through introduction of oxygen into the SG secondary bulk via various possible reactions.

A flow diagram showing the sequence of events postulated in this hypothesis is shown in Figure 2-1. The first two steps of this hypothesis are well documented and will not be addressed in this report. The third and fourth steps, however, have not been well understood. The purpose of this report is to review the literature regarding these phenomena and to present the results of recent theoretical and experimental investigations conducted in support of this project by the authors. It is hoped that an increased understanding of the oxidation and reduction of steam

generator deposits will lead to the development of scientifically-based guidelines for shutdown, layup and startup oxidant control.

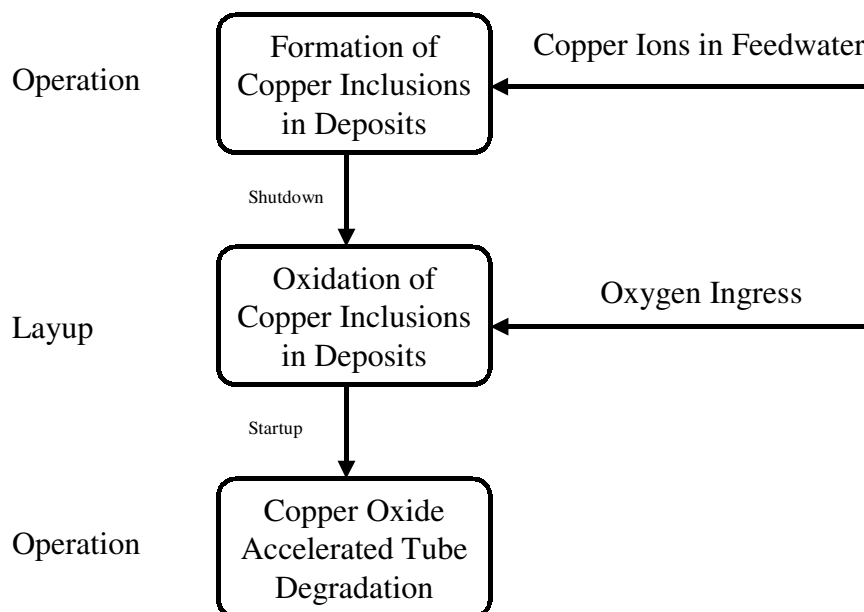


**Figure 2-1**  
**Schematic of the Working Hypothesis**

Steam generator deposits contain several species that might participate in the hypothesis described above. Most deposits are composed primarily of magnetite ( $\text{Fe}_3\text{O}_4$ ). It is possible that the conversion of magnetite to hematite ( $\text{Fe}_2\text{O}_3$ ) might occur during SLS and could contribute to steam generator tube degradation. However, it has been demonstrated in both caustic [1] and acidic environments [17] that copper oxides can raise the corrosion potential of Alloy 600, accelerating SG tube degradation. Furthermore, even “copper free” plants have deposits with some copper content due to the presence of copper as a tramp element in many secondary-side components. Copper in deposits is primarily found as copper metal, which is much more easily oxidized than magnetite. Therefore, although magnetite has been included in some portions of this project, the focus has mainly been on copper.

## Report Organization

This report presents the results of the current project in three parts:

- Literature Review
- Deposit Oxidation-Diffusion Model
- Experimental Test Program

The information from each of these sources is reviewed in a separate section.

## ***Literature Review***

Section 3 presents the data found in the literature. A comprehensive review of the literature included a search of several commercial databases. The literature gathered included journal articles, workshop and conference presentations, EPRI reports and books. The literature review covered four main topics:

- Deposit Characterization
- Effects of Copper Deposits on Steam Generators
- Oxidation Reaction Rates
- Reduction Reaction Rates

In addition to the topical review given in Section 3, Appendix A contains summaries of the individual papers and reports reviewed during the literature survey.

## ***Deposit Oxidation-Diffusion Model***

Section 4 presents the results of the theoretical portion of this study. A mathematical investigation was conducted to predict the diffusion of oxygen into porous deposit structures at the same time that the oxygen was consumed by reaction with imbedded copper particles to form copper oxide. The purpose of this investigation was to determine if diffusional resistance would significantly slow the oxidation of imbedded copper, or if imbedded copper would react at the same rate as copper exposed to the bulk secondary fluid. Three different methods were used to make this determination:

- A steady-state reaction/diffusion model
- An evaluation of the effectiveness factor
- An evaluation of the characteristic time scales

These three evaluation techniques compare the relative influence of the diffusion and reaction rates to determine whether diffusion through deposits will slow the rate of oxidation of copper particles imbedded in tube scale. The reaction/diffusion model approach allowed the consideration of wet and dry layup situations.

## ***Experimental Test Program***

Section 5 presents the results of the experimental portion of this project. The experimental program consisted of four different investigations:

- Characterization of SG Deposit Copper Inclusions
- Aqueous Oxidation Experiments (copper and magnetite under wet-layup conditions)
- Atmospheric Oxidation Experiments
- Reduction Experiments for Copper under Startup Conditions

## Characterization of SG Deposit Copper Inclusions

In the deposit characterization investigation, copper inclusions from two different plants were analyzed using an electron microprobe to determine their elemental makeup. This investigation was conducted primarily to validate the use of synthetic copper powder to simulate copper inclusions in steam generator deposits. If the copper inclusions were found to be nearly pure copper, then the inclusions would have the same oxidation chemistry as synthetic copper powders. The presence or absence of zinc in the inclusions was of particular interest due to the strong effect of zinc alloying on copper oxidation chemistry.

## Oxidation of Copper under Wet-Layup Conditions

In the wet-layup copper oxidation experiments, X-ray diffraction was used to determine the extent to which copper was converted to a more oxidized species (cuprite,  $\text{Cu}_2\text{O}$ ) over the course of one month. These experiments tested the influence of three parameters on the rates of oxidation:

- pH
- Temperature
- Initial hydrazine concentration

The wet-layup experiments also tracked changes in the solution chemistry during the test period. These measurements included:

- pH
- Hydrazine concentration
- Oxidation-reduction potential

## Oxidation of Magnetite under Wet-Layup Conditions

Wet-layup experiments identical to those performed with copper were performed with synthetic magnetite and deposit powder from the steam generators of a PWR commercial power plant. The following measurements were made during the course of one month's exposure of the magnetite and deposit powders to the simulated layup solution:

- pH
- Hydrazine concentration
- Oxidation-reduction potential
- Fractional conversion of magnetite ( $\text{Fe}_3\text{O}_4$ ) to hematite ( $\text{Fe}_2\text{O}_3$ )

## Atmospheric Oxidation Experiments

In the atmospheric experiments, the oxidation of copper powders was measured using thermogravimetric analysis (TGA). TGA measures the extent of the oxidation reaction by measuring the weight gain of a copper sample due to the addition of oxygen molecules. The atmospheric experiments determined the effect of the following parameters on the rate of oxidation:

- Temperature
- Relative humidity

The results from the atmospheric oxidation experiments were analyzed by fitting the data to models presented in the literature.

## Reduction Experiments for Copper under Startup Conditions

In the reduction experiments, cuprite films around copper metal particles were reduced by exposure to hydrazine and high temperatures. The extent of the conversion of cuprite to copper metal was measured by X-ray diffraction. These experiments measured the effect on the extent and rate of reduction of the following parameters:

- pH
- Temperature
- Initial hydrazine concentration



# 3

## LITERATURE REVIEW

---

### Summary

The literature review was conducted by searching several commercial databases for references to copper oxidation and reduction and the influence of copper oxides on steam generator (SG) performance. Several types of document were found and reviewed, including journal articles, workshop and conference presentations, EPRI reports and books.

The literature search led to several broad conclusions. Steam generator deposits, although consisting mainly of magnetite, also contain metallic copper. The copper in deposits is generally found as inclusions within a porous magnetite matrix. When copper is oxidized, it can significantly accelerate steam generator tube degradation. There is a large body of data in the literature regarding the kinetics of oxidation and reduction of copper. However, there are few data specific to steam generator layup conditions.

The literature search focused on four main topics:

- Deposit Characterization
- Effects of Copper Deposits on Steam Generators
- Oxidation Reaction Rates
- Reduction Reaction Rates

The findings in these areas are reviewed below. Additionally, summaries of each of the documents reviewed during the course of the literature survey are given in Appendix A.

### Deposit Characterization

The characterization of steam generator deposits falls into two main categories: chemical and physical. In general, the chemical analysis consists of determining the elemental composition of the deposit and determining the degree of oxidation of the elements. For example, one can determine the weight fraction of iron and then determine whether the iron is metallic iron (Fe), hematite ( $\text{Fe}_2\text{O}_3$ ) or magnetite ( $\text{Fe}_3\text{O}_4$ ). Physical characterization includes the determination of bulk properties, such as porosity and density, and of morphology, such as types of inclusions and the general location of various elements. The literature data regarding these two aspects are summarized below.

## **Chemical Characterization**

Steam generator deposits are composed (elementally) overwhelmingly of iron. Typically, over 85% of the solids found in SG deposits are iron compounds. However, most of the iron deposits exist in the form of magnetite,  $\text{Fe}_3\text{O}_4$ , which is generally considered benign since the compactness of magnetite layers is believed to prevent oxygen diffusion and help form a passivation layer on metal surfaces.

Of primary significance with regard to the hypothesis of copper-oxide-accelerated steam generator tube degradation is the presence of copper-containing species in the deposits. Copper tubing in the secondary-coolant-cycle heat transfer equipment (such as condensers and feedwater heaters) account for the bulk of the copper transported to the steam generator [19]. In many plants (generally referred to as “copper-free”) these components do not use copper tubing. Nevertheless, copper still deposits in the steam generator due to its presence as a tramp element in many non-copper alloys. Copper typically accounts for about 5% of the secondary-side deposits in an SG [2], although it can account for significantly less (~0.3%) in “copper-free” systems and significantly more than 5% at some plants, and even more than 50% at one plant [3]. Copper in SG deposits is primarily found as copper metal (Cu), but also as cuprite ( $\text{Cu}_2\text{O}$ ) and tenorite (CuO) in minor amounts [4].

## **Physical Characterization**

The physical nature of steam generator deposits as determined by their hardness, porosity or distribution of constituent elements is highly dependent not only on the chemistry of the secondary coolant but also on the location of the deposit within the steam generator [2]. However, there are some general trends that are of note.

Although some types of deposit (tube sheet or sludge pile deposits) are quite dense, tube scales and free span deposits often have a void fraction of about 50% [2]. Often these scales are layered, with the region near the tube wall being considerably denser than the region exposed to the bulk secondary coolant. The relatively high void fraction is due to the porous nature of the deposits. The deposit structure is often seen as a network of capillaries [2]. One way to characterize such networks is to define a tortuosity. Tortuosity reflects the degree to which the capillaries are not straight and is a unitless quantity. Typical tortuosity values ( $\tau$ ) for tube scales are about 1 to 3 [20]<sup>1</sup>. Roughly, this means that molecules will diffuse as much as three times slower through the scale as they would through an equivalent length of straight capillaries. The scale porosity  $\varepsilon$  also has a direct effect on the effective diffusion rate  $D_{eff}$ .

$$D_{eff} = \frac{\varepsilon}{\tau} D \quad [3-1]$$

where  $D$  is the molecular diffusivity of a species of interest in water.

---

<sup>1</sup> There are various definitions of the tortuosity of a porous medium in the literature including  $1/\tau$  as  $\tau$  is used in Equation 3-1. See Bear [56] for the theoretical basis of the tortuosity and a discussion of the various definitions.



Typically, the copper found in these deposits is located in inclusions of about 5  $\mu\text{m}$  or less in diameter. These inclusions are often found in a layer near the tube wall [2]. One mechanism that has been proposed to explain the formation of this morphology is that copper is complexed with ammonia in the bulk secondary coolant. When these copper-ammonia complexes reach the elevated temperatures near the tube wall by transport through the deposit void spaces, the ammonia is volatilized, leaving behind copper metal, which fills what was once a void space [21].

## Effects of Copper Deposits on Steam Generators

Evidence of the effect of copper in steam generator deposits on the accelerated degradation of steam generator tubes falls into two categories: anecdotal plant data and laboratory data. Unfortunately, the link between the two data sets is not clear due to differences in the way parameters are varied in the laboratory experiments and the mechanisms through which these parameters affect real steam generators. This section presents a brief review of the two data categories and gives an explanation of why the two cannot easily be compared.

### ***Plant Observations***

The hypothesis of a link between the presence of copper oxides in steam generator deposits and accelerated corrosion of steam generator tubes began with a number of anecdotal observations. For example, at South Korea's Kori 1 significant corrosion of steam generator materials was observed in conjunction with an unusually high degree of copper in the steam generator deposits (approximating 50%). When tighter control of oxygen ingress and reduction of oxidized deposits during startup were imposed, the corrosion of the steam generator tubes decreased significantly [3]. Additional evidence of an SLS link to accelerated corrosion was found in a Belgian study that found that corrosion corresponded more closely with the number of cycles than with the duration of operation. Likewise, it has been observed that in Swedish plants, which exercise stringent control over SLS oxygen ingress, there is very low IGA/SCC [22].

A recent EPRI workshop [23] was devoted to investigating the effects of startup oxidants on steam generator tube degradation. The general conclusions of this conference were that, although there is considerable anecdotal evidence regarding the hypothesis that deposit oxides accelerate corrosion of steam generator tubes, there is not enough evidence to make a firm conclusion. EPRI report TR-112967 [57], *Source Book on Limiting Exposure to Startup Oxidants*, September 1999, details the technical bases for limiting exposure to startup oxidants and makes specific recommendations for plant operation.

### ***Laboratory Data***

In laboratory tests, it has been shown that the presence of copper oxides significantly raises the corrosion potential of Alloy 600 in caustic solutions [1, 5]. The corrosion potential (like the oxidation-reduction potential, ORP) is a measure of the tendency of an electrode to dissolve in the test solution. A rise in the corrosion potential therefore indicates a greater tendency toward corrosion. Other studies, in acidic conditions, have observed the acceleration of corrosion of Alloy 600 in the presence of copper oxides [17]. Although a similar study in acidic conditions

concluded that the rise in the corrosion potential of Alloy 690 due to small amounts of copper oxides was not enough to accelerate corrosion, accelerated corrosion was nonetheless observed. The authors concluded that copper oxides might act through some catalytic effect rather than through the corrosion potential [6].

Although there has been one study that concluded that copper must be present in high concentrations to be detrimental to Alloy 600 [18], there is a substantial amount of information indicating that even small quantities can accelerate corrosion. One study has examined several levels of copper oxides and their impact on both the corrosion potential and the corrosion rate of Alloy 600. This study determined that, in caustic solutions, a concentration of 0.1% CuO was enough to raise the corrosion potential while 0.01% was not. In the presence of additional sludge components, a level of 0.045% CuO was found to raise the corrosion potential significantly. The study concluded that the level of CuO that would produce the maximum acceleration in stress corrosion cracking probably lies somewhere between 0.1% and 0.01% [1]. Another study used capsule experiments to determine the influence of copper oxides on stress corrosion cracking. It was determined that, in acid environments, there was a decline in the acceleration of SCC when the copper oxide levels were changed from 0.64% to 0.16%, but corrosion was still significantly accelerated at the lower level [6].

### ***Relating Laboratory Data to Plant Operations***

Since the mechanism through which copper oxides accelerate corrosion is probably related to an electrochemical reaction involving the oxide, it is likely that it is a surface effect. In other words, because the oxide is insoluble, the ratio of the oxide mass to the solution mass is not as important as the ratio of the oxide wetted surface area to the tube wetted surface area. Thus, in regard to accelerated corrosion of steam generator tubes, the important parameter is the ratio of surface areas, not the concentration of the oxide. Unfortunately, none of the research done to date on the effect of copper oxides has included information on the specific surface area (surface area per unit mass) of the copper oxides, which might allow comparison to effects in a steam generator. Ideally, the levels of copper oxide in a given test would be expressed as a relative surface area, i.e., the ratio of oxide surface area to Alloy 600 or carbon steel surface area. An additional problem is the lack of data on the distance over which copper oxides might influence corrosion rates. It is probable that the distance over which copper oxides act is relatively small, so it is the local relative area—or possibly in combination with the local copper oxide volumetric concentration—that most likely controls the extent of corrosion acceleration. Therefore, significant assumptions must be made with little foundation in order to draw conclusions about steam generator degradation from the studies available in the literature.

The question of the relative surface area effect also raises questions about the size and shape of the copper deposits. Although copper in steam generator deposits is usually present as small particles, other possibilities exist. Of specific concern would be those instances in which copper might be dissolved and re-plated (e.g., during layup-startup evolutions) in a way that drastically increases the surface area available for oxidation and subsequent promotion of corrosion.

## Oxidation Reaction Rates

Copper has a long history of extensive use in many industries due to its excellent thermal and electrical conductivity and convenience of use. Because of this wide usage, many studies have been performed on copper's susceptibility to oxidation. The data available in the literature fall into four general categories:

- Types of Reaction
- Models of Atmospheric Oxidation
- Aqueous Oxidation
- Type of Oxide Formed

The literature data in each of these categories are summarized below.

### *Types of Reactions*

Several copper oxidation reactions may occur in a steam generator during layup (either wet or dry):

1.  $\text{Cu} + 1/8 \text{O}_2 \rightarrow \text{Cu}_4\text{O}$
2.  $\text{Cu} + 1/128 \text{O}_2 \rightarrow \text{Cu}_{64}\text{O}$
3.  $\text{Cu} + 3/32 \text{O}_2 \rightarrow \text{Cu}_4\text{O}_{0.75}$
4.  $\text{Cu} + 1/2 \text{O}_2 \rightarrow \text{CuO}$
5.  $2\text{Cu} + 1/2 \text{O}_2 \rightarrow \text{Cu}_2\text{O}$

Reactions 1, 2 and 3 characterize the initial phases of copper oxidation. When the first few molecules of oxygen begin to react, crystal structures are formed on the metal surface in which the copper atoms can be considered to be of mixed valence. These crystal structures are metastable and represent a transition from a clean metallic copper surface to one which is oxidized [9, 24]. In consideration of the oxidation of copper metal in SGs, these reactions should be considered negligible since their kinetics will be included in any measurements of the more common Reaction 4 and Reaction 5.

### *Models of Atmospheric Oxidation*

The kinetics of copper oxidation are usually investigated using one of several models developed by Cabrera and Mott [7]. Cabrera and Mott defined three phases of oxidation: very thin film growth, thin film growth and thick film growth. During the early stages of oxidation a very thin film ( $\ll 10$  nm) of oxide forms on the metal surface. Over time, the film thickens to a thin film ( $\leq 10$  nm) and finally to a thick film ( $\gg 10$  nm). The rate of oxidation in this model depends on the relative disjunction between the rate of cation diffusion and electron diffusion. Linear oxidation, in which the oxidation proceeds at a constant rate, is also possible. Additionally, there

are empirical models, which predict the rate of oxidation based on experimental findings, rather than theoretical derivations. Models of atmospheric oxidation thus fall into five categories:

- Very Thin Film Oxidation
- Thin Film Oxidation
- Thick Film Oxidation
- Linear Oxidation Models
- Empirical Oxidation Models

A summary of the literature regarding each of these categories is given below.

### Very Thin Film Oxidation

In very thin films ( $\ll 10$  nm) the electric potential created by oxidation is dissipated over a very short distance, creating a very strong flux of cations from the metal surface through the oxidation film. Thus, the rate limiting step is the escape of metal cations from the bulk metal. This leads to a logarithmic growth law that predicts that the film thickness  $x$  will grow as:

$$\frac{dx}{dt} = ue^{\frac{x_1}{x}} \quad [3-2]$$

where  $t$  is the time and  $x_1$  and  $u$  are constants that have theoretical meanings but are only known to an order of magnitude, thus necessitating experimental derivation of their values. The values of  $u$  and  $x_1$  were measured for room temperature oxidation of highly polished copper in air by Krishnamoorthy and Sircar [8]. They found that  $x_1$  was independent of the oxygen pressure at a value of  $x_1 = 2.89$  nm. They also reported a dependence of  $u$  on the partial oxygen pressure as shown in Table 3-1.

**Table 3-1**  
**Kinetic Parameter Dependence on the Partial Pressure of Oxygen**

<b>O<sub>2</sub> Partial Pressure (atm)</b>	<b><math>u</math> (nm/hr)</b>
0.0135	0.0045
0.027	0.007
0.068	0.0085
0.123	0.012
0.21	0.02

Using small value approximations (i.e., Taylor series expansions), Equation 3-2 can be simplified to a more tractable form [25, 26]:

$$x = A \ln(Bt + 1) \quad [3-3]$$

where  $A$  and  $B$  are constants either fitted to the data or derived from Equation 3-2. There are considerable additional data on oxidation in this regime. However, there is little agreement among the many measurements. Figure 3-1 shows the data from several studies under various conditions. Although there is some general agreement, the various techniques used and the variability in the initial condition of the copper make quantitative conclusions difficult to reach. For example, Allen [27] determined that the chemical preparation of the copper surface before running an oxidation experiment had a large effect on the kinetic data collected. Bradley and Uhlig [28] found that if the copper was annealed before oxidation, the annealing gas had a significant impact on the subsequent oxidation rates. Swanson and Uhlig [26] argue that pretreatment of copper can affect the orientation of the copper crystals, which may have a large impact on the reactivity of the exposed surfaces.

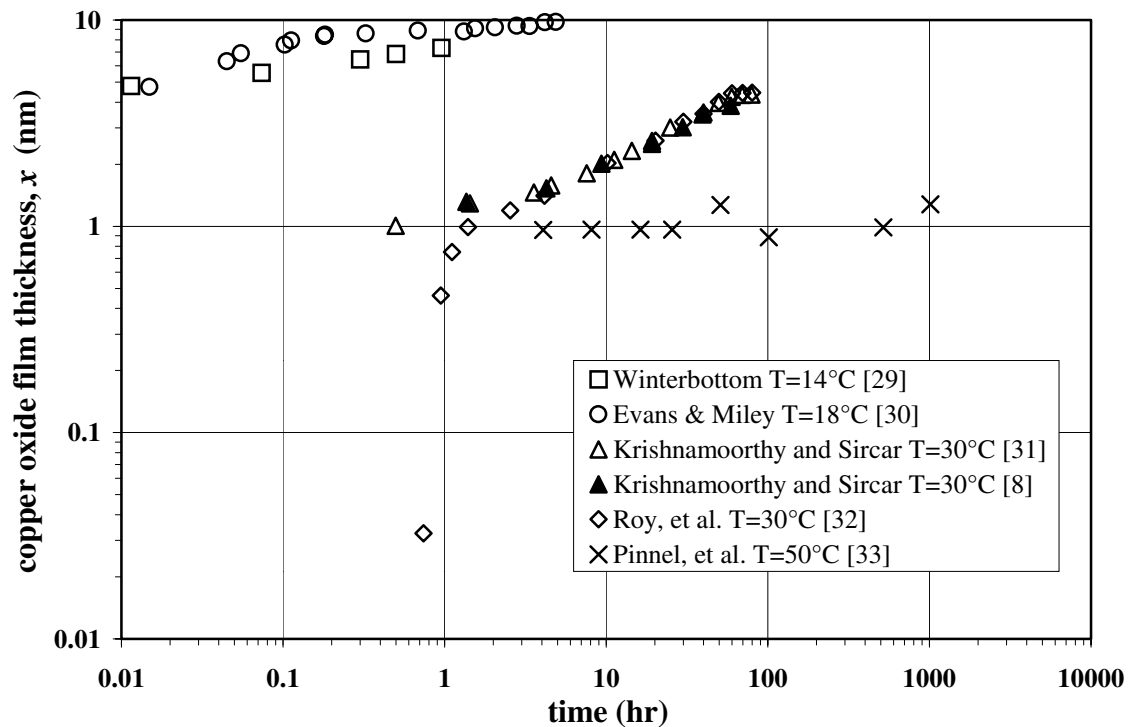


**Figure 3-1**  
**Literature Data for Copper Oxide Thin Film Growth**

### Thin Film Oxidation

In oxide films that are thin ( $\leq 10$  nm) the film is thick enough to support a finite potential drop, yet thin enough that the potential gradient is significant compared to the concentration gradient of ions and electrons [7]. The rate limiting step is transport of cations through the already formed oxide film. This transport is primarily driven by electric potential, yielding a parabolic growth law:

$$\frac{dx}{dt} = \frac{a}{x} \quad [3-4]$$

In Equation 3-4,  $a$  is a theoretically derived parameter:

$$a = \Omega v_i V n_i \quad [3-5]$$

in which  $\Omega$  is the volume of oxide per ion,  $v_i$  is the ion mobility,  $V$  is the potential across the oxide film and  $n_i$  is the concentration of metal ions in the solution. There are apparently no data in the literature directly addressing the parabolic growth of copper oxides in the thin film region (as opposed to parabolic growth in the thick film region, see below).

### Thick Film Oxidation

In thick films ( $\gg 10$  nm) the variations in electrical charge are small compared to variations in the concentration of copper species across the oxide layer. It is assumed that the oxidation reaction provides a perfect sink for the diffusing species. Hence, the process of oxidation is controlled solely by Fickian diffusion:

$$Flux = D_i \frac{dC_i}{dz} = D_i \frac{C_i(0)}{x} \quad [3-6]$$

In Equation 3-6,  $D_i$  is the diffusion coefficient of the ions,  $C_i$  is their concentration and  $z$  is the direction normal to the film growth. Since the concentration drop does not change as the film becomes thicker, the rate of reaction (equal to the flux) must slow. Using  $\Omega$  to relate the thickness to the concentration yields a parabolic growth law:

$$\frac{dx}{dt} = \frac{D_i \Omega C_i(0)}{x} \quad [3-7]$$

$$x^2 = 2D_i \Omega C_i(0)t = kt \quad [3-8]$$

Mrowec and Stoklosa [10] report parabolic growth rates for several partial pressures of oxygen. Roy, Bose and Sircar [34] give similar data.

### Linear Oxidation Models

Another possible model is based on the assumption that growth is limited by the reaction rate. This leads to a linear growth law. No literature data are available which indicate that this model is valid under layup-type environments. However, a theoretically sound basis for the existence of linear oxidation rates exists. If the oxide film is formed in such a way that it is significantly porous or has cracks, it will provide no protection to the underlying metal, and the oxidation will proceed at a constant rate.

## Empirical Oxidation Models

In addition to the models of Cabrera and Mott [7], a strictly empirical model is given by Khoviv and Malevskaya [35], predicting the thickness of the film to be:

$$x = Kt^n \quad [3-9]$$

where  $n$  and  $K$  are fitted parameters. Their data are in the appropriate range for parabolic growth, and their data could be reformatted and analyzed according to that model.

Another empirical model is the two region logarithmic model [25, 26]. Experimental observations indicate that the oxidation reaction of copper can be modeled as having two regions of logarithmic growth with different rate constants. Growth is observed to be fast in the initial stage and slower in the later stage. Some observers attribute this two region growth to a change in mechanism during the oxidation [25].

## Aqueous Oxidation

All of the kinetics studies cited above were conducted with copper exposed to dry air. There have been several studies that have investigated the dissolution of copper in various aqueous solutions [16, 19, 36, 37, 38, 39]. The results of these studies are highly specific to the particular chemistries studied, but a few general observations can be made. Increasing temperature leads to increased dissolution rates [19]. Lower pH leads to higher dissolution rates [19, 38]. Higher oxygen concentrations lead to higher dissolution rates [19]. Additionally, there are conflicting data on the effect of the fluid flow on the dissolution rate [19, 39].

The oxidation of copper by water with low dissolved oxygen levels to produce copper oxides and hydrogen has been discussed in several controversial articles. Hultquist [12] claims to have observed the evolution of hydrogen in conjunction with the oxidation of copper in water at room temperature. However, Simpson and Schenk [13] claim that the reaction between copper metal and water is thermodynamically unfavorable. Nevertheless, it appears likely that some additional mechanism of oxidation is possible in aqueous environments. It is possible that this reaction does not require dissolved oxygen but may be sustained by the oxygen provided by water molecules.

## Type of Oxide Formed

Several investigations [9–11] have observed the formation of two different types of copper oxides (Reactions 4 and 5 from above). Mrowec and Stoklosa found that the rate of oxidation is dependent on the nature of the oxide formed [10]. Lenglet *et al.* found that a layer of CuO forms at the air-oxide interface [9]. Mrowec and Stoklosa determined that the saturation concentration of oxygen in the CuO became the limiting factor in determining the oxidation rate when the partial pressure of oxygen in the air exceeded the partial pressure of oxygen in the saturated CuO layer. They found that the saturation pressure (equivalent to the dissociation pressure) was a function of temperature [10]. This dependency of the saturation pressure on temperature is shown in Figure 3-2 (based on theory). In addition, the findings of Mrowec and Stoklosa are in good agreement with those of several other studies [14, 40, 41]. Note that the kinetic data cited

above were determined experimentally and then plotted in Figure 3-1 by converting the reported data to oxide film thicknesses and assuming formation of a single oxide layer of cuprite. Although there may in fact be two layers present, the kinetics data can still be useful in determining the overall growth rate of the entire layer.

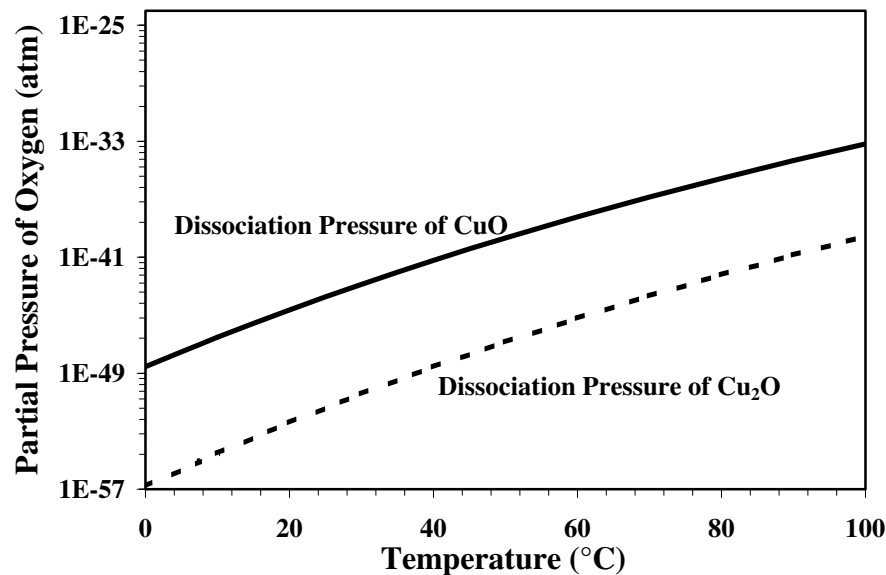


**Figure 3-2**  
**The Dissociation Pressures of Copper Oxides [10]**

## Reduction Reaction Rates

The data available in the literature regarding the reduction of copper oxides are much more limited than that regarding oxidation. The following reduction reactions may take place in a steam generator during startup or early operation:

6.  $\text{Cu}_x\text{O} \rightarrow x \text{Cu} + 1/2 \text{O}_2$
7.  $\text{CuO} + \text{M} \rightarrow \text{Cu} + \text{MO}$
8.  $\text{CuO} \rightarrow \text{Cu} + 1/2 \text{O}_2$
9.  $\text{Cu}_2\text{O} \rightarrow 2 \text{Cu} + 1/2 \text{O}_2$

where M might be any available metal (*e.g.* Fe or Ni). Reaction 6 represents the reverse of Reactions 1–3 above and likewise involves metastable compounds which are expected to exist in only a small amount at any specific time during the reaction [9, 24]. Therefore, the metastable compounds should not significantly accelerate SG tube degradation. Reaction 7 does represent a potential source of increased corrosion in the SG due to the presence of copper oxides. (Note that Reaction 7 may not be exactly representative of the reactions taking place, which may involve other valences of copper and the oxidized metal.) Reactions 8 and 9 may be considered to act in



competition with Reaction 7, and therefore are quite relevant to the hypothesis under discussion. Thus, there are two general reactions that must be considered: the release of oxygen to another metal and to the solution or a scavenger.

### ***Release of Oxygen to Another Metal***

Reaction 7 is the most important of the reduction reactions in the consideration of copper-related corrosion of SGs. Unfortunately, there are almost no data in the literature regarding the kinetics of this reaction. However, in addition to the anecdotal data discussed above, an investigation by Hur *et al.* [16] has shown that in the presence of copper-containing sludge (2.5% CuO, 10.0% Cu<sub>2</sub>O, 45.0% Cu as weight of sludge) the corrosion of carbon steel was increased by a factor of 30 over corrosion in the absence of sludge. Again, it should be noted that no data are available upon which to conclude the stoichiometry and valences involved in Reaction 7.

### ***Release of Oxygen to Solution or Scavenger***

Reactions 8 and 9 must be driven by one of two methods: extreme heating, in excess of 1000°C, [14] or removal of oxygen gas (i.e., an O<sub>2</sub> sink) [15]. While the use of extreme heating is not relevant here, the use of an oxygen sink is particularly relevant. Bowers *et al.* [15] used hydrazine (N<sub>2</sub>H<sub>4</sub>), long known as a powerful reducing agent, to convert copper oxides back to metallic copper. The temperatures in these experiments were moderate (22°C to 108°C) and the hydrazine was used in the vapor state.

When thick (>20 nm) copper oxide films were reduced by hydrazine in Bowers's experiments, they were found to undergo three distinct phases: an induction period during which there was no reduction, a fast reduction phase which followed a parabolic rate law and a slow reduction phase which also followed a parabolic growth law. The cause of the induction was not evident from the kinetics. However, it was clear that thinner films had a longer induction period. The induction periods lasted up to 25 minutes. The kinetics of the fast reduction period were found to follow a parabolic growth rate, indicating diffusion control. The experiments were performed at several temperatures, and the rate constant was found to follow an Arrhenius model with a pre-exponential factor of  $32 \pm 4 \text{ s}^{-1}$  and an activation energy of  $32 \pm 2 \text{ kJ/mol}$ . The value of the activation energy is also suggestive of diffusion control. It is of note that the rate law found by Bowers *et al.* is based on a total conversion factor rather than a molar factor. This is due to their finding that the reaction proceeded faster in thicker films. From this observation two hypotheses were formulated: the reaction was limited by intragranular diffusion with relatively free passage of oxygen outside the grain boundary or the reaction was limited by pore diffusion which became increasingly difficult as the reaction progressed. Porosity testing indicated that the latter hypothesis was more likely correct. The slower reduction in the third phase was attributed to a change in the nature of the oxide (i.e., packing density or size of grains) in the layer closest to the metal/oxide interface [15].



# 4

## DEPOSIT OXIDATION-DIFFUSION MODEL

---

### Introduction

In order to evaluate laboratory data on the oxidation of copper, it is necessary to consider, not only the fundamental reaction kinetics, but also the effect of diffusional resistances due to the location of the copper in the tube scale and the porosity of the scale. Microscopic examination of typical tube scales shows that copper in PWR steam generator deposits is usually concentrated in inclusions which tend to lie near the tube wall. The top half of Figure 4-1 shows a cross section of a typical dense tube scale sample from a PWR steam generator. The bottom half shows the presence of copper in the same sample using what is referred to as a copper map, obtained from energy dispersive spectroscopy (EDS). The copper map shows the presence of embedded copper particles close to the tube wall. In Figure 4-1 the left edge of the scale would be adjacent to the tube wall.

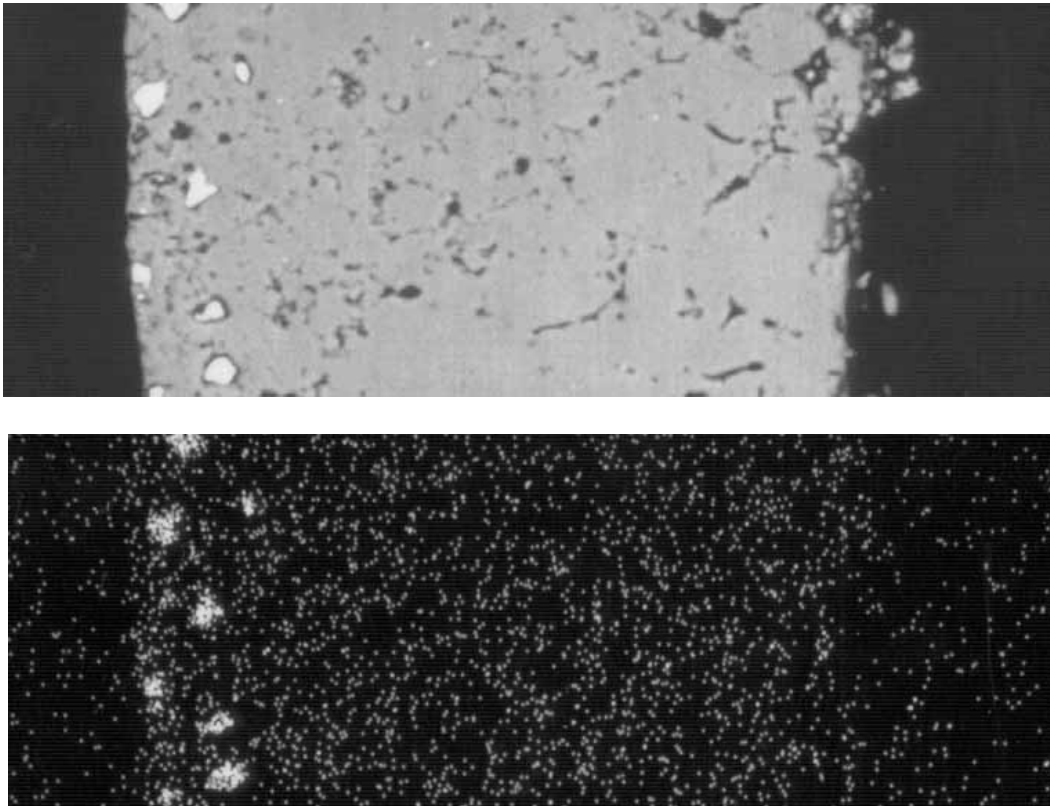


**Figure 4-1**  
**Typical Dense Tube Scale: SEM Microphotograph (top) and Copper Map (bottom)**

Because copper in steam generator deposits is not directly in contact with the bulk fluid, it is conceivable that the diffusion of dissolved oxygen through the scale structure may slow the rate of oxidation of the copper. In other words, diffusion may be the rate-limiting step. To determine the relative influences of the oxidation reaction rate and the oxygen diffusion rate, three theoretical tools were used:

- Steady-State Reaction/Diffusion Model
- Effectiveness Factor
- Comparison of Characteristic Time Scales

The steady-state model was developed by the present authors. The other two techniques were based on literature descriptions. The implementation and results of these techniques are discussed below. Note that a scale temperature of 30°C was assumed in the calculations presented in this section, but the conclusions are more generally applicable.

### **Steady-State Reaction/Diffusion Model**

In order for oxygen in the steam generator bulk environment to react with embedded copper particles, it must first diffuse through the tube scale. This diffusion process could conceivably slow the observed oxidation rate, providing some protection to the copper. One way in which to evaluate the magnitude of this effect is to compare the concentration of oxygen at the copper particle surface with that in the bulk environment. If diffusion provides significant resistance to the oxidation of copper particles, the oxygen concentration will be significantly lower at the copper surface than in the bulk environment. The determination of the oxygen concentration at the copper surface requires the solution of the diffusion equation using the consumption of oxygen at the copper surface as a boundary condition.

The development and evaluation of a steady-state reaction/diffusion model for the oxidation of embedded copper particles requires four steps:

- Determination of Physical and Chemical Parameters
- Determination of the Diffusion Characteristic Time Scale
- Derivation of the Steady-State Model
- Evaluation of the Model and Parameter Effects

Each of these steps is discussed in detail in the following sections.

#### ***Determination of Physical and Chemical Parameters***

The parameters needed to describe the diffusion and reaction of oxygen in steam generator tube scale can be divided into three categories:

- Scale Parameters
- Diffusion Parameters
- Reaction Parameters

Scale parameters describe the morphology of the tube scale. Diffusion parameters describe the rate at which oxygen molecules travel through the medium of interest (nitrogen for steam generators in dry layup or liquid water for steam generators in wet layup). Reaction parameters describe the kinetics of the oxidation reaction. The specific values of the parameters used are discussed below.

### Scale Parameters

The first set of parameters necessary to describe the diffusion of oxygen through tube scale are the variables that describe the physical nature of the scale. The parameters required to describe the morphology of the scale are shown in Figure 4-2, which gives a schematic of the diffusion model. (Note that the existence of a copper film is an approximation. Copper generally exists as particles, close to the tube wall, as shown in Figure 4-1.) Typically, steam generator tube scale consists of two distinct layers. The inner layer (nearest the tube) is dense and is typically characterized by small pores and low porosity. The outer layer (nearest the bulk environment) is generally less dense, characterized by larger pores and higher porosity. Two scale properties are of particular interest for each layer: the porosity ( $\epsilon$ ) and the tortuosity ( $\tau$ ). Together with the thickness of each layer, these parameters sufficiently describe the morphology of the scale.

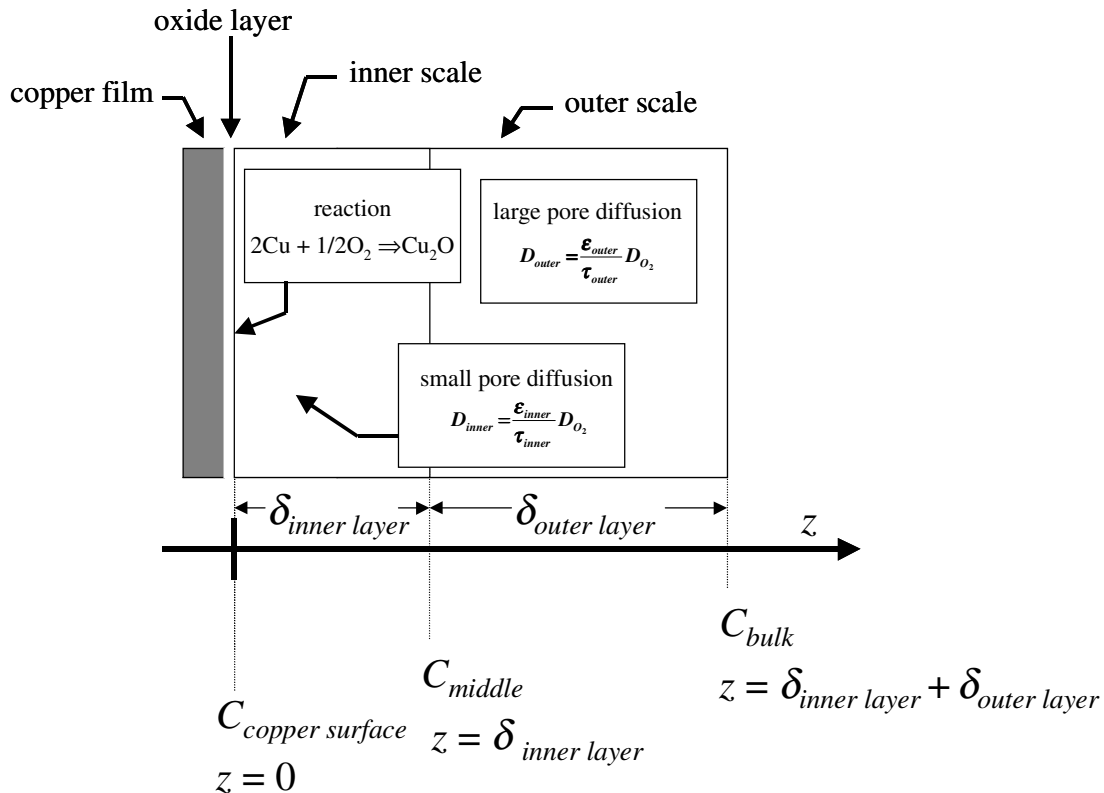


**Figure 4-2**  
**Schematic of the Diffusion Model**

The porosity of steam generator tube scale is a measurement of the volume fraction of the scale which is filled by pores. A solid layer of magnetite would have a porosity of zero. Since scale

would not exist without a solid skeleton, the maximum possible porosity is always less than unity. As a base case, a porosity of  $\varepsilon_{\text{outer layer}} = 0.5$  is used for the outer scale. This value is typical of isotropic deposits formed in steam generators using all volatile treatment (AVT) chemistry [2]. In the base case, the inner scale porosity is taken as  $\varepsilon_{\text{inner layer}} = 0.1$ . This is the lower end of the range for isotropic deposits [2]. In the subsection “Evaluation of the Model and Parameter Effects” below, the impact of other scale porosity values will be evaluated.

The tortuosity of a porous medium reflects the increased distance molecules must travel due to the curvature of the pores. A straight pore would have a tortuosity of unity, indicating that the diffusion through the pore takes place at the same rate as diffusion would take place through the fluid filling the pore in an unrestricted environment. High tortuosity indicates highly non-linear pores. Values of the tortuosity of steam generator tube scale are believed to range from unity to about three [58]. For the base case, a tortuosity of  $\tau = 2$  was chosen for both the inner and outer layers. Since there are no available data regarding the relative tortuosities of the inner and outer layers, these tortuosities were assumed to be equal.

Microscopic analysis of tube scale from several plants by the present authors indicates that the inner layer is often about half the thickness of the outer layer. Typical total scale thicknesses range from about 25 to 250  $\mu\text{m}$  [2]. As a base case, a value of 75  $\mu\text{m}$  is used. The scale parameters used for the base and conservative cases are given in Table 4-1. Note that the ratio of the inner to outer layer thicknesses was reversed for the conservative case.

**Table 4-1**  
**Scale Parameter Values for Base and Conservative Cases**

Parameter	Base Case	Conservative Case
$\varepsilon_{\text{inner layer}}$	0.1	0.01
$\varepsilon_{\text{outer layer}}$	0.5	0.1
$\tau$	2	3
$\delta$	75 $\mu\text{m}$	250 $\mu\text{m}$
$\delta_{\text{inner layer}}$	25 $\mu\text{m}$	167 $\mu\text{m}$
$\delta_{\text{outer layer}}$	50 $\mu\text{m}$	83 $\mu\text{m}$

## Diffusion Parameters

The diffusion of oxygen through the porous scale is governed in part by the diffusion of oxygen in the fluid filling the pores. The fluid in the pores may be either nitrogen (if the steam generator is in dry layup with a nitrogen blanket) or water (if the steam generator is in wet layup). A third possibility exists when steam generators are in dry layup in air. However, the diffusion of oxygen in air is essentially the same as the diffusion of oxygen in nitrogen.

The physical property that governs the diffusion rate is the diffusivity. The diffusivity of one gas in another can be calculated by the Fuller/Schettler/Giddings Relation [43]:

$$D_{O/N} = \frac{10^{-3} T^{1.75} [(M_O + M_N)/(M_O M_N)]^{1/2}}{P [V_O^{1/3} + V_N^{1/3}]^2} \quad [4-1]$$

where  $D_{O/N}$  is the diffusivity in  $\text{cm}^2/\text{s}$ ,  $T$  is the absolute temperature in K,  $M_O$  is the molecular weight of oxygen (32),  $M_N$  is the molecular weight of nitrogen (28),  $P$  is the pressure in atmospheres,  $V_O$  is the diffusion volume of oxygen (given as 16.6 in Reference [43]) and  $V_N$  is the diffusion volume of nitrogen (given as 17.9 in Reference [43]). At  $30^\circ\text{C}$  and 1 atmosphere, Equation 4-1 gives:

$$D_{O/N}(T = 30^\circ\text{C}) = \frac{10^{-3} \cdot 303^{1.75} [(32 + 28)/(32 \cdot 28)]^{1/2}}{1 \cdot [16.6^{1/3} + 17.9^{1/3}]^2} = 0.21 \frac{\text{cm}^2}{\text{s}} = 2.1 \times 10^7 \frac{\mu\text{m}^2}{\text{s}} \quad [4-2]$$

The diffusivity of oxygen in water at  $25^\circ\text{C}$  is  $2.5 \times 10^{-5} \text{ cm}^2/\text{s}$  [43] or  $2.5 \times 10^3 \mu\text{m}^2/\text{s}$ . According to the Stokes-Einstein theory of diffusion, the diffusivity is a linear function of absolute temperature. Assuming the validity of this theory for the case of oxygen in water, the diffusivity does not change significantly between 25 and  $30^\circ\text{C}$ , a change of less than 2% on the absolute temperature scale.

Finally, it is necessary to confirm that there is no significant diffusion of oxygen through the magnetite skeleton of the scale. Because the diffusivities in solid media are so small, there are very few data available concerning them. There are apparently no data present in the literature regarding the diffusivity of oxygen in magnetite. However, the magnitude of the diffusivity of oxygen in magnetite can be estimated by comparing typical values of diffusivities in solids. Table 4-2 shows the diffusivities of hydrogen in various solids, nitrogen and liquid water. Based on these data, it is expected that the diffusion through magnetite would be on the order of  $10^8$  times slower than diffusion in  $\text{N}_2$ , or  $10^4$  times slower than in liquid water. Hence, diffusion through the magnetite is negligible.

**Table 4-2**  
**Comparison of Diffusivities in Solids and Fluids**

	Value ( $\text{cm}^2/\text{s}$ )	Temperature ( $^\circ\text{C}$ )	Reference
$D_{\text{H}_2/\text{SiO}_2}$	$10^{-8}$	500	[44], Table 16.2-4
$D_{\text{H}_2/\text{Ni}}$	$1.16 \times 10^{-8}$	85	[44], Table 16.2-4
$D_{\text{H}_2/\text{Fe}}$	$0.26 \times 10^{-8}$	20	[45], Table A.8
$D_{\text{H}_2/\text{N}_2}$	0.68	0	[45], Table A.8
$D_{\text{H}_2/\text{H}_2\text{O}}$	$0.63 \times 10^{-4}$	25	[45], Table A.8

## Reaction Parameters

In order to compare the rates of diffusion and reaction, it is necessary to know the reaction rate of oxygen in contact with the copper particles embedded within the tube scale. It is assumed that the reaction is first order with respect to oxygen. That is, the reaction rate varies linearly with the oxygen concentration at the copper surface. However, for atmospheric reactions, there is some evidence in the literature that the reaction rate varies with the 1/4 power of the oxygen concentration [34]. Assuming a linear dependence over-estimates the effect of varying oxygen concentrations and will, therefore, present a conservative estimate of the degree to which diffusion influences the reaction rate. The form of the reaction rate equation is given by:

$$R_{O_2} = k \frac{MW_O}{MW_{Cu_2O}} \rho_{Cu_2O} \frac{C_{copper\ surface}}{[O_2]_0} = k' \frac{C_{copper\ surface}}{[O_2]_0} \quad [4-3]$$

where the reaction rate  $R_{O_2}$  and the reaction rate constant  $k'$  have units of  $\text{kgO}_2/\text{s}\cdot\text{m}^2$  and the oxygen concentration  $C_{copper\ surface}$  ( $\text{kgO}_2/\text{m}^3$ ) is scaled by the concentration for a standard reference state. (The molecular weights of oxygen and cuprite and the cuprite density are used to convert  $k$  to  $k'$ .) The standard state for atmospheric oxidation is taken as the concentration of oxygen in air, about 0.2 atm. The standard state for aqueous oxidation is taken as the saturation level at room temperature for water exposed to air at one atmosphere, about 7 ppm [43].

In Section 5, several reaction rates are determined from oxidation experiments. Under atmospheric conditions, the oxidation of copper is found to follow a logarithmic rate law. Under aqueous conditions, it is found to follow a linear rate law. For ease of analysis, a linear rate law is used in the diffusion-reaction model derived here. To account for the kinetics under various environmental conditions, four rate constants are used. The rate constants and the conditions under which they apply are given in Table 4-3. For a full explanation of the conditions under which these reaction rates are appropriate, see Section 5.

**Table 4-3**  
**Experimental Reaction Rate Constants for Copper Oxidation**

Reaction Rate, $k$ (nm/day)	Reaction Rate, $k'$ ( $\text{kgO}_2/\text{s}\cdot\text{m}^2$ )	Conditions
24	$1.9 \times 10^{-10}$	early phase (1 <sup>st</sup> hour) atmospheric
2.4	$1.9 \times 10^{-11}$	late phase (20 <sup>th</sup> hour) atmospheric
0.8	$6.2 \times 10^{-12}$	low-pH aqueous
0.08	$6.2 \times 10^{-13}$	high-pH, low-temperature aqueous

## Determination of the Diffusion Characteristic Time Scale

In order to characterize the relative influence of the diffusional resistance on the oxidation rate of copper embedded in steam generator tube scale, it is necessary to model the diffusion through the



scale. Typically, diffusional processes such as this are described by the partial differential equation called the *diffusion equation*:

$$D \frac{\partial^2 C}{\partial z^2} = \frac{\partial C}{\partial t} \quad [4-4]$$

In order to simplify the model to a more tractable form, it is desirable to solve the steady-state version of the equation. However, in order to determine whether the steady-state approach is appropriate, it is first necessary to determine whether the characteristic time scale of diffusion is longer or shorter than the time scale of interest (i.e., the duration of a stage of layup).

The Fourier series solution of Equation 4-4 will involve an exponential function of the ratio of the actual time to some characteristic time scale. This time scale is the ratio of the square of a characteristic length divided by the diffusivity. If the time scales under consideration (lengths of either hours or days, depending on the layup situation) are much longer than the characteristic time scale, then use of the approximation of steady state is appropriate to investigate the relative influence of diffusion.

The characteristic length appropriate to this evaluation is the total thickness of the tube scale. This choice leads to a characteristic time scale of:

$$\tau_{diffusion} = \frac{(\delta_{inner\ layer} + \delta_{outer\ layer})^2}{D_{O/H_2O}} = \frac{(25\ \mu\text{m} + 50\ \mu\text{m})^2}{2.5 \times 10^{-5}\ \text{cm}^2/\text{s}} = 2.25\ \text{s} \quad [4-5]$$

The diffusivity of oxygen in water was chosen for this case because it is slower than that in nitrogen, leading to a higher (more conservative) estimate of the characteristic time scale. The time scale of diffusion (on the order of 2 seconds) is much shorter than the time scale of the stages of layup (which can be as short as a few hours but tend to be on the order of days). Therefore, a steady-state approximation is appropriate for evaluating oxidation of copper particles in tube scale.

### ***Derivation of the Steady-State Model***

The purpose of the steady-state model is to evaluate the change in the oxidation rate of embedded copper particles due to the resistance caused by diffusion of oxygen through the scale. In order to make this evaluation, it is necessary to compare the concentration of oxygen present at the copper surface ( $C_{copper\ surface}$ ) with that present at the outer scale surface ( $C_{bulk}$ ). Equation 4-4 can be solved to determine  $C_{copper\ surface}$ . As shown above, Equation 4-4 can be appropriately approximated by the corresponding steady-state equation:

$$D \frac{d^2 C}{dz^2} = 0 \quad [4-6]$$

The diffusivity can be divided out of this equation, leaving the second derivative equal to zero. This is the equation for a line. The differences between the inner layer and the outer layer necessitate the use of two equations to describe the concentration profile:

$$C_{outer\ layer} = b_{outer\ layer} + zm_{outer\ layer} \quad [4-7]$$

$$C_{inner\ layer} = b_{inner\ layer} + zm_{inner\ layer} \quad [4-8]$$

The variables  $m_{outer\ layer}$ ,  $m_{inner\ layer}$ ,  $b_{outer\ layer}$  and  $b_{inner\ layer}$  are the undetermined coefficients from the integration of Equation 4-6. The unknown concentration at the copper surface ( $C_{copper\ surface}$ ) and the concentration at the layer boundary:

$$C_{inner\ layer}(z = z_{middle}) = C_{outer\ layer}(z = z_{middle}) \quad [4-9]$$

can be substituted into Equations 4-7 and 4-8 to yield:

$$C_{outer\ layer} = C_{middle} + (z - z_{middle})m_{outer\ layer} \quad [4-10]$$

$$C_{inner\ layer} = C_{copper\ surface} + zm_{inner\ layer} \quad [4-11]$$

At the boundary between the scale and the bulk environment, the concentration in the scale is equal to that in the bulk. Therefore, Equation 4-10 becomes:

$$C_{bulk} = C_{middle} + \delta_{outer\ layer}m_{outer\ layer} \quad [4-12]$$

Likewise, at the boundary between layers, Equation 4-11 gives the value of the oxygen concentration as:

$$C_{middle} = C_{copper\ surface} + \delta_{inner\ layer}m_{inner\ layer} \quad [4-13]$$

Substituting Equation 4-13 into Equation 4-12 gives:

$$C_{bulk} = C_{copper\ surface} + \delta_{inner\ layer}m_{inner\ layer} + \delta_{outer\ layer}m_{outer\ layer} \quad [4-14]$$

The slopes  $m_{inner\ layer}$  and  $m_{outer\ layer}$  can be determined by noting that in a steady-state situation, the flux across any plane is equivalent to the flux across every other plane. The flux at the copper surface is equal to the reaction rate. The flux at the boundary between the layers is given by the effective diffusivity times the concentration gradient (Fick's Law):

$$k' \frac{C_{copper\ surface}}{[O_2]_0} = D_{inner\ layer}^{eff} \frac{dC_{inner\ layer}}{dz} = D_{outer\ layer}^{eff} \frac{dC_{outer\ layer}}{dz} \quad [4-15]$$

The effective diffusivities describe diffusion through porous media and are defined by:

$$D_{inner\ layer}^{eff} = \frac{\varepsilon_{inner\ layer}}{\tau_{inner\ layer}} D \quad [4-16]$$

$$D_{outer\ layer}^{eff} = \frac{\varepsilon_{outer\ layer}}{\tau_{outer\ layer}} D \quad [4-17]$$

Since the concentration gradients are constant, the derivatives are equal to the slopes. Substituting the slope for the gradient in the inner layer yields:

$$k' \frac{C_{copper\ surface}}{[O_2]_0} = D_{inner\ layer}^{eff} m_{inner\ layer} \quad [4-18]$$

which can be rearranged to give an expression for the slope:

$$m_{inner\ layer} = \frac{k' C_{copper\ surface}}{[O_2]_0 D_{inner\ layer}^{eff}} \quad [4-19]$$

Similarly, an expression for the slope in the outer layer can be derived:

$$m_{outer\ layer} = \frac{k' C_{copper\ surface}}{[O_2]_0 D_{outer\ layer}^{eff}} \quad [4-20]$$

Substituting these expressions for the slopes into Equation 4-14 yields:

$$C_{bulk} = C_{copper\ surface} + \delta_{inner\ layer} \frac{k' C_{copper\ surface}}{[O_2]_0 D_{inner\ layer}^{eff}} + \delta_{outer\ layer} \frac{k' C_{copper\ surface}}{[O_2]_0 D_{outer\ layer}^{eff}} \quad [4-21]$$

Equation 4-21 can be rearranged into the form of the conduction equation:

$$k' \frac{C_{copper\ surface}}{[O_2]_0} = (C_{bulk} - C_{copper\ surface}) \left( \frac{\delta_{inner\ layer}}{D_{inner\ layer}^{eff}} + \frac{\delta_{outer\ layer}}{D_{outer\ layer}^{eff}} \right) \quad [4-22]$$

where the flux (left hand side of Equation 4-22) is equated to a driving force (the difference in concentrations) divided by an overall resistance. The overall resistance is given by the formula for resistances in series: the overall resistance is the sum of the individual resistances.

For evaluating the effect of diffusion on the concentration of oxygen at the copper surface, it is more useful to rearrange Equation 4-21 to yield an expression for the ratio of the concentration at the copper surface to the concentration in the bulk:

$$\frac{C_{copper\ surface}}{C_{bulk}} = \frac{1}{1 + \frac{k'\delta_{inner\ layer}}{[O_2]_0 D_{inner\ layer}^{eff}} + \frac{k'\delta_{outer\ layer}}{[O_2]_0 D_{outer\ layer}^{eff}}} \quad [4-23]$$

Finally, the expressions for the effective diffusivities (Equations 4-16 and 4-17) can be substituted into Equation 4-23 to yield:

$$\frac{C_{copper\ surface}}{C_{bulk}} = \frac{\frac{[O_2]_0}{k'}}{\frac{[O_2]_0}{k'} + \frac{\delta_{inner\ layer} \tau_{inner\ layer}}{\epsilon_{inner\ layer} D} + \frac{\delta_{outer\ layer} \tau_{outer\ layer}}{\epsilon_{outer\ layer} D}} \quad [4-24]$$

Evaluation of Equation 4-24 will indicate whether copper particles embedded in steam generator tube scale will be protected from oxidation by the resistance to diffusion through the scale. Note that Equation 4-24 was rearranged to emphasize that the concentration ratio depends on the ratio of the kinetic resistance to the total transport resistance, which is the sum of the kinetic resistance and the diffusional resistances for each layer. One minus the concentration ratio represents the fraction of the total transport resistance that is due to the diffusional resistances, so a concentration ratio near unity indicates that the total diffusional resistance is negligible.

### **Evaluation of the Model and Parameter Effects**

The model developed above allows the comparison of the oxygen concentration at the copper particle surface with that in the bulk fluid through Equation 4-24. When this ratio is close to unity, diffusion does not retard the oxidation process. When the ratio falls significantly below unity, diffusion through the surrounding scale is predicted to provide some protection.

Using the scale parameters listed in Table 4-1, Equation 4-24 was used to calculate the concentration ratios for the four sets of representative conditions, two for atmospheric oxidation and two for aqueous oxidation. The results are given in Table 4-4 for the base case and conservative sets of scale parameters.

**Table 4-4**  
**Model Results for Base and Conservative Cases**

Conditions	Reaction Rate $k'$ (kgO <sub>2</sub> /s-m <sup>2</sup> )	Molecular Diffusivity $D$ (m <sup>2</sup> /s)	Reference Oxygen Conc. $[O_2]_0$ (kgO <sub>2</sub> /m <sup>3</sup> )	$1 - (C_{\text{copper surface}}/C_{\text{bulk}})$	
				Base Case	Conserv. Case
early phase (1 <sup>st</sup> hour) atmospheric	$1.9 \times 10^{-10}$	$2.1 \times 10^{-5}$	0.27	$2 \times 10^{-8}$	$2 \times 10^{-6}$
late phase (20 <sup>th</sup> hour) atmospheric	$1.9 \times 10^{-11}$	$2.1 \times 10^{-5}$	0.27	$2 \times 10^{-9}$	$2 \times 10^{-7}$
low-pH aqueous	$6.2 \times 10^{-12}$	$2.5 \times 10^{-9}$	0.007	$2 \times 10^{-4}$	0.018
high-pH, low-temperature aqueous	$6.2 \times 10^{-13}$	$2.5 \times 10^{-9}$	0.007	$2 \times 10^{-5}$	$2 \times 10^{-3}$

In all the cases studied, the ratio of the concentration of oxygen at the surface of the copper particle to that in the bulk fluid was greater than 0.982. That is, the fraction of the total resistance to oxidation that is due to diffusion is conservatively less than 1.8%. The steady-state reaction/diffusion model predicts that copper particles embedded in steam generator deposits will not receive significant protection due to the necessity for oxygen to diffuse through the deposit before reacting with the copper. Moreover, the closeness of the concentration ratio to unity means that this conclusion is not too sensitive to the assumption of steady state. However, the conclusion does depend on the existence of a small level of porosity (e.g., 1%) in the consolidated inner scale layer, which is believed to be the case for the vast majority of plants.

## Effectiveness Factor

Methods for comparing reaction rates and diffusion rates have been well developed by engineers interested in modeling reactions in catalyst pellets [44]. The standard measure of the effect of diffusion on the overall reaction rate is the effectiveness factor  $\eta$ :

$$\eta = \frac{r_d}{r_s} \quad [4-25]$$

where  $r_d$  is the reaction rate with the diffusional resistance and  $r_s$  is the reaction rate that would occur on a bare surface. The effectiveness factor  $\eta$  is a function of the Thiele modulus  $\phi$ . When the geometry under consideration is a flat surface (thin disk), that function is [44]:

$$\eta = \frac{\tanh(\phi)}{\phi} \quad [4-26]$$

The functional form of Equation 4-26 is shown in Figure 4-3. Note how the effectiveness factor is unity for small values of the Thiele modulus, which is a non-dimensional parameter that quantifies the relative importance of the fundamental reaction rate versus the diffusion rate in determining the rate limiting step of a surface reaction.

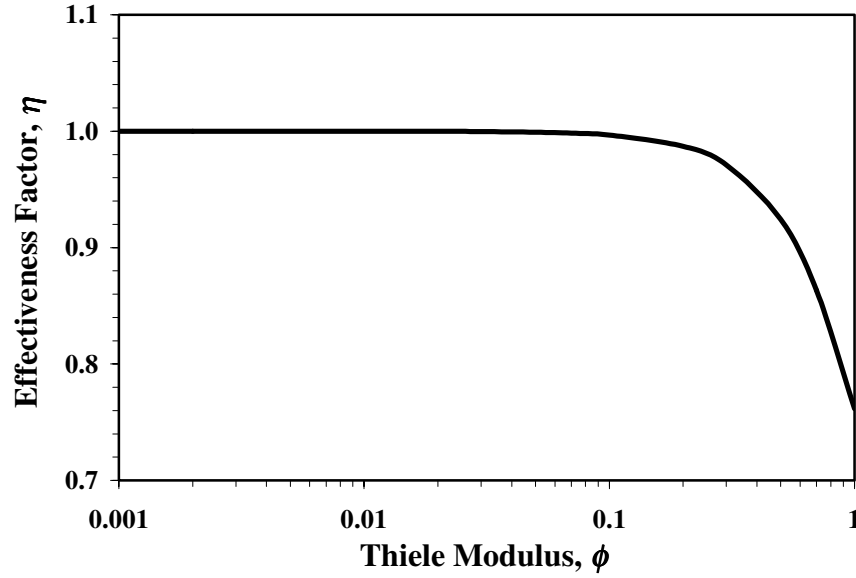


**Figure 4-3**  
**The Effectiveness Factor as a Function of the Thiele Modulus**

The Thiele modulus takes many forms depending on the kinetics of the reaction. For the oxidation of copper in a deposit it can be expressed as [47]:

$$\phi = L \sqrt{\frac{k_{absolute}}{\frac{\varepsilon}{\tau} D}} \quad [4-27]$$

where  $L$  is the diffusion length,  $\varepsilon$  is the void fraction or porosity,  $\tau$  is the tortuosity and  $D$  is the diffusion of the reacting species through the pores of the catalyst.

The absolute reaction rate  $k_{absolute}$  for oxygen can be calculated from the reaction rate  $k$  using the oxygen mass fraction in cuprite, the density of cuprite  $\rho_{Cu_2O}$  and the specific surface area of steam generator deposits  $a$ :

$$k_{absolute} = k \frac{MW_o}{MW_{Cu_2O}} \rho_{Cu_2O} a \quad [4-28]$$

Using Equations 4-26 through 4-28, an effectiveness factor is calculated in Table 4-5 based on inputs that conservatively underestimate the effectiveness factor. This simple calculation supports the conclusion that the diffusional resistance is negligible and does not significantly

slow the oxidation rate. The Thiele modulus is sufficiently small that the oxidation rate is not significantly affected.

**Table 4-5**  
**Effectiveness Factor Calculation**

Parameter	Symbol	Value	Basis
Reaction Rate	$k$	24 nm/day	Conservatively High Value for Cu oxidation (at 30°C in dry air; see Table 4-3)
Oxygen Mass Fraction	$MW_O/MW_{Cu_2O}$	0.112	Periodic Table
Oxide Density	$\rho_{Cu_2O}$	6.0 g/cm <sup>3</sup>	[46]
Scale Specific Surface Area	$a$	1.0 m <sup>2</sup> /g	Typical Value
Reaction Rate	$k_{absolute}$	$1.86 \times 10^{-7} \text{ s}^{-1}$	Equation 4-28
Diffusion Length	$L (\delta)$	250 $\mu\text{m}$	Conservative Value
Diffusivity in Water	$D$	$2.5 \times 10^{-5} \text{ cm}^2/\text{s}$	[43]; Oxygen in Water
Porosity	$\varepsilon$	0.01	Conservative Value
Tortuosity	$\tau$	3	Conservative Based on [58] (for “unconsolidated” layer)
Thiele Modulus	$\phi$	0.037	Equation 4-27
Effectiveness Factor	$\eta$	0.9995	Equation 4-26

The relationship between the effectiveness factor and the Thiele modulus is derived for a catalyst pellet, which assumes a surface reaction on the walls of the pores throughout the scale matrix (uniform volumetric reaction rate). While some reaction could be occurring throughout the scale matrix (conversion of magnetite to hematite, for example), it is likely that the reaction would preferentially occur at the deep locations of the metallic copper inclusions. Since on average the diffusional distance is greater for a layer with the reaction preferentially located deep in the layer, the relationship expressed in Equation 4-26 may somewhat overestimate the overall reaction rate and the actual effectiveness factor. However, this observation is balanced by the rather conservative choice of scale parameters in Table 4-5.

## Comparison of Characteristic Times

A third way to determine the relative importance of the diffusional resistance is to compare the time scales associated with the diffusion process and the reaction process. If one of these processes happens on a very short time scale compared to the other, then it can be neglected. That is, if the time scale of diffusion is short compared to the time scale of the reaction, then

diffusion will not be a limiting factor in determining the overall oxidation rate. This method requires the derivation of characteristic time scales for diffusion and oxidation.

Models of diffusion processes generally lead to a set of partial differential equations, such as the one-dimensional *diffusion equation* (Equation 4-4). When possible, the solution of these equations proceeds by various permutations of the technique of separation of variables. This technique leads to the determination of eigenvalue solutions that generally contain the parameter group  $\tau_{diffusion}$ , which is usually referred to as the diffusion *time constant*. As the name implies, the diffusion time constant provides an estimate of the time scale at which the diffusion process takes place. As shown previously in Equation 4-5,  $\tau_{diffusion}$  is approximately 2 seconds.

The estimation of the reaction time scale is not as straightforward. One possibility is the grouping  $\tau_{r1}$ :

$$\tau_{r1} = \frac{\delta}{k} = \frac{75 \mu\text{m}}{24 \text{ nm/day}} = 3125 \text{ days} \quad [4-29]$$

However, it is obvious that the length scale  $\delta$  is not physically related to the oxidation process. A more appropriate measure might be the oxide thickness at which the reaction begins to slow  $\xi$ . Roy, Krishnamoorthy and Sircar [32] determined this thickness to be about 1 nm at 30°C. Therefore, a more appropriate measure of the time scale of reaction would be  $\tau_{r2}$ :

$$\tau_{r2} = \frac{\xi}{k} = \frac{1 \text{ nm}}{24 \text{ nm/day}} = 0.04 \text{ day} = 3600 \text{ s} \quad [4-30]$$

This is about the time at which the oxidation reaction in air begins to significantly slow (see Figure 5-20).

The time scale of diffusion (2 s) is much shorter than the time scale of reaction (3600 s), indicating that oxygen can diffuse to the surface of embedded copper particles much faster than it can react to form oxide. Therefore, this simple comparison of characteristic time scales shows that diffusion is not a limiting factor in the oxidation of embedded copper particles.

## Conclusions

Based on the results of a steady-state reaction/diffusion model and two related dimensional analyses, the resistance to oxidation due to the diffusion of oxygen through porous deposits is small. In all the cases examined, the oxidation of copper embedded in scale will proceed at practically the same rate as it would if the copper were exposed directly to the bulk environment. Thus, although there may be some protection due to masking (i.e., the direct blocking of the copper surface by a solid magnetite particle), there is no significant protection due to the diffusional resistance. This implies that the behavior of copper inclusions embedded within tube scales is similar to that of copper particles directly exposed to layup solutions. Note that this conclusion depends on the existence of at least a small level of porosity (e.g., 1%) in any consolidated scale layer, which is believed to be the case for the vast majority of plants.



Note that the possibility of advective transport of oxygen through the scale is conservatively neglected in the analyses of this section. Any circulation of fluid through the scale would tend to decrease the effective resistance to oxidation provided by the tube scale. The possibility of circulation through the scale depends on the particular SLS stage being considered.



# 5

## EXPERIMENTAL TEST PROGRAM

---

### Introduction

In order to evaluate the working hypothesis that copper oxides formed during layup accelerate PWR steam generator tube degradation and to prepare SLS chemistry guideline recommendations based on this hypothesis, additional data, not available in the literature, are needed. Specifically, information on the nature of the copper inclusions in PWR steam generator deposits and the rates of oxidation and reduction of copper and iron species in steam generator deposits are required. In order to obtain these data, an experimental test program was conducted consisting of five investigations:

- Characterization of SG Deposit Copper Inclusions
- Oxidation of Copper and Magnetite under Wet-Layup Conditions
- Oxidation of Copper under Atmospheric Conditions
- Reduction of Copper under Startup Conditions

This section begins with a description of each of the analytical techniques used and then progresses to the presentation of the experimental procedures and results associated with each of the four investigations listed above. These discussions are followed by a listing of the materials used during the course of the five investigations.

### Analytical Techniques

In order to conduct these experiments, the following analytical techniques were used:

- Electron Microprobe Analysis
- Thermogravimetric Analysis
- X-Ray Diffraction (XRD)
- Oxidation-Reduction Potential Measurement
- pH Measurement
- Oxygen and Hydrazine Detection
- BET (Brunauer-Emmett-Teller) Specific Surface Area Analysis

Each of these techniques is described below.

### ***Electron Microprobe Analysis***

When a sample is bombarded with high-energy electrons, some of those electrons impart energy to the sample by exciting the electrons of the sample atoms to a higher energy state. Over a short period of time, these excited electrons will lose the extra energy they gained from bombardment by releasing X-rays. The energy (i.e., the wavelength) of the X-rays is determined by the atomic number of the atom which captured the incident electron and is measured while a small area of the sample is bombarded. This allows the elemental composition of the target area to be measured. For electron microprobe analysis, the electron beam is focused on a very small area (e.g., 5 nm across), allowing the elemental content of small inclusions to be determined.

### ***Thermogravimetric Analysis (TGA)***

Thermogravimetric analysis (TGA) uses a precision torque meter to measure the weight of a sample. The instrument used for these studies was the ATI Cahn TG131. A schematic of the instrument is pictured in Figure 5-1. The balance operates by measuring the current necessary to produce the electromotive force required to maintain the beam in a balanced position. The torque meter provides weight measurements that are nominally accurate to one microgram, and temperature probes in the reaction chamber provide the temperature with  $\pm 1^\circ\text{C}$  accuracy. A feedback control loop allows the control of the temperature in the reaction chamber to  $\pm 1^\circ\text{C}$  of the setpoint. However, at this level of accuracy, thermal fluctuations induce weight changes due to buoyancy forces, and the instrument sensitivity is reduced to about  $\pm 10\text{ }\mu\text{g}$ . Note that the counter weight is roughly the same mass as the powder sample in order to insure that the balance operates in the optimal range.

The glass reaction chamber includes several features. An insulated heating jacket surrounds the glass reaction chamber for the purpose of maintaining the sample at a uniform temperature. Inside the chamber the powder is suspended from the balance in a quartz crucible. From a port at the bottom of the reaction chamber, a single reaction gas or multiple reaction gases can be introduced. The reaction gas flows around the crucible and out through an exit port at the top of the reaction chamber. The gas flow rates used in these experiments are small enough that no significant drag force is exerted on the crucible, i.e., the flow rate of the gas does not affect the weight measurements.

Data acquisition and reduction for TGA require several steps. The balance reading and the temperature of the reaction chamber are exported to a personal computer and recorded every ten seconds. The subsequent data reduction requires several manipulations of the raw data. First, the effect of buoyancy must be eliminated. A high temperature reaction gas is less dense and therefore provides less buoyancy than a low temperature reaction gas. Likewise, a low density gas such as hydrogen provides less buoyancy than air or oxygen. In order to analyze experiments in which either the gas or the reaction chamber temperature change, the raw data must be adjusted for buoyancy. The measured weight of a one gram sample varies about  $2\text{ }\mu\text{g}/^\circ\text{C}$ .

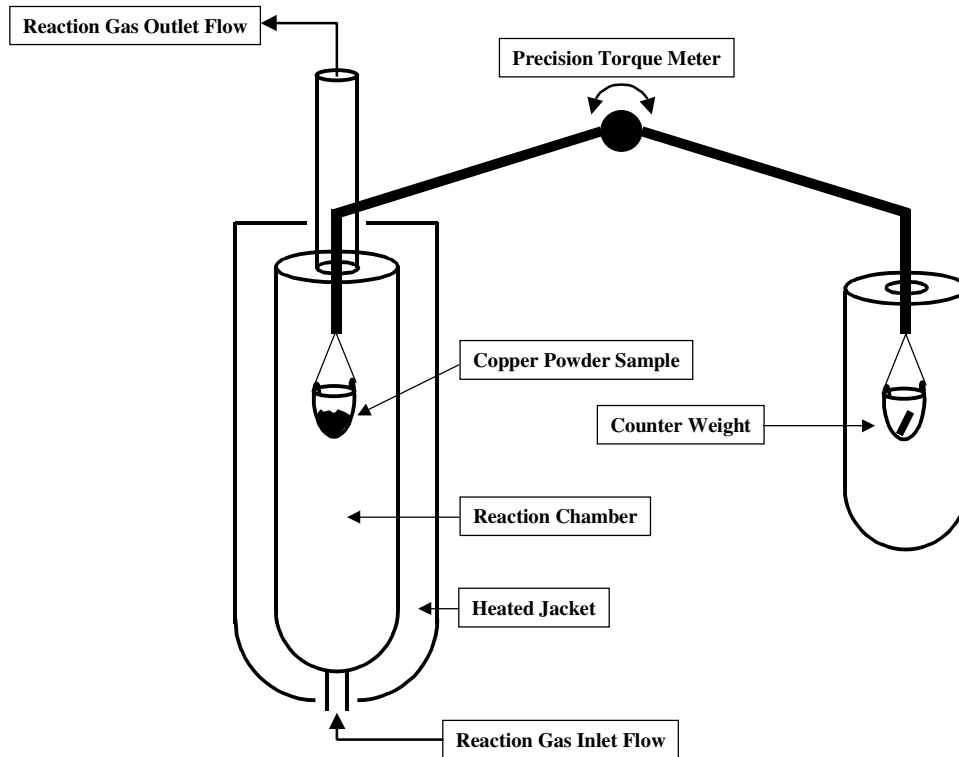


**Figure 5-1**  
**Thermogravimetric Analysis (TGA) Schematic**

Since thermal fluctuations, mechanical vibration and other sources of noise produce apparent weight changes of similar magnitude as those produced by an oxidation reaction, some smoothing of the data is required. Smoothing is only required when the reaction rate has slowed to the point at which the noise fluctuations are comparable to the incremental weight changes in the sample. Therefore, there is no significant loss of information due to the smoothing. For example, when the reaction has slowed to the point at which significant changes occur only on the time scale of an hour or more, the smoothing process averages data over 10 or 15 minutes. Because the data will eventually be used for linear fitting routines, the data are culled so that more data points are used when fast changes are occurring and fewer data points are used when the reaction has slowed.

Finally, the weight changes measured using TGA are converted into oxide film thicknesses. This conversion (which uses a measurement of the surface area made with a BET specific surface area analyzer) allows the data to be interpreted and applied to other cases in which the particle size or shape may be quite different. The conversion of TGA data to film thicknesses was performed using a planar approximation model. The details of this calculation are given in Appendix B.

## **X-Ray Diffraction**

Powder X-ray diffraction (XRD) measures the atomic structure of ordered materials using X-ray energy. The instrument used in this study is a Shimadzu XRD-6000. The X-rays are generated by electron bombardment of a copper target. Electrons strike the copper target, exciting the electrons of the copper atoms to a higher energy level. Subsequently, these electrons return to the unexcited energy level by releasing energy as radiation. In the case of an electron from the K orbital of the copper atom, this radiation is a  $K\alpha$  X-ray. The X-rays are directed toward the powder sample and are diffracted by the electrons surrounding each atom of the sample. Because of their wave-like nature, the X-rays diffracted by the many atoms in the sample interfere with each other. This generates a diffraction pattern that is directly related to the spacing of the atoms in the sample, i.e., the structure of the crystal lattice. Different crystalline structures generate different spectra, and differences between the spectra of two compounds can be used to determine which species is present in the sample. Reference [48] discusses the XRD technique in additional detail.

A prerequisite for using X-ray diffraction as a quantitative analysis tool is the generation of a calibration curve to verify the correspondence between signal strength at a given angle and the concentration of a particular species. In the case of cuprite, the 2-theta peak at  $61.3^\circ$  was chosen as the optimal peak for calibration (based on its relative strength and separability from the peaks produced by copper or the aluminum sample holder). Mixtures containing known amounts of copper metal powder and cuprite ( $\text{Cu}_2\text{O}$ ) were analyzed in the same manner in which oxidized copper powders were to be analyzed. The integrated peak intensity (i.e., the number of scintillation counts contributing to the peak) was thus determined as a function of concentration. As shown in Figure 5-2, this function is roughly linear, leading to a direct relationship between the oxide content of the powder mixture and the integrated peak intensity. Similar curves were also generated for mixtures of copper metal and tenorite ( $\text{CuO}$ ) (Figure 5-3) and magnetite ( $\text{Fe}_3\text{O}_4$ ) and hematite ( $\text{Fe}_2\text{O}_3$ ) (Figure 5-4). These calibration curves allow the determination of the fractional conversion to oxide. Subsequently, the fractional conversion can be used to determine an oxide film thickness. This step required use of the spherical approximation as detailed in Appendix B.

Attenuation of the X-ray energy by the sample must also be considered. The penetration of copper  $K\alpha$  X-rays into copper powder is only diminished by 25% over a length of  $6\text{ }\mu\text{m}$ . Therefore, since both the copper and copper oxide particles used in calibration are smaller than  $6\text{ }\mu\text{m}$ , the X-rays penetrate a layer of several particles. The calibration curve generated using mixtures of particles is therefore applicable to testing the oxide content of a sample of similarly sized or smaller copper particles with oxide coatings. The details of the penetration calculation are provided in Appendix C.

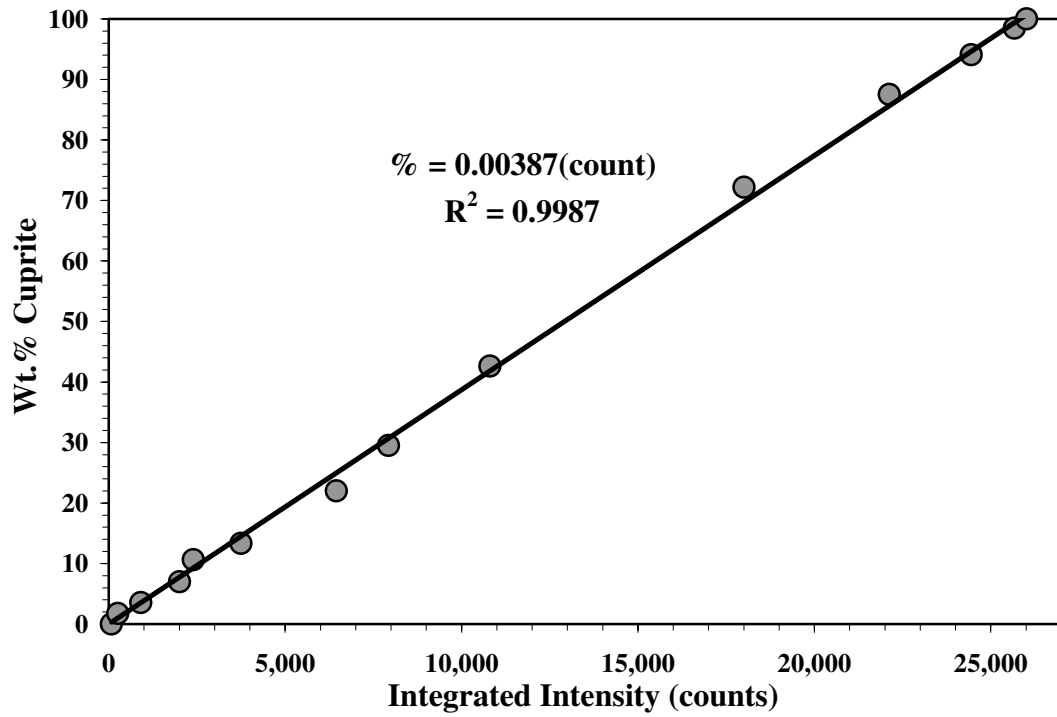


**Figure 5-2**  
XRD Calibration Curve for Mixture of Cuprite ( $\text{Cu}_2\text{O}$ ) and Copper Powders

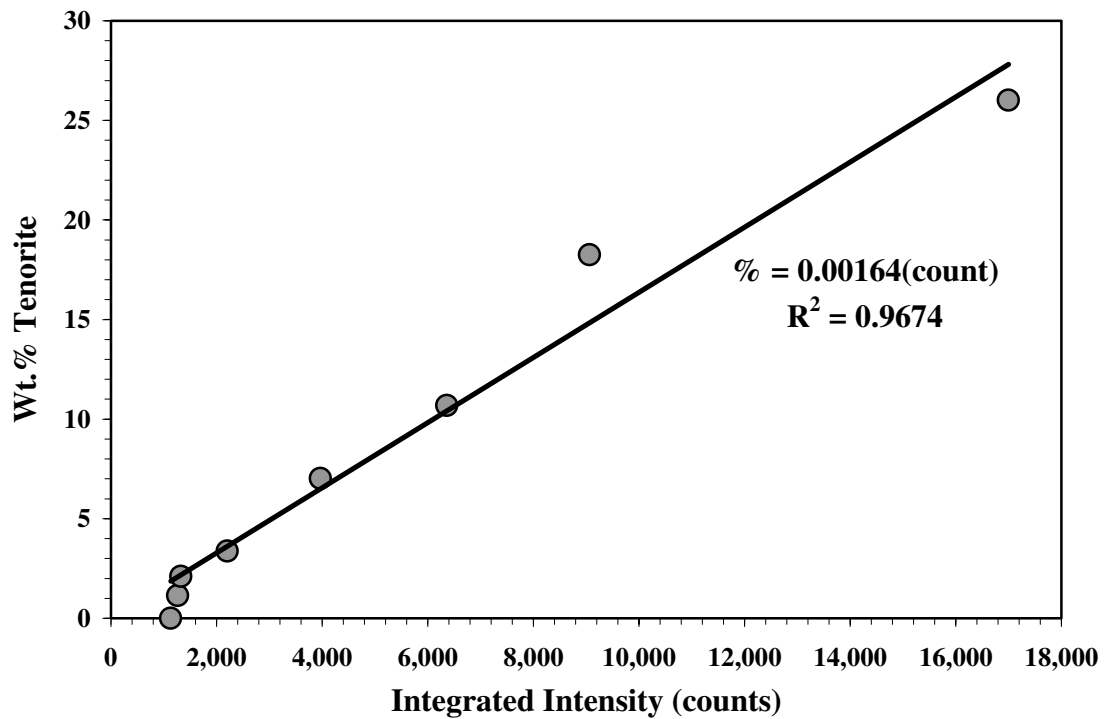


**Figure 5-3**  
XRD Calibration Curve for Mixture of Tenorite ( $\text{CuO}$ ) and Copper Powders

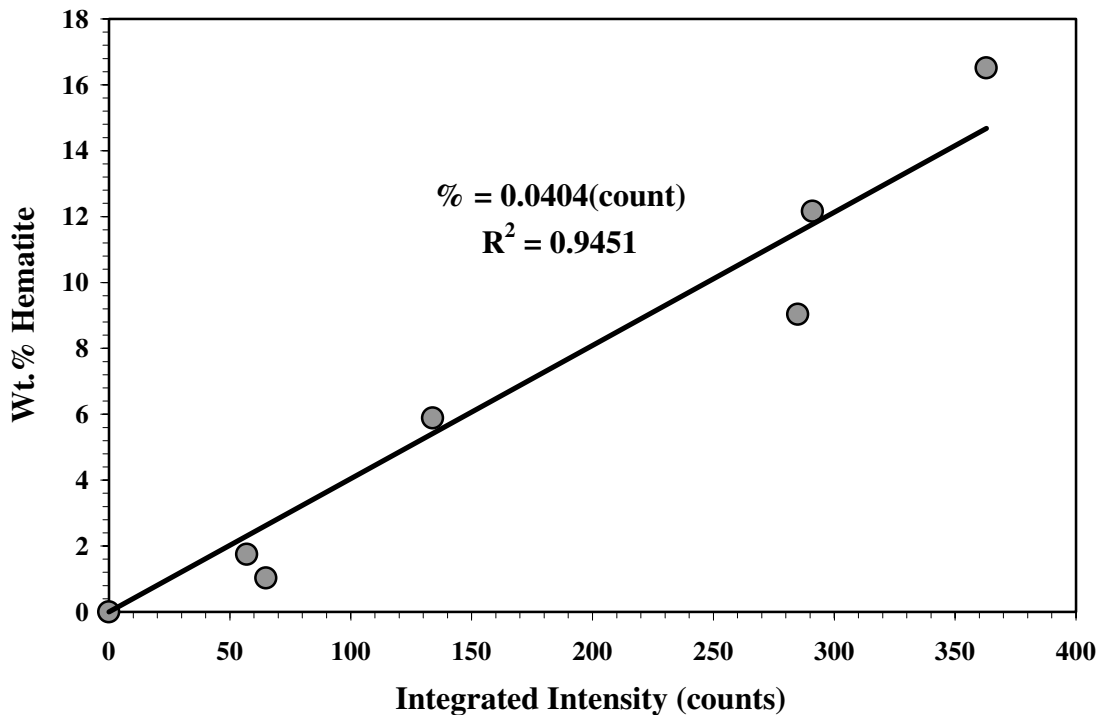


**Figure 5-4**  
XRD Calibration Curve for Mixture of Hematite ( $\text{Fe}_2\text{O}_3$ ) and Magnetite ( $\text{Fe}_3\text{O}_4$ ) Powders

### ***Oxidation-Reduction Potential (ORP) Measurement***

#### **The Theoretical Electrochemical Potential (ECP)**

Electrons in metals are only loosely associated with any given atom of metal. Consequently, there is some dissociation between metal cations and their corresponding electrons. This dissociation is self-limiting due to the energy required to maintain the separation of charges. However, when an energy source is available, the dissociation can become significant.

In an aqueous environment, additional energy to maintain the dissociation of metal cations from their electrons is provided by the interaction of the cations with the solution. The bonding energy between the solution and the cations provides the energy needed to maintain the dissociation of charges. For any given metal and a specified aqueous environment an equilibrium will develop in which the chemical energy released by the association of the metal cations with the solution balances the energy consumed in maintaining the separation of charges between the cations and their electrons. The stable separation of charges leads to a measurable electric potential on the remaining metal. Figure 5-5 shows schematically the electrochemical configuration of such a system.

When the system is in chemical equilibrium, the electric potential on the remaining metal is called the electrochemical potential (ECP). The ECP is related to the free energy of the association of the cations with the solution through Faraday's Law (which merely provides a



conversion constant for expressing chemical potentials as electric potentials). With the free energies of the dissolution reaction (which correspond to the half-cell potentials) one can predict the electrochemical potential of a given metal as a function of pH and other variables such as temperature, charge and the presence of other species. This is the basis for potential-pH or Pourbaix diagrams.

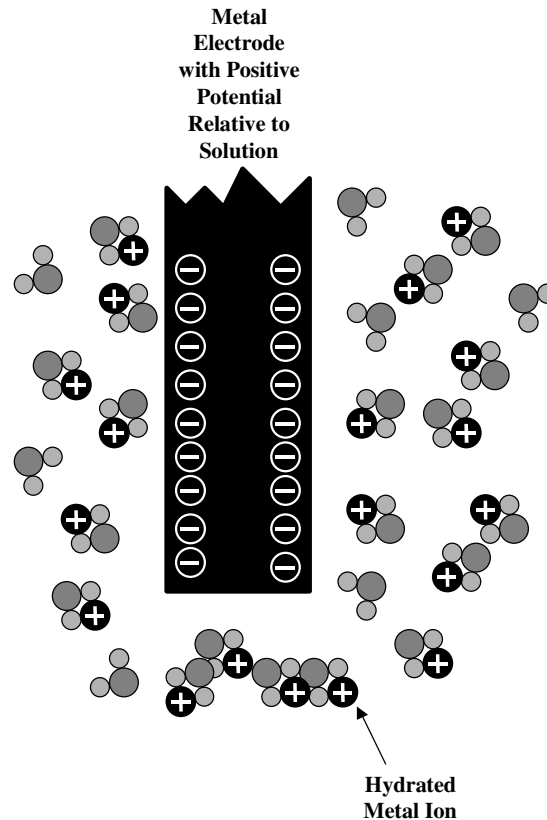


**Figure 5-5**  
**Schematic of Oxidation-Reduction Potential (ORP) Configuration**

### Oxide Surface Layers and the ORP

However, in actual systems, thermodynamic equilibrium is almost never achieved. The presence of oxygen leads to the formation of protective oxides. These oxides create a diffusion barrier to further reaction with the solution. The reaction with the solution continues toward equilibrium, but at a much slower pace. Thus the process becomes kinetically controlled, and thermodynamic parameters based on equilibrium conditions cannot properly be applied.

The oxidative processes that interfere with the approach to equilibrium are relatively slow. This makes it possible to measure a transient electrical potential on the remaining metal. Although kinetic factors make this potential different from the thermodynamic ECP, it is still a useful measurement of the affinity of the solution for metal cations. To emphasize that this measurement is not the ECP, it is often referred to as a corrosion potential or, more commonly, an oxidation-reduction potential (ORP).

## **ORP Measurement Technique**

In these experiments, the ORP was measured at room temperature using a platinum electrode with a silver/silver chloride internal reference. The potential measured is that between the reference and the platinum. The electrons left behind when platinum cations dissolve into the solution generate the potential on the platinum electrode (see Figure 5-5). Thus, ORP is used here as a measure of the tendency of platinum to dissolve in the experimental solution. Since the electrode used was not one for which corrosion rates are of specific interest (e.g., Alloy 600 or carbon steel), there is no direct quantitative way to compare the ORP measured in these experiments with those determined by various authors to be detrimental to steam generators. However, general trends in the ORP will be qualitatively the same from metal to metal, and general conclusions can be drawn. For example, a higher measured ORP is expected to reflect an increase in corrosion rates. Thus, it might be observed that higher hydrazine levels lower the ORP and are thus beneficial. However, the ORP measurements of this report cannot be used to determine an optimal hydrazine level that balances the specific decrease in corrosion against the potential handling costs associated with use of high concentrations of hydrazine.

Note that the ORP values measured in reference to the silver/silver chloride reference electrode can be converted to values in reference to a standard hydrogen electrode (SHE) by adding 200 mV. To convert to values in reference to a standard calomel electrode (SCE), subtract 45 mV. As per the manufacturer instructions, the ORP meter was calibrated using pH buffer solutions saturated in quinhydrone.

## ***pH Measurement***

The pH measurements made during this investigation used an off-the-shelf pH meter and a silver/silver chloride pH electrode. Prior to measurement, the meter was calibrated using three buffer solutions at pH's of 4.0, 7.0 and 10.0. All pH measurements (both for experimental purposes and for calibration) were made at room temperature.

## ***Oxygen and Hydrazine Detection***

The concentration of dissolved oxygen was determined using a colorimetric technique using commercially available glass ampoules. This technique is described in ASTM Method D-5543-94, "Standard Test Methods for Low-Level Dissolved Oxygen in Water" [49]. Oxygen concentrations of up to 1 ppm were distinguishable using this method. Hydrazine levels were also detected using colorimetric ampoules. The technique allows measurements of hydrazine levels between 1 and 500 ppm. Both of these colorimetric techniques are off-line methods that require a liquid sample at room temperature and atmospheric pressure.

## ***BET Specific Surface Area Analysis***

For the purposes of determining the thickness of oxide films and the applicability of using XRD to measure them, the value of the specific surface area of the various powders used in these experiments was necessary. A Micromeritics Flowsorb II specific surface area analyzer was used to make the required measurements. The Flowsorb II measures the conductivity of a flowing

mixture of nitrogen and helium in order to determine the relative quantity of nitrogen. The powder sample is placed in the gas flow path and cooled with liquid nitrogen. When the sample is at the temperature of liquid nitrogen, nitrogen from the flowing gas precipitates onto the powder according to the Brunauer-Emmett-Teller (BET) multilayer adsorption isotherm theory. When the sample is allowed to return to room temperature, the adsorbed nitrogen is released causing a change in the concentration of nitrogen in the gas stream, which is detected and integrated to yield a measurement of the amount of nitrogen adsorbed. The amount of nitrogen adsorbed is directly related to the surface area of the sample. The specific surface area is determined by dividing the measured total surface area of the sample by its mass. Table 5-1 gives the specific surface areas of the materials used in this study. Note that because the BET theory represents an approximation, there is some uncertainty in the oxide thickness calculation due to the use of this method.

**Table 5-1**  
**Specific Surface Areas of Experimental Materials**

<b>Powder</b>	<b>Specific Surface Area (m<sup>2</sup>/g)</b>	<b>Density (g/cm<sup>3</sup>)</b>	<b>Area Averaged Radius (nm)</b>
metallic copper	1.09	8.9	310
cuprite (Cu <sub>2</sub> O)	0.67	6.0	750
tenorite (CuO)	0.36	6.3	1300
magnetite (Fe <sub>3</sub> O <sub>4</sub> )	6.16	5.0	97
hematite (Fe <sub>2</sub> O <sub>3</sub> )	5.17	5.2	110
plant steam generator deposit	1.42	5.0	420
oxidized metallic copper (8% cuprite)	1.10	8.7	310

### Characterization of SG Deposit Copper Inclusions

Of particular interest to the application of the results of this study to steam generator deposits is the purity of the copper inclusions in the steam generator deposits. For example, if the copper inclusions are significantly alloyed with zinc, then the oxidation of the inclusions would proceed at a much slower pace and data from the oxidation of pure copper particles would not be applicable. Electron microprobe analysis was conducted for this study on copper inclusions from scale samples from two plants. The copper inclusions examined are shown in Figure 5-6. Plant A scale typically had an overall (i.e., considering the entire deposit, not just the inclusions) zinc content of about 8%, while Plant B scale typically had an overall zinc content of about 2%.

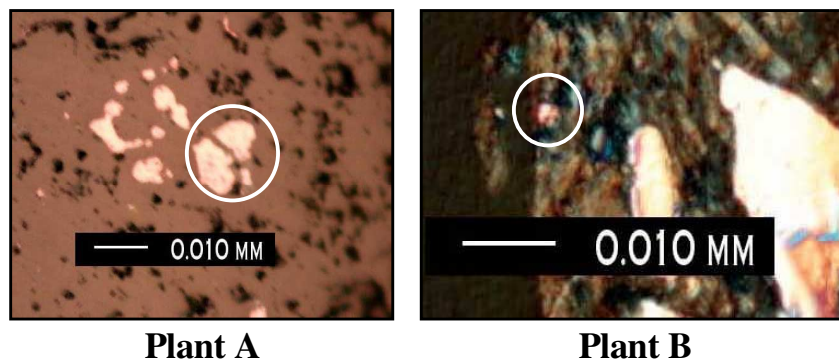


**Figure 5-6**  
**Copper Inclusions Examined by Electron Microprobe**

Microprobe analyses of two copper inclusions from the scale of these two plants indicated that copper accounted for over 90% of the inclusion mass. Zinc was not detected in any of the copper inclusions analyzed, despite the significant amount of zinc present in the total scale. By measurement, iron compounds made up the majority of the remaining mass of the inclusions. However, since the copper inclusions were surrounded by magnetite, it is reasonable to assume that the iron signal came from the surrounding material. Since metallic iron is not generally formed in deposits, it is unlikely that this iron signal was generated by iron alloyed with the copper. Thus, the results from electron microprobe analyses indicated that the inclusions are primarily made of pure copper, with no detectable zinc and perhaps minimal amounts of iron. The complete results of the electron microprobe analyses are given in Table 5-2. It is therefore reasonable to assume that the kinetics of oxidation of the copper inclusions are roughly the same as those of pure copper particles.

**Table 5-2**  
**Elemental Composition of Copper Inclusions**

Element	Element Weight Percent		
	Plant A Inclusion #1	Plant A Inclusion #2	Plant B Inclusion #1
Mg	0.03	0.01	0.03
Al	0.10	0.41	0.10
Si	0.00	0.00	0.03
Cr	0.01	0.00	0.52
Mn	0.04	0.05	1.58
Fe	5.81	7.22	6.36
Ni	0.02	0.01	1.41
Cu	94.0	92.3	89.97
Zn	0.00	0.00	0.00
Pb	0.00	0.00	0.00

## Aqueous Oxidation Experiments

The working hypothesis that copper accelerates PWR steam generator tube degradation is based on the assumption that copper in SG deposits will oxidize. In order to evaluate the hypothesis and formulate layup guidelines, the extent of oxidation possible during layup must be determined. Toward this end, a series of aqueous oxidation experiments were conducted.

### ***Aqueous Oxidation Experimental Technique***

Experimental procedures were developed for controlling and measuring the aqueous environment for the oxidation of powder samples. As illustrated in Figure 5-7, glass test tubes sealed with rubber stoppers were used as reaction chambers. To each test tube was added a small beaker with 0.30 g of reaction powder (either copper powder, magnetite powder or steam generator deposits) and 30 ml of reaction solution. The test tubes were then sealed and immersed in a constant temperature water bath (30°C or 60°C). At each time point, a test tube was opened and an analysis performed (pH, ORP, oxide content, etc.). Each test tube provided data at only one time point; a new test tube was used for each measurement. Efficient use of the water baths required that different test tubes be started at different times. Although this may have introduced some noise into the data, the procedure has the important benefit of assuring that each test tube is exposed to the same conditions (i.e., sealed at constant temperature) throughout the entire length of the test.

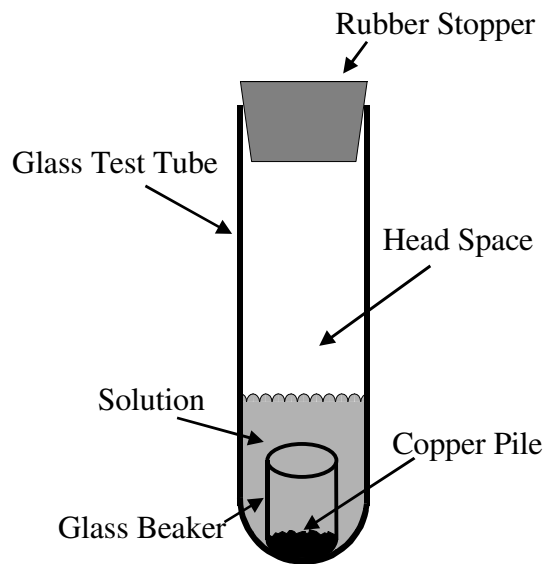


**Figure 5-7**  
**Aqueous Oxidation Experimental Setup**

Four different solutions were used to provide reaction conditions that mimicked layup conditions in a steam generator. De-ionized water was used in all cases. The first solution was adjusted to a pH of 7.0 with dilute  $\text{NH}_4\text{OH}$ , while the second solution was adjusted to a pH of 10.0 with dilute  $\text{NH}_4\text{OH}$ . The third and fourth solutions were made by the addition of hydrazine to a concentration of 400 ppm ( $\text{N}_2\text{H}_4$  weight basis). No other adjustments were made to the first three

solutions. The fourth solution was adjusted to a pH of 10.0 with dilute  $\text{NH}_4\text{OH}$ . Table 5-3 lists the relevant features of the four solutions.

**Table 5-3**  
**Aqueous Solutions Used**

<b>Solution #</b>	<b>Hydrazine (ppm)</b>	<b>pH</b>	<b>ORP (mV)</b>
1	0	7.0	160
2	0	10.0	46
3	400	unadjusted	-229
4	400	10.0	-243

For collection of data, the test tube was removed from the water bath and allowed to cool to room temperature. The pH and ORP of the solution were measured and recorded. The beaker containing the reaction sample was removed and the solution in the beaker decanted back into the test tube. For solutions that had originally contained hydrazine, a hydrazine test was performed on the solution in the test tube. The moist powder was removed from the beaker and partially dried on a clean glass plate. The powder-paste was then examined using XRD to determine the oxide content.

### ***Experimental Results for Oxidation of Copper under Wet-Layup Conditions***

The results of the aqueous oxidation tests provided three types of data:

- Hydrazine Decomposition
- pH and ORP Data
- Degree of Oxidation

Hydrazine is found to decompose rather quickly in the presence of copper. After about a week, it falls below the detection limit of 1 ppm. The ORP was found to be a function only of the pH. The extent of oxidation varied depending on the conditions. It was slowest at high pH (10) and low temperature (30°C). The details of each of these types of data are summarized below.

#### **Hydrazine Decomposition**

In the presence of copper, hydrazine was found to decompose rather quickly. The time at which the hydrazine completely decomposed is between the last time at which it was detected and the first time at which it was not detected. These times are given in Table 5-4. At 60°C, the concentration of hydrazine dropped from 400 ppm to less than 1 ppm (the detection limit in these studies) within two days at both the pH values included in the study. At 30°C, decomposition was somewhat slower. At pH=10.0, there was less than 1 ppm of hydrazine remaining after 3 days (first measurement). However, in the solution in which the pH was not adjusted but raised

to about 9 to 9.5 only by the addition of hydrazine, the hydrazine level was at 20 ppm after 3 days. Hydrazine decomposition is known to be catalyzed by copper ions, and this rapid degradation is to be expected considering the high copper surface area in the test tube compared to the total liquid volume.

**Table 5-4**  
**Detection of Hydrazine Decomposition Time, Copper Powder Experiments**  
**(1 ppm detection limit)**

Solution #	Temperature (°C)	Hydrazine Detection (days)	
		Last Time Present	First Time Absent
3	30	3	7
	60	0	2
4	30	0	3
	60	0	2

#### pH and ORP Data

In the absence of hydrazine (whether due to lack of addition or degradation of that which was added), the ORP correlated linearly with the pH as shown in Figure 5-8. This correlation simply demonstrates the tendency of metal to dissolve much more readily at low pH than at high pH. No significant conclusions can be drawn from this trend, except that pH is a strong factor in determining corrosion rates. Hydrazine, when it was present, created a dramatic drop in the ORP (see Figure 5-8), indicating that it may significantly decrease the rate of oxidation. Note that no significant changes in pH or ORP with time were observed in any of the solutions studied.

#### Degree of Oxidation

The powder samples were analyzed for oxide content by XRD as described on page 5-4. Figures 5-9 through 5-12 show the oxide contents measured in the several experiments conducted. Three parameters were varied in this study: hydrazine dosing, temperature and pH. Since a full factorial experimental design was used, the independent examination of each of these parameters was possible. Note that the dissolved oxygen level in these tests was the saturated value at the particular experimental temperature (and atmospheric pressure). Also, the linear curve fits are least squares fits to the measured data points, and the uncertainty bands are based on relative experimental errors calculated from special repeated measurements.

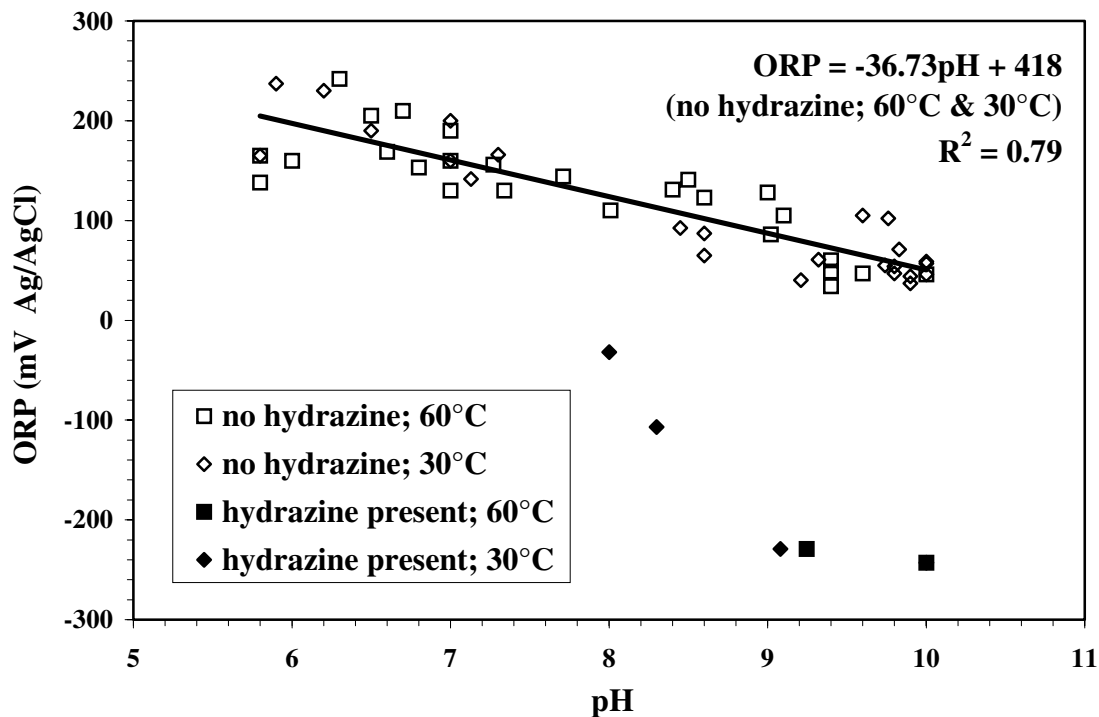


**Figure 5-8**  
**ORP of Aqueous Solutions with Copper Powder as a Function of pH**

#### *Effect of Hydrazine*

Examination of the results showed that dosing with hydrazine affected the oxidation rate only as long as hydrazine was present. In both 60°C experiments and in the high-pH 30°C experiments, all in which hydrazine decomposed rapidly, only small differences between the samples with and without an initial hydrazine content were observed (see Figures 5-10 through 5-12). In the case of the low-pH, 30°C experiments, during the first week, when hydrazine was still present in the test solution, a significant reduction was observed in the degree of oxidation of the copper sample. However, after the hydrazine had decomposed, the copper proceeded to oxidize at the same rate as the copper that had not been exposed to hydrazine (see Figure 5-9). Although the degree of oxidation is lower in the samples that originally were dosed with hydrazine, the rate of oxidation, after a short initial period, is essentially the same as that for those samples that were never exposed to hydrazine. Thus, the initial hydrazine dosing did not lead to the passivation of the copper, but merely reduced the rate of oxidation while it was present. This phenomenon contrasts with the action of hydrazine on iron, which is passivated by a hydrazine catalyzed reaction converting  $\text{Fe(OH)}_2$  to  $\text{Fe}_3\text{O}_4$  [50]. This finding highlights the fact that measures taken to prevent corrosion of steam generator construction materials during layup may not be the same measures required for preventing oxidation of steam generator deposits.



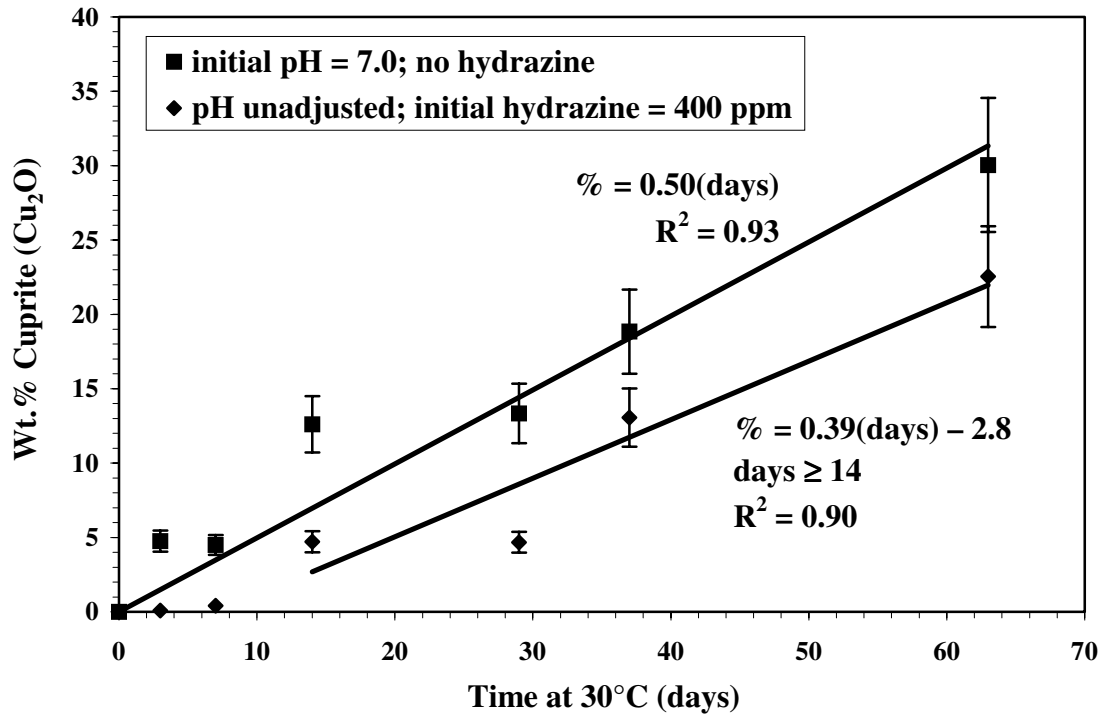


Figure 5-9  
Degree of Copper Oxidation, 30°C, Low pH Solutions

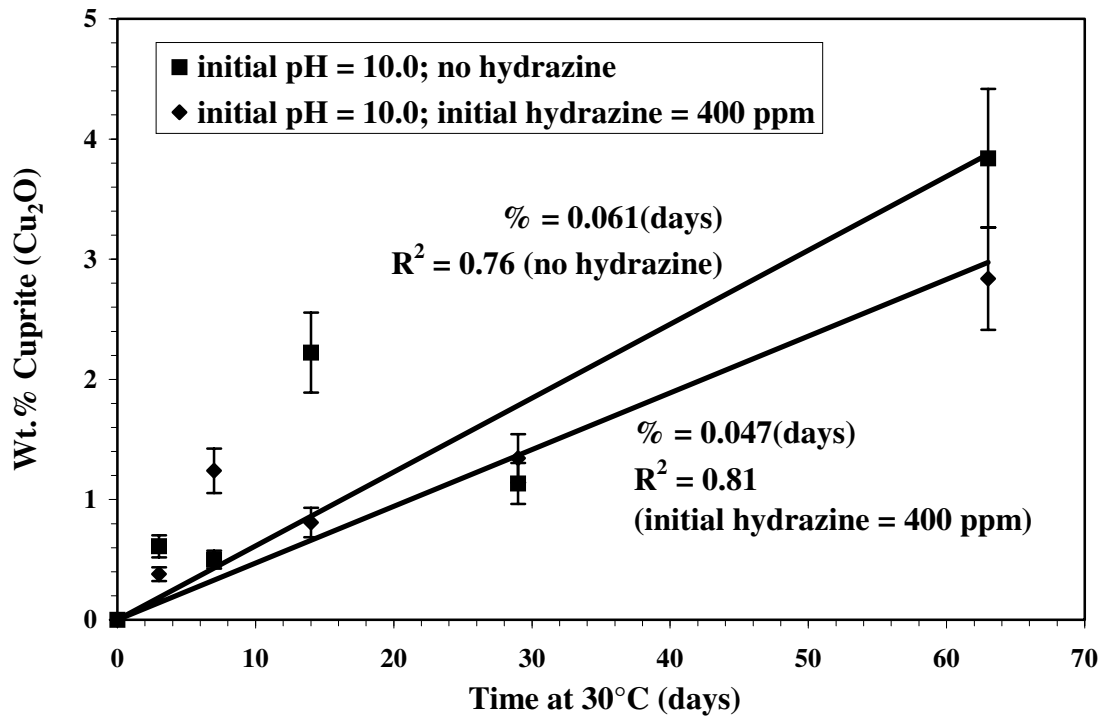
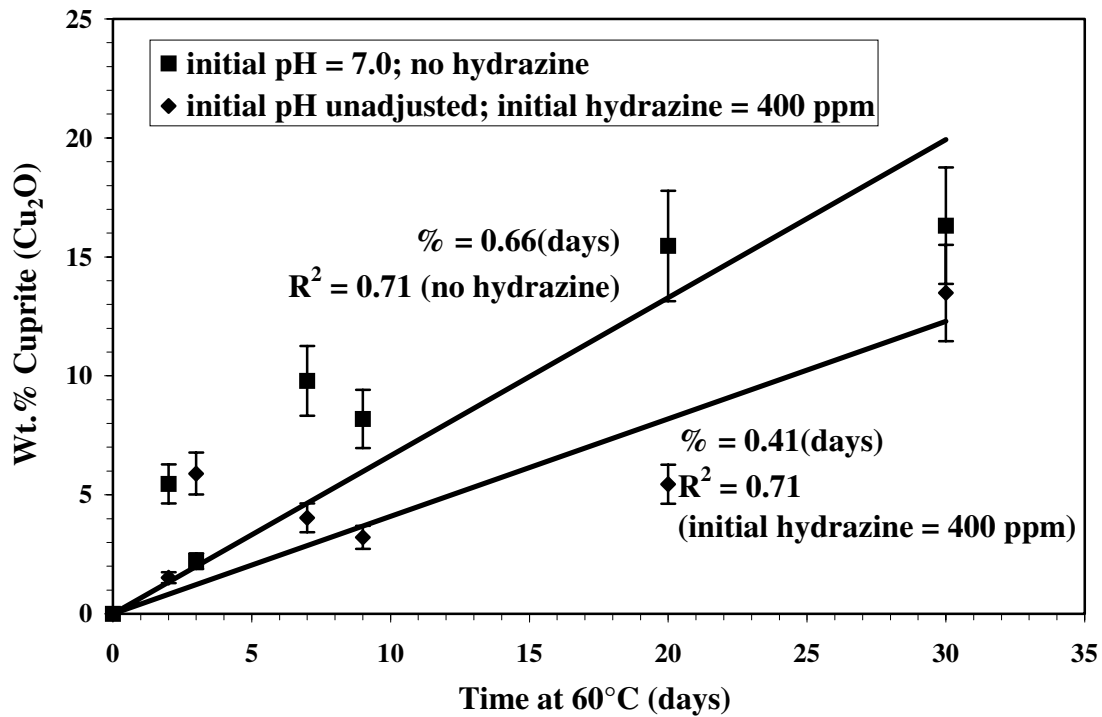
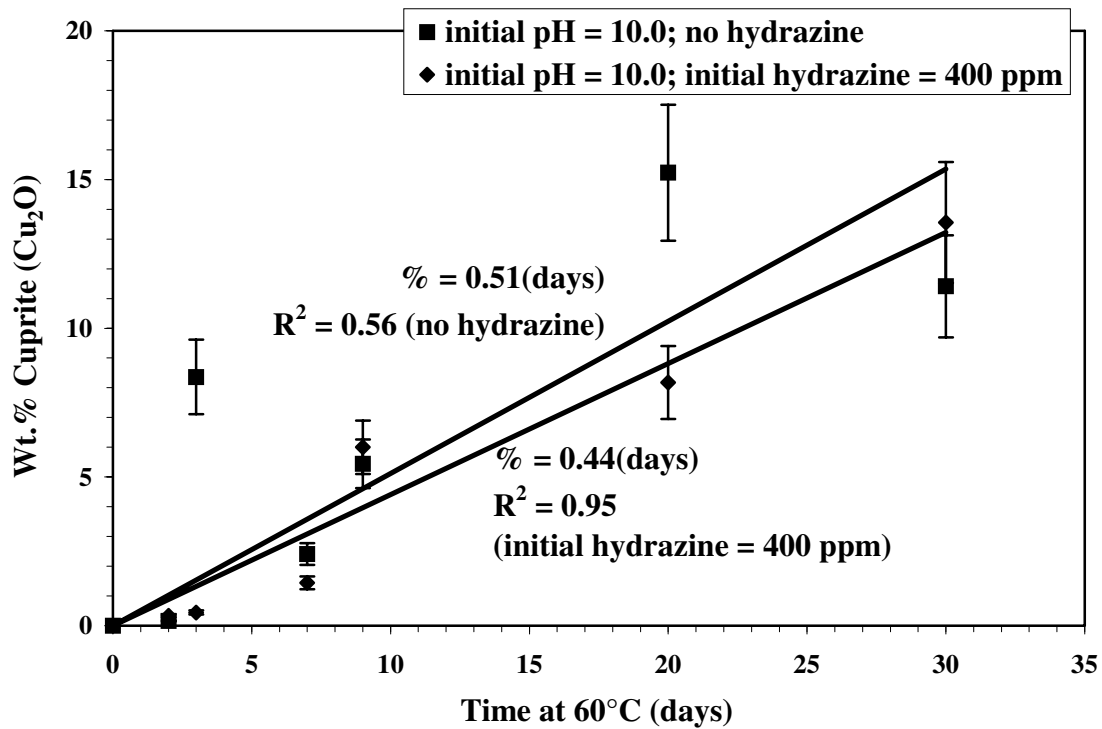


Figure 5-10  
Degree of Copper Oxidation, 30°C, High pH Solutions



**Figure 5-11**  
Degree of Copper Oxidation, 60°C, Low pH Solutions



**Figure 5-12**  
Degree of Copper Oxidation, 60°C, High pH Solutions

### *Effect of Temperature*

The effect of temperature was complicated by its interactions with other parameters. In the low-pH experiments, the temperature had no significant impact on the rate of oxidation other than through its effect on the decomposition rate of hydrazine. Thus, for low-pH experiments at both 30°C and 60°C, about 15% of the copper was oxidized after about 30 days (see Figures 5-9 and 5-11). In the high-pH experiments, there was a dramatic difference due to temperature: an order of magnitude increase in the oxidation rate at 60°C. At 30°C, the copper was about 1.5% converted after 30 days (Figure 5-10), but at 60°C, it was about 15% converted after 30 days (Figure 5-12).

### *Effect of pH*

The effect of pH is manifested through its interaction with the temperature. At 60°C, pH differences did not produce any significant changes in the oxidation rate (Figures 5-11 and 5-12). For both high- and low-pH experiments at this temperature, the oxidation was about 15% after 30 days. However, at 30°C, the pH had a dramatic impact, lowering the 30-day oxidation from about 15% at low pH to about 1.5% at high pH (Figures 5-9 and 5-10).

According to the results, the factors that make a significant reduction in the oxidation rate are (1) the continuing presence of hydrazine, (2) the lowering of temperature at high pH and (3) the elevation of the pH at low temperatures, which can reduce the oxidation rate by an order of magnitude. The general trends in oxidation rate with temperature and pH are summarized in Figure 1-1 (for the case of no existing hydrazine).

## ***Experimental Results for Oxidation of Magnetite under Wet-Layup Conditions***

PWR steam generator deposits are primarily composed of magnetite. The conversion of magnetite ( $\text{Fe}_3\text{O}_4$ ) to hematite ( $\text{Fe}_2\text{O}_3$ ) is a possible source of oxidants. Aqueous oxidation experiments similar to those conducted with copper powders were conducted with synthetic magnetite and actual steam generator deposit powders. As with the copper powder experiments, the results of this investigation fall into three categories:

- Hydrazine Decomposition
- pH and ORP Data
- Degree of Oxidation

The results of these experiments are summarized below. See page 5-36 for details regarding the magnetite and plant deposit materials tested.

### **Hydrazine Decomposition**

Although the steam generator deposit powder was primarily composed of magnetite, there were significant chemistry differences between these experiments. In experiments with steam generator deposits, hydrazine completely decomposed before the first measurement. Table 5-5

gives the times of the last measurement at which hydrazine was present and the first measurement at which it was completely decomposed (< 1 ppm). In experiments with commercial magnetite, hydrazine did not decompose at all at 30°C (still at initial levels after 30 days) and was present for at least a week at 60°C. The hydrazine decomposition results for the steam generator deposits are nearly exactly those obtained with copper powder. These rates are compared in Figure 5-13, which shows the times at which hydrazine decomposition completed. These results call into question the use of synthetic magnetite powders for simulating the layup chemistry of SG deposits. The hydrazine decomposition behavior of the SG deposits is likely due to the presence of copper (11% by weight) and/or minor constituents such as zinc and nickel, or possibly due to the particular surface properties of the deposit particles.

**Table 5-5**  
**Detection of Hydrazine Decomposition Time, Magnetite and SG Deposit Experiments**

Solution #	Powder	Temperature (°C)	Hydrazine Detection (days)	
			Last Time Present	First Time Absent
3 (pH unadjusted)	SG deposit	30	0	4
		60	0	3
	synthetic magnetite	30	28	—
		60	7	11
4 (pH = 10)	SG deposit	30	0	4
		60	0	3
	synthetic magnetite	30	28	—
		60	7	11

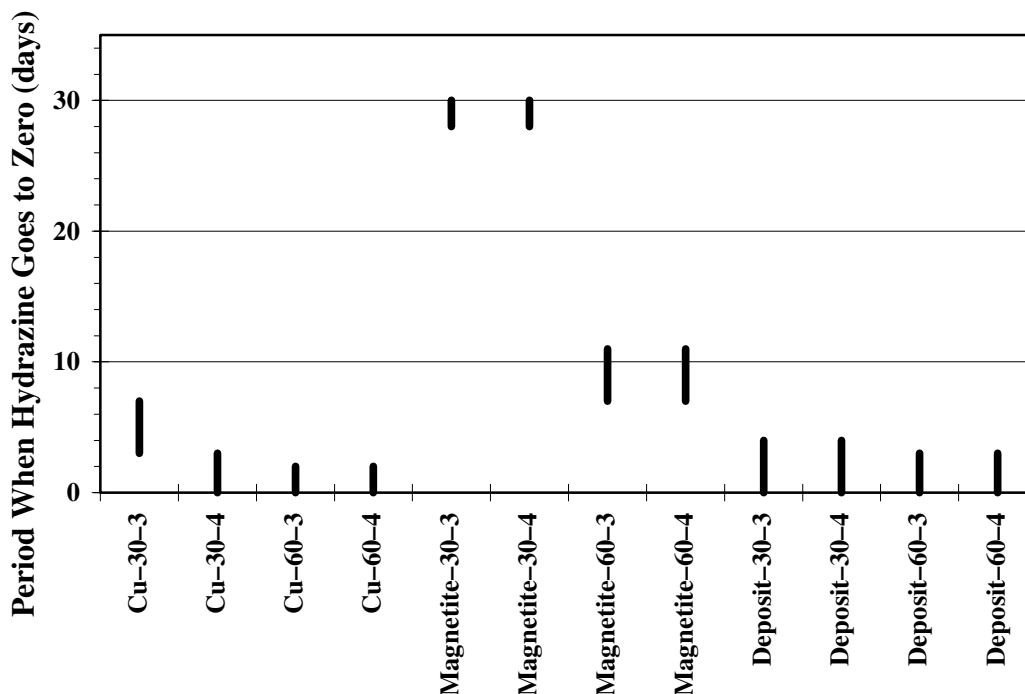


**Figure 5-13**  
**Hydrazine Decomposition (Powder-Temperature (°C)-Solution #)**

### pH and ORP Data

In the absence of hydrazine the ORP correlated linearly with the pH in experiments with magnetite (see Figure 5-14) as well as those with steam generator deposits (see Figure 5-15). However, there was a significant difference between the ORP of a solution with steam generator deposits and one with synthetic magnetite. A student t-test was performed using measurements of the ORP between pH=9 and pH=10 only. The results are shown in Figure 5-16. The SG deposit and synthetic magnetite samples overlap at a 99.8% confidence interval, indicating that there is a 99.8% probability that the ORPs of these two solutions are different. Generally, the confidence interval of 95% is considered statistically significant. Furthermore, the difference in ORP due to the presence of steam generator deposits instead of magnetite is consistent over a pH range from less than six to greater than 10 (see Figure 5-17).

Another student t-test showed that the ORP of a solution ( $9 < \text{pH} < 10$ ) with copper powder overlaps that of one with steam generator deposits at a 37% confidence interval, indicating that there is not a significant difference in influence on ORP between copper powder and steam generator deposits (see Figure 5-16). This equivalence holds over a pH range of less than six to greater than 10 (see Figure 5-17). These results indicate that the electrochemical nature of the steam generator deposit powder is more like that of copper powder than the synthetic magnetite powder that was tested.

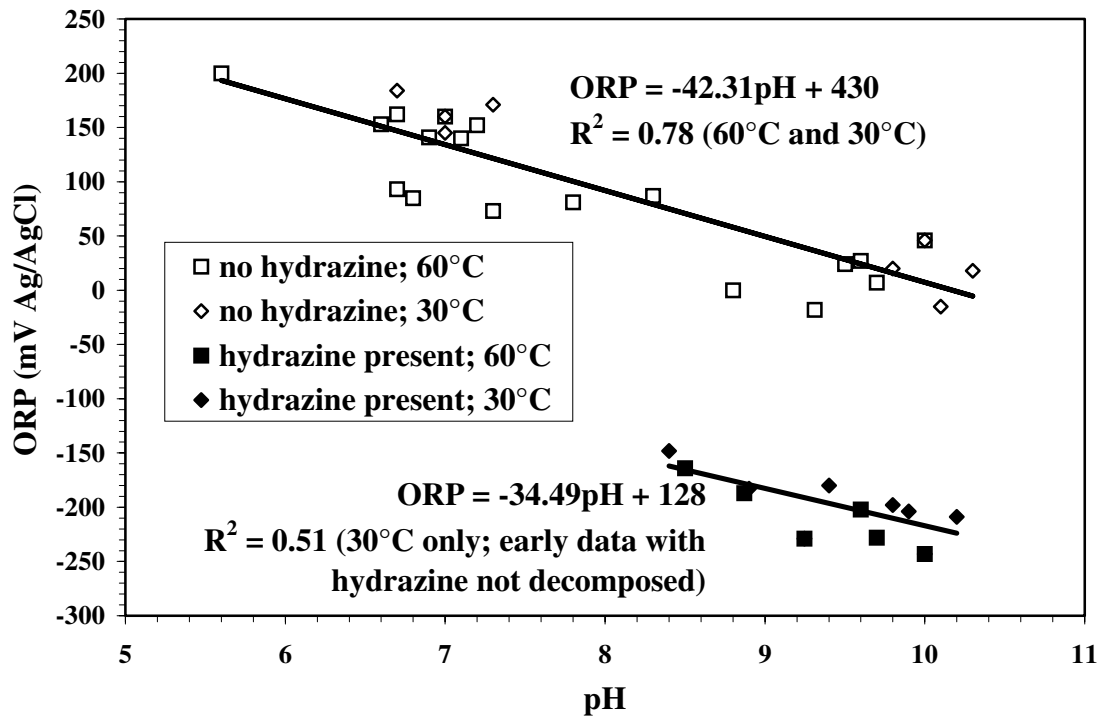


Figure 5-14  
ORP of Aqueous Solutions with Magnetite Powder

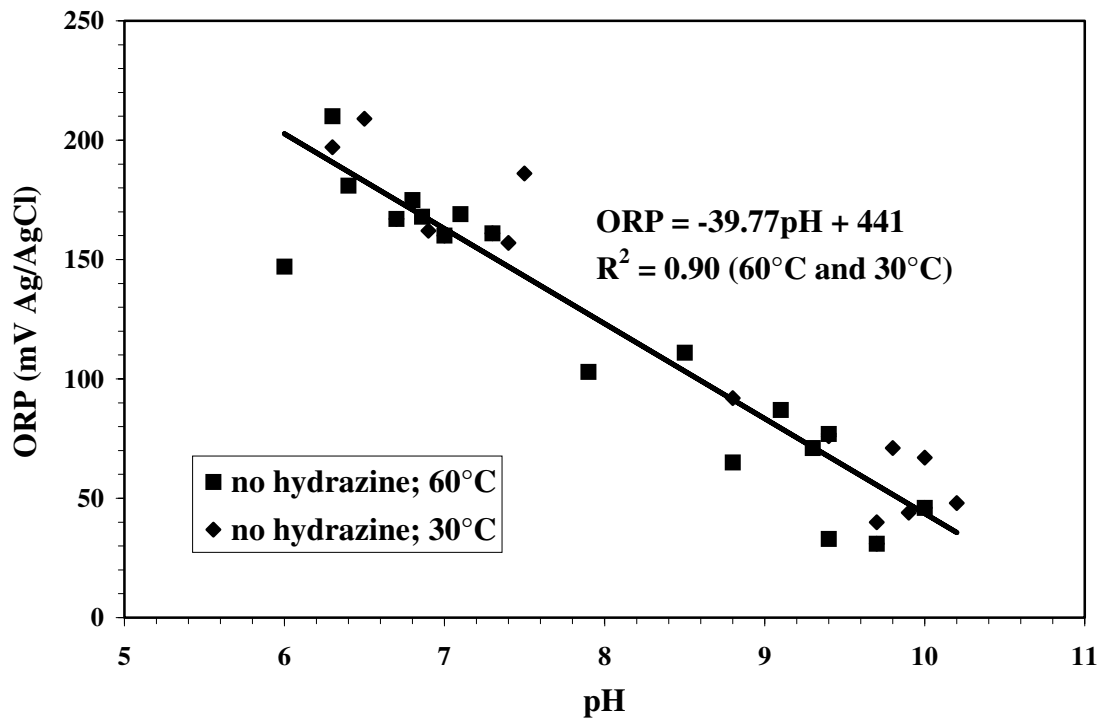


Figure 5-15  
ORP of Aqueous Solutions with Steam Generator (SG) Deposits

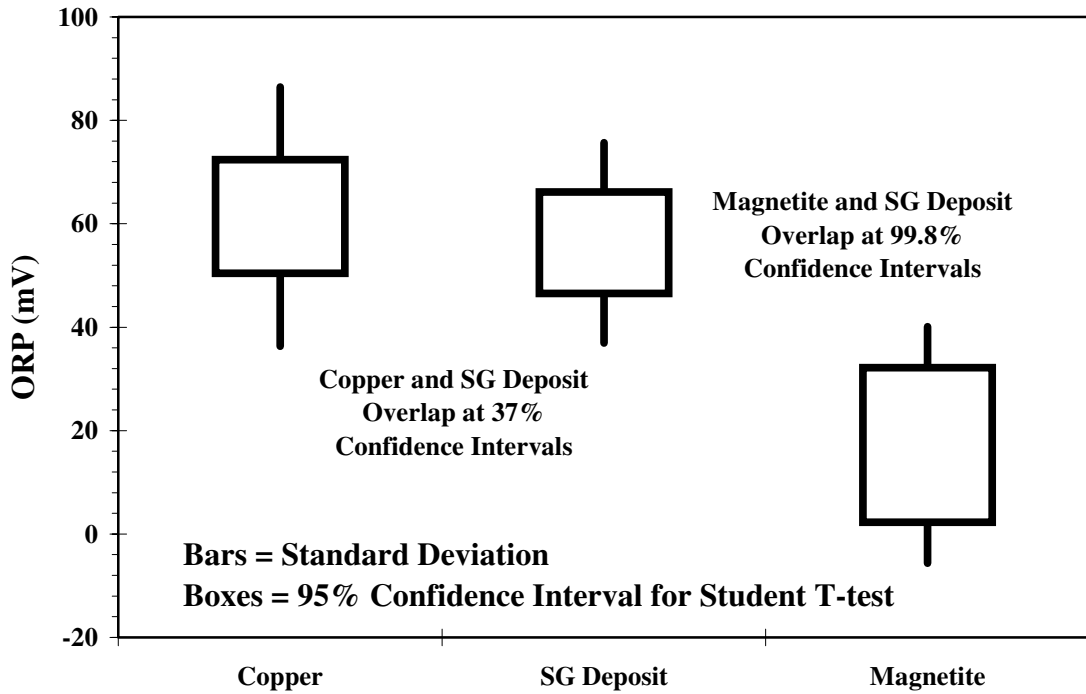


Figure 5-16  
Student T-test for ORP (9<pH<10)

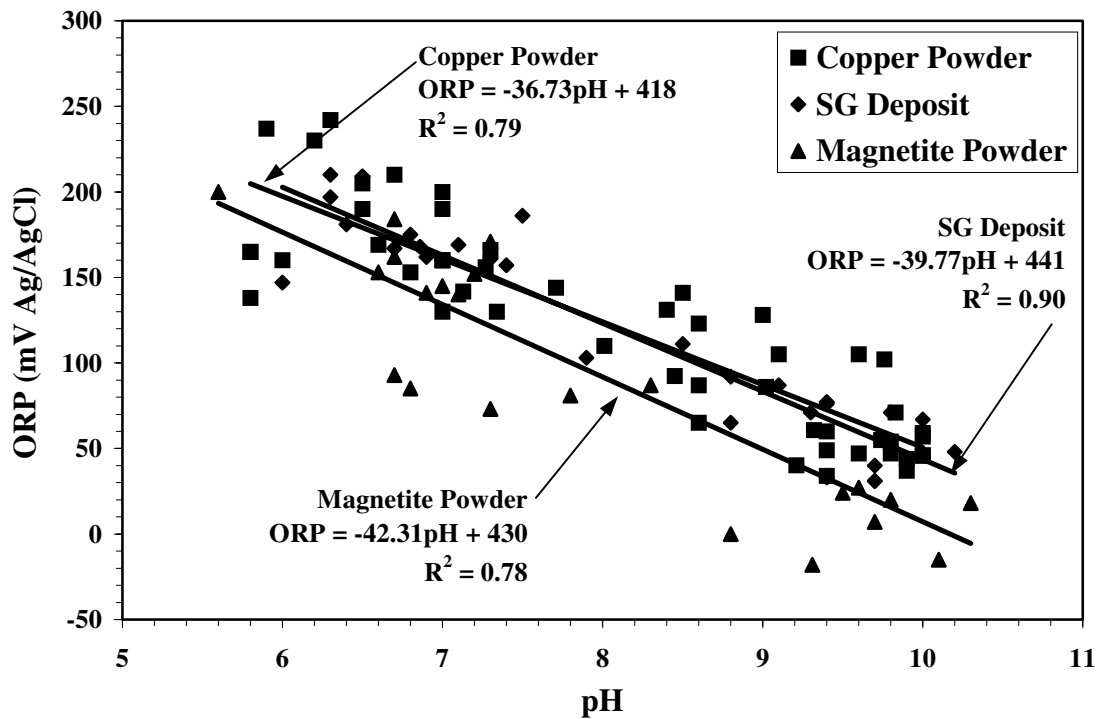


Figure 5-17  
ORP of Various Powder Types (with no hydrazine and at 30°C and 60°C)

In the presence of hydrazine (magnetite experiments only due to rapid degradation of hydrazine during experiments with SG deposit) the ORP was again linearly dependent on the pH. The slope was roughly the same as in the absence of hydrazine but with the ORP about 200 mV lower. This relationship is shown in Figure 5-14. Note that, as was the case for the copper oxidation experiments, no correlation was found between experimental duration and the pH or the ORP of the solution (except that hydrazine decomposition would change the ORP).

## **Degree of Oxidation**

No conversion of synthetic magnetite to hematite was observed over the course of one month of testing. This was true for the full set of experimental conditions including one month of the conditions expected to be most oxidizing: 60°C with pH=7.0 and no hydrazine present. Quantification of hematite in a magnetite powder through XRD was limited to conversions greater than about five percent. However, qualitative detection of the presence of hematite was possible with less than one percent hematite present. Therefore, the conversion of magnetite to hematite over the course of one month was less than 1%. Using the planar approximation (Appendix B), a 1% conversion corresponds to a hematite film thickness of 0.5 nm for the average synthetic magnetite particle radius of 97 nm.

Similarly, no conversion of the magnetite in the steam generator deposit to hematite was detectable. However, the detection of hematite in the steam generator deposit powder was complicated by the presence of several additional elements, leading to a complicated spectrum. Consequently, the detection limit for the deposit powder was closer to the five percent limit of quantitative detection because the small signals which would otherwise indicate lower (i.e., about one percent) levels of hematite were masked by additional signals from the non-iron components of the powder. The detection of copper oxidation in the steam generator deposits was not feasible due to the relatively low levels of copper in the tested deposit.

## **Atmospheric Oxidation Experiments**

During layup, the layup solution is sometimes drained from the steam generators for maintenance or sludge lancing. This may expose the deposits in the steam generator to atmospheric conditions. An investigation was made to determine if copper in steam generator deposits might oxidize when exposed to air. Copper powder was used to assure that the effects of oxidation would be measurable using thermogravimetric analysis (TGA). Using this technique, a logarithmic rate law was found to describe the kinetics of atmospheric oxidation. A description of the TGA experimental technique is given below (also see page 5-2 for a general introduction to TGA) and followed by a summary of the results.

### ***Thermogravimetric Analysis (TGA) Experimental Technique***

The TGA experimental technique consisted of a pretreatment step to control the initial oxide content, a humidity control system for the bottled air reaction gas and measurements at various combinations of temperature and humidity.



## Pretreatment Step

Although high purity copper powder with low oxide content was used for the experiments in this study, the possibility existed that previous oxide formation would affect the results of any experiments performed. Therefore a pretreatment technique was used before all TGA runs to ensure that a consistent starting oxide content was used. Generally, a sample of about one gram was used. Larger and smaller samples were also run to confirm that sample size had little effect on the kinetics of the reaction. After inserting the sample into the TGA reaction chamber and taring the balance, forming gas (90% nitrogen and 10% hydrogen) was used as the reaction gas. The sample was held at 200°C for four hours. Typically, there was a weight loss of about 0.4% during the pretreatment phase. This weight loss was probably due to the combination of moisture loss (due to heating) and oxygen loss (due to reduction of oxides by the hydrogen) with the former accounting for most of the change. After completion of the pretreatment, the sample was allowed to cool to the experimental temperature while forming gas was continuously passed through the reaction chamber.

## Control of Relative Humidity

The reaction gas for the oxidation studies was bottled air at varying degrees of relative humidity. For low humidity experiments the air was passed through an anhydrous calcium sulfate bed to remove any water vapor present. To achieve non-zero values of relative humidity, the air was bubbled through a chilled water bed to create a stream of water saturated air. A schematic of this operation is shown in Figure 5-18. When this stream of air was raised to the reaction temperature, the relative humidity fell to the desired level. The requirements for setting the relative humidity were determined through the use of a psychrometric chart. Figure 5-19 shows an example of one such determination. Air at 30°C (86°F) and 30% relative humidity contains about 0.008 grains of moisture per pound of dry air. Water saturated air at about 11°C (51°F) contains the same amount of water on a weight basis. Therefore, air that is saturated with water at 11°C and is raised to 30°C (86°F) has a relative humidity of 30%. Fully saturated air is easily achieved by bubbling it through water at the desired temperature. In this manner, the desired degree of humidity can be achieved at any specified temperature less than 100°C.

## Measurement Step

When the sample had cooled from the pretreatment temperature to the experimental temperature, the reaction gas was switched from forming gas to air at the specified humidity level. The change in the measured weight due to the density difference between forming gas and air indicated that there is a nearly instantaneous change in the gas content of the reaction chamber upon switching. Then, the sample was held at the desired experimental temperature as the reaction gas flowed continuously through the reaction chamber, maintaining a constant humidity and oxygen concentration. The extent of the reaction was monitored under constant conditions for an extended period, generally greater than 20 hours. Some longer experiments were also conducted to characterize better the later stages of the reaction.

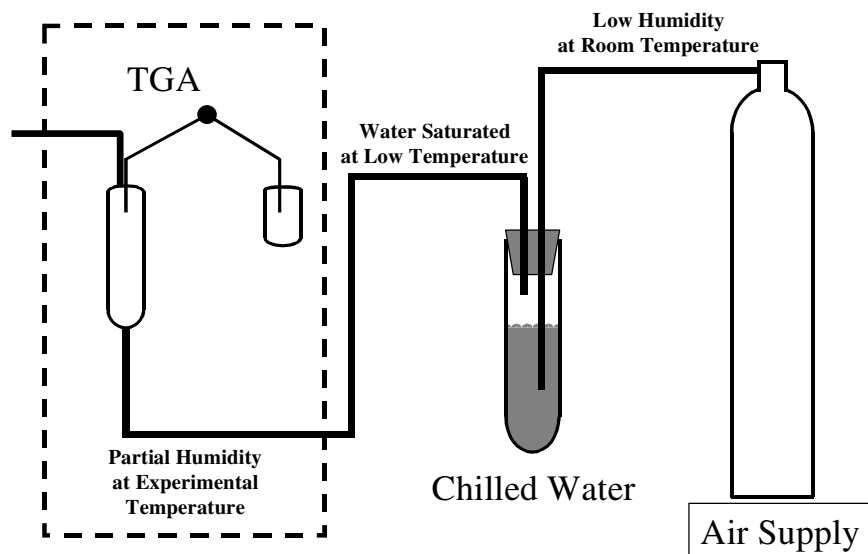


**Figure 5-18**  
**Schematic of Relative Humidity Control Process**

Experiments were conducted at several temperatures ranging from 30 to 90°C. Due to condensation of water from saturated air between the chilled water bath and the TGA, experiments above 60°C were not possible at nonzero humidities. Experiments with 30% and 60% relative humidity were conducted at 30 and 60°C. Note that the results obtained at 60°C may have been affected by undetected condensation.

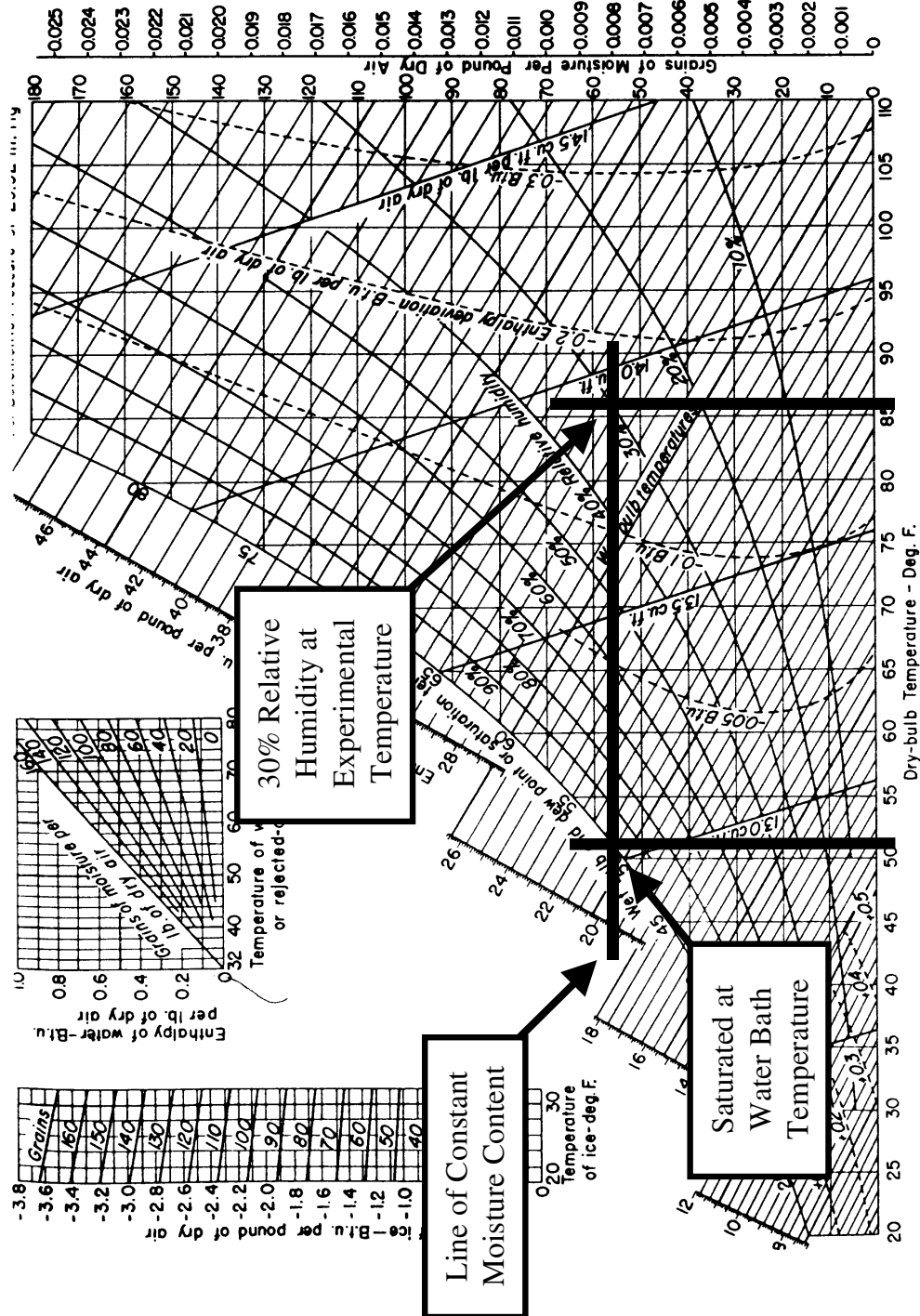


**Figure 5-19**  
**Psychrometric Chart**

[43, Perry, R.H. and D.W. Green, *Perry's Chemical Engineering Handbook*, Sixth Edition, McGraw-Hill Companies, New York, 1984. Reproduced with permission of The McGraw-Hill Companies.]

### TGA Results for Atmospheric Oxidation of Copper

After adjusting the raw data as described in the section on analytical techniques (page 5-2), the resultant data were fitted to several of the models that are described in the literature. The best model was found to be the logarithmic model. An example of a data series fitted with a logarithmic model is shown in Figure 5-20. In Figure 5-20 the circles represent measured data (averaged over relatively short time periods of 50 to 1000 seconds). The solid line represents the two parameter fit of the logarithmic growth law to the data using a least squares fitting routine. Note that the close fit to a logarithmic curve shown in Figure 5-20 is typical of the results for lower temperatures and that the fits were not quite as good at the higher temperatures tested.

When used to express the film thickness ( $x$ ) as a function of time ( $t$ ), the logarithmic model contains two kinetic parameters,  $A$  and  $B$ , giving the relationship:

$$x = A \ln(Bt + 1) \quad [5-1]$$

The units of  $A$  and  $B$  are chosen to conform with the units of  $x$  and  $t$ .  $A$  and  $x$  are given in nanometers (nm);  $B$  and  $t$  are given in inverse seconds (1/s) and seconds (s), respectively. The logarithmic model describes well the two prominent features of the film thickness growth curve: the fast increase in thickness at short times and the slow increase at longer times. With a kinetic model chosen, comparing reactions at different conditions becomes a matter of comparing the kinetic parameters. In the subsections below, the dependence of the kinetic parameters on the temperature and on the relative humidity is presented.

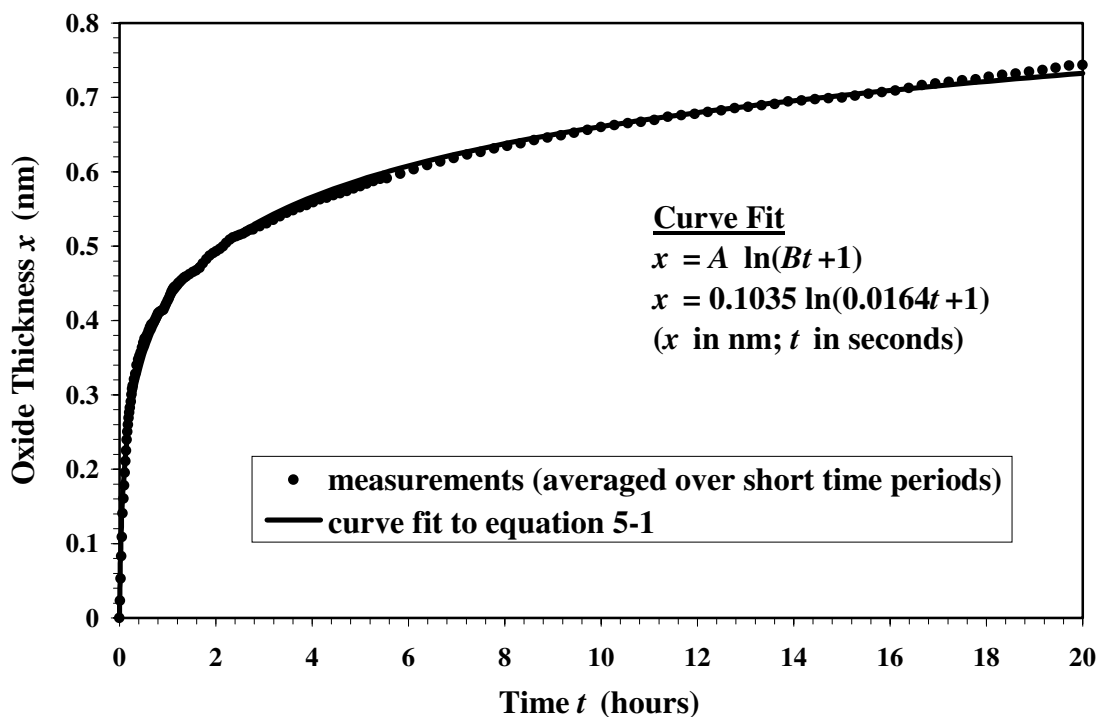


**Figure 5-20**  
Copper Oxidation in Dry Air at 30°C

## Thermal Dependence of the Reaction Rate Constants

Figures 5-21 and 5-22 show the thermal dependence of the logarithmic rate law constants  $A$  and  $B$ , respectively, under zero humidity conditions. The thermal dependence of the reaction rate constants was found to have two distinct regions. Because the temperature range covered in these experiments (30°C to 90°C) encompasses the temperature at which it is known that the reaction mechanism changes (50°C to 75°C) [32, 51], this result is not unexpected. In this study, it was found that the boundary between regions was near 60°C.

### Parameter A

Traditionally, rate constants are interpreted by evaluating the change in their logarithm with respect to the inverse absolute temperature. That approach was used here. At 60°C and above, the logarithm of the reaction rate constant  $A$  was found to be a linear function of the inverse temperature (see Figure 5-21). This type of relationship is referred to as an Arrhenius relationship and follows the form:

$$A = A_o e^{\frac{-E_{act}}{RT}} \quad [5-2]$$

where  $R$  is the ideal gas constant. The activation energy,  $E_{act}$ , and the pre-exponential factor,  $A_o$ , are constants that depend on the specifics of the reaction. The experimental data collected during this study indicate that  $E_{act}$  above 60°C is about 24 kcal/mol. For the case of  $\text{Cu}_2\text{O}$  forming on copper, Cabrera and Mott [7] suggest that the activation energy is about 1.1 eV or 25.4 kcal/mol. This value is somewhat smaller than that which would be expected from a pure vacancy diffusion reaction (about 2 eV) [52] and may indicate that the reaction mechanism involves a significant adsorption barrier.

Below 60°C, there is a change in the mechanism of the reaction which leads to a departure from the Arrhenius relationship. Between 60°C and 30°C, this departure can be modeled as a parabolic decay in the logarithm of the reaction constant  $A$ :

$$\ln(A) = 1.4495 \times 10^7 / T^2 - 95,857 / T + 156.25 \quad [5-3]$$

Although this relationship correctly describes the change in the reaction rate constant  $A$  between 60°C and 30°C, it does not necessarily describe the physics of a reaction mechanism. Clearly, at lower temperatures, a slow reaction with a small activation energy dominates the reaction rate. At higher temperatures, a second mechanism with a much larger activation energy begins to dominate. The region between 30°C and 60°C is a transition zone in which it is not possible to make an accurate measurement of a traditional activation energy. Nevertheless, it is still possible to use the relationship described above to predict the reaction rate at various temperatures in this region.

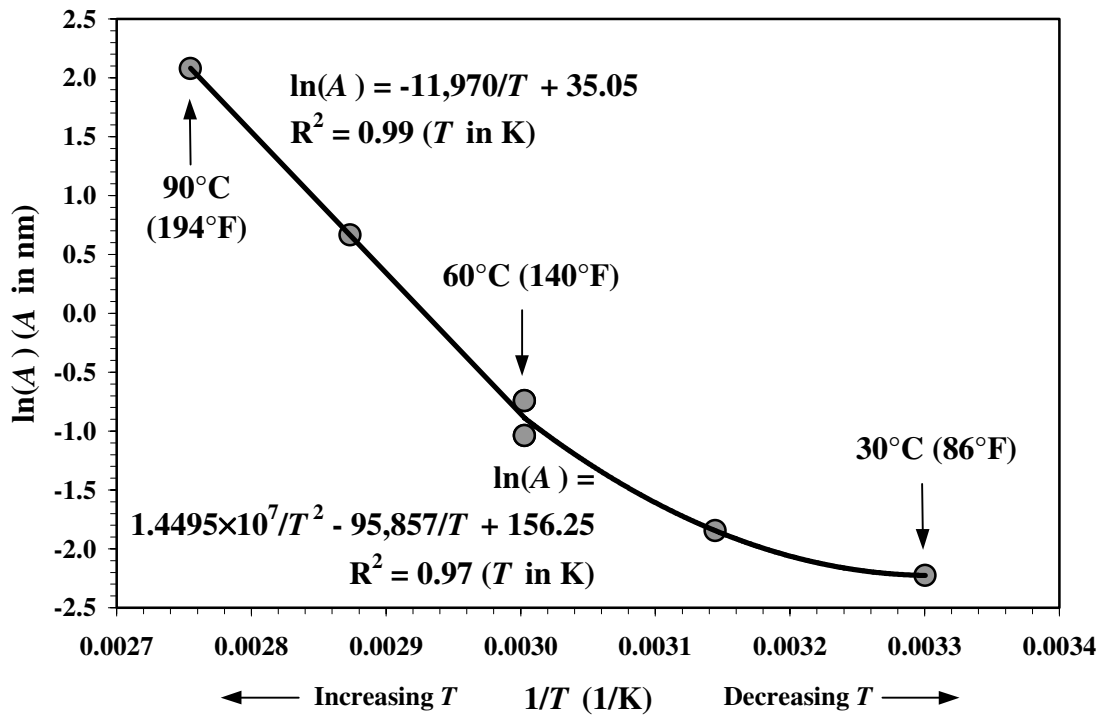


**Figure 5-21**  
Thermal Dependence of Rate Constant  $A$  for Atmospheric Copper Oxidation

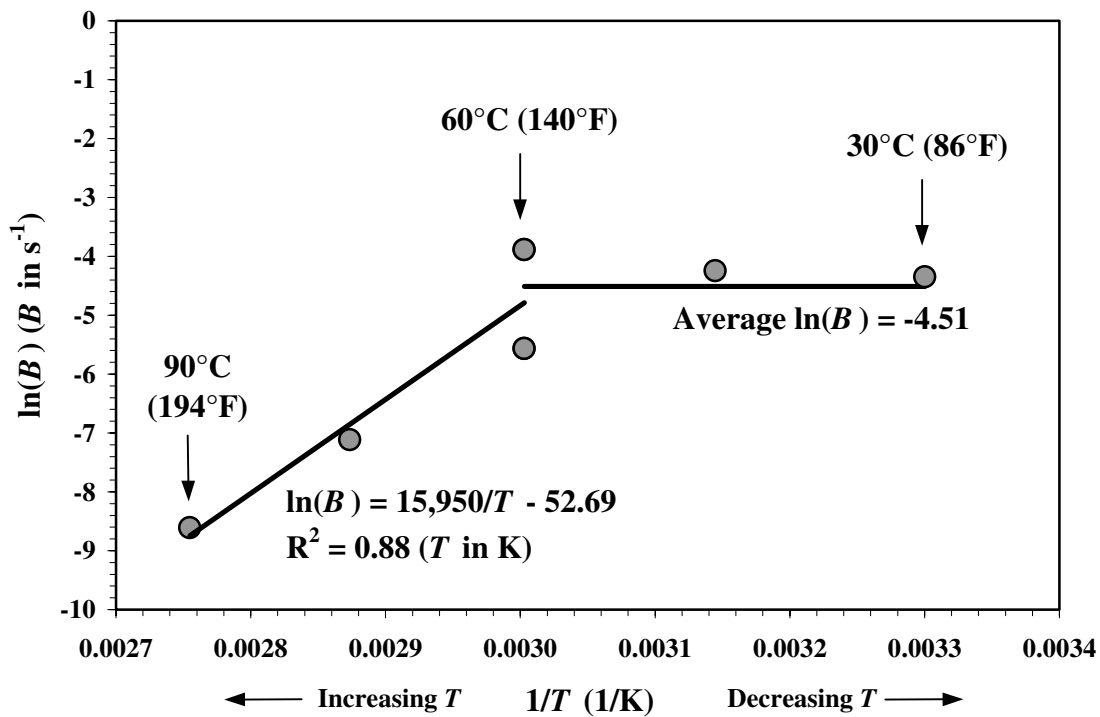


**Figure 5-22**  
Thermal Dependence of Rate Constant  $B$  for Atmospheric Copper Oxidation

### Parameter B

Although the reaction rate parameter  $B$  is not a rate constant that would be expected to follow an Arrhenius relationship, it is nonetheless convenient to examine its thermal dependence in the same manner. Again, when examining the dependence of the logarithm of  $B$  on the inverse temperature, different forms of the dependence are observed in the two temperature regions examined. At 60°C and above (see Figure 5-22), the logarithm of  $B$  has a linear dependence on the inverse temperature:

$$\ln(B) = 15,950/T - 52.69 \quad [5-4]$$

This form of the equation is used rather than the standard Arrhenius formulation so that it is clear that an activation-energy-type relationship is not implied. The form chosen here is for convenience, rather than to describe any underlying physical principles. Below 60°C, the rate parameter  $B$  is roughly constant, its logarithm having a value of -4.5.

With the temperature dependence of the two rate parameters known, it is possible to calculate the film thickness at any given temperature and time (assuming the effect of humidity is considered).

### Humidity Dependence of the Reaction Rate Constants

During dry layup of steam generators, the humidity of the air is considered to be an important factor in determining the rate at which oxides are formed. To examine the effect of humidity, experiments were performed at 30 and 60°C at varying relative humidities. The relative humidity is the ratio of the molar fraction of water in air to the molar fraction of water in a saturated air/water mixture of the same temperature and pressure. Therefore, the concentration of water in a 30% relative humidity atmosphere depends on the temperature (see Figure 5-19). However, as relative humidity is the most common and readily available measure of the moisture content of air, this parameter was chosen as the independent variable in these experiments.

At 60°C, the relative humidity was found not to significantly affect the progress of the oxidation reaction. Both rate parameters  $A$  and  $B$  showed no significant change over a range of relative humidity from 0% to 60% (see Figures 5-23 and 5-24). As previously mentioned, these results may have been affected by undetected condensation in the TGA apparatus. However, at 30°C, the reaction rate constant was significantly increased by the presence of moisture, nearly double at 60% relative humidity compared with zero humidity. This is made evident by the roughly linear increase in the logarithm of the rate parameter  $A$  with relative humidity (see Figure 5-23). As was the case with temperatures below 60°C, humidity had no observable effect on the rate parameter  $B$ . At 30°C, there is a high confidence that there was no significant undetected condensation in the TGA apparatus.

It is important to note that, even at 60% relative humidity, the oxidation of copper proceeds more slowly at 30°C than at 60°C and all humidity levels. Therefore, raising the temperature of the air, which effectively lowers the relative humidity, will accelerate oxidation, not retard it, even for humid air. Temperature is the more important factor. In fact, there is a factor of 70 increase in oxide thickness for a temperature increase from 30 to 90°C (zero humidity).

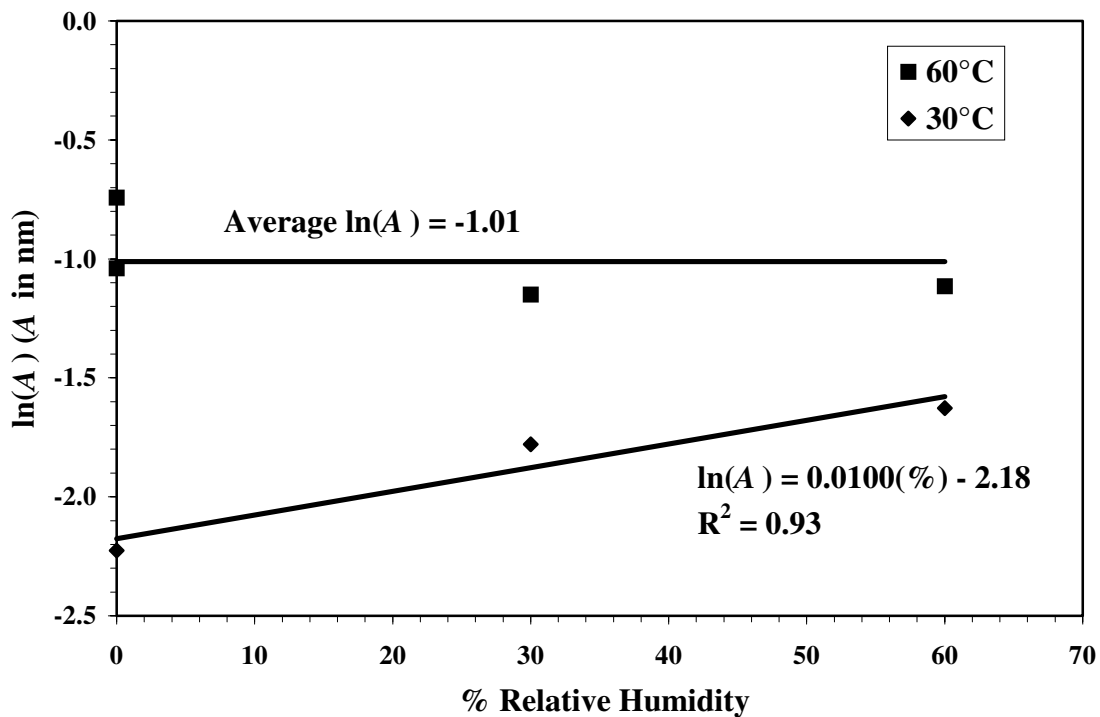


**Figure 5-23**  
Humidity Dependence of Rate Constant  $A$  for Atmospheric Copper Oxidation

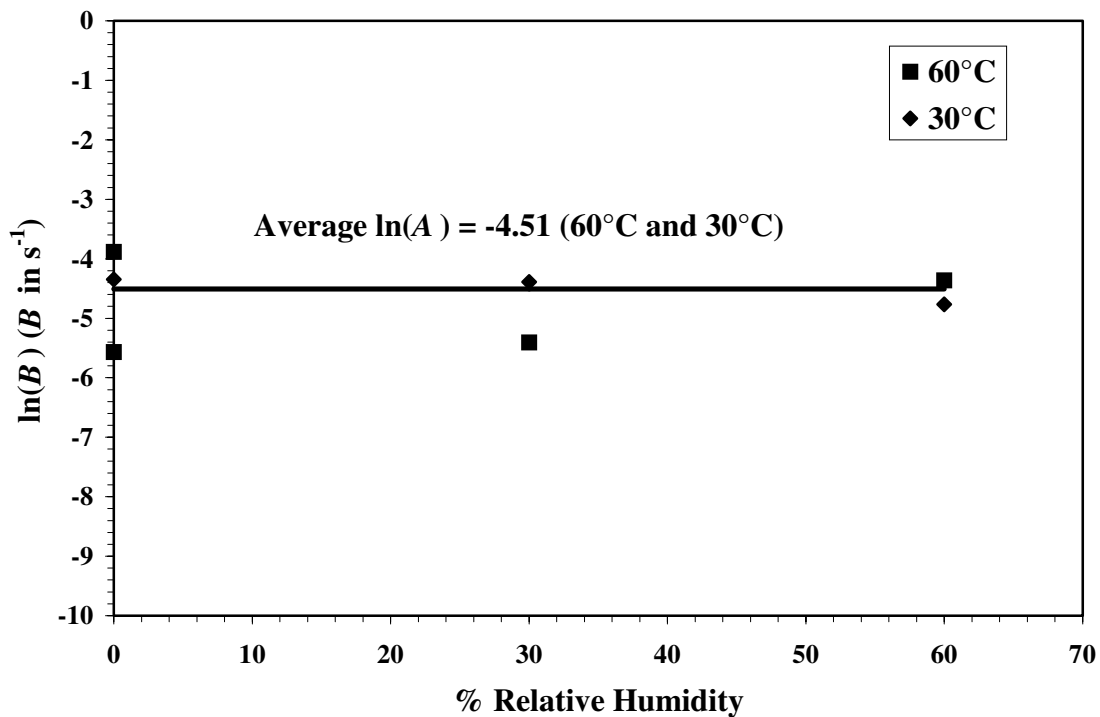


**Figure 5-24**  
Humidity Dependence of Rate Constant  $B$  for Atmospheric Copper Oxidation



The existence of a critical humidity below which corrosion is not accelerated by relative humidity is well documented for many reactions [53]. For iron this level is about 60%. However, it is important to note that, although keeping relative humidity levels below 30% or 45% may prevent humidity-accelerated corrosion of carbon steels, copper may behave differently. This is but one example of situations in which measures taken to prevent corrosion of steam generator construction materials during layup may not be the same measures needed to prevent the oxidation of steam generator deposits prior to operation under boiling conditions.

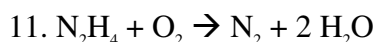
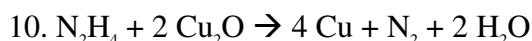
## Reduction Experiments for Copper under Startup Conditions

PWR steam generator layup practices are based on factors in addition to corrosion concern such as economic restraints and maintenance requirements. Because copper oxidizes so readily, some oxidation of copper in steam generator deposits during layup may be unavoidable. In order to minimize deposit oxide acceleration of tube degradation, it may be necessary to implement startup procedures to reduce these oxides to a less harmful state, rather than attempt to completely prevent their formation. In order to explore this possibility, a number of reduction experiments were conducted to gather data on copper oxide reduction kinetics. A summary of the experimental technique and a discussion of the results are presented below.

### *Reduction Experimental Technique*

The experimental setup used for the aqueous oxidation experiments was unsuitable for the high temperature reactions being investigated in the reduction phase of this study. Therefore, several small reaction bombs were created using short lengths of 1/4-inch stainless steel tubing. The bombs were sealed using compression fitting end caps.

The reaction powder used was the copper powder that had been oxidized in the aqueous oxidation studies described above. It therefore consisted of particles with a metallic copper core surrounded by a film of cuprite ( $\text{Cu}_2\text{O}$ ). The reaction tubes were filled with 0.30 g of the reaction powder. Under a low oxygen, low carbon dioxide nitrogen cover, deaerated water (less than 400 ppb  $\text{O}_2$ ) with 400 ppm hydrazine was loaded into the reaction tube until it was filled (~1.5 ml). In some cases, additional hydrazine was added to the deaerated water before filling the reaction tube. Cuprite and oxygen compete for hydrazine according to the following two reduction reactions:



After filling, the tubes were sealed and placed in an oven at the appropriate temperature (100 or 200°C). When an oxide content measurement was desired, the tube was removed from the oven and placed on ice until chilled. The water in the bomb was then opened and tested for hydrazine, and the copper powder was partially dried in air. The oxide content of the copper paste was then determined by XRD after either 5 or about 25 hours at temperature.

## Reduction Experimental Results

Three sets of experiments were run with deaerated water ( $\text{DO}_2 \sim 0.4$  ppm) in order to investigate the effects of hydrazine concentration, pH and temperature on the reduction of partially oxidized copper.

### Stoichiometric Shortage of Hydrazine with Respect to Cuprite

The first set used a hydrazine level of 400 ppm (0.04%) with pH adjusted to either 10.3 or 9.3 with dilute ammonia. These levels of oxygen, copper and hydrazine led to a large stoichiometric excess of hydrazine with respect to oxygen (1000 times stoichiometric in Reaction 11), but a large stoichiometric shortage of hydrazine with respect to the copper oxide (20% of stoichiometric in Reaction 10). Thus, no significant reduction of the particles would be expected, nor would significant oxidation. Unexpectedly, the results in Figure 5-25 showed that the degree of oxidation increased significantly. No significant effect of pH or temperature was observed.

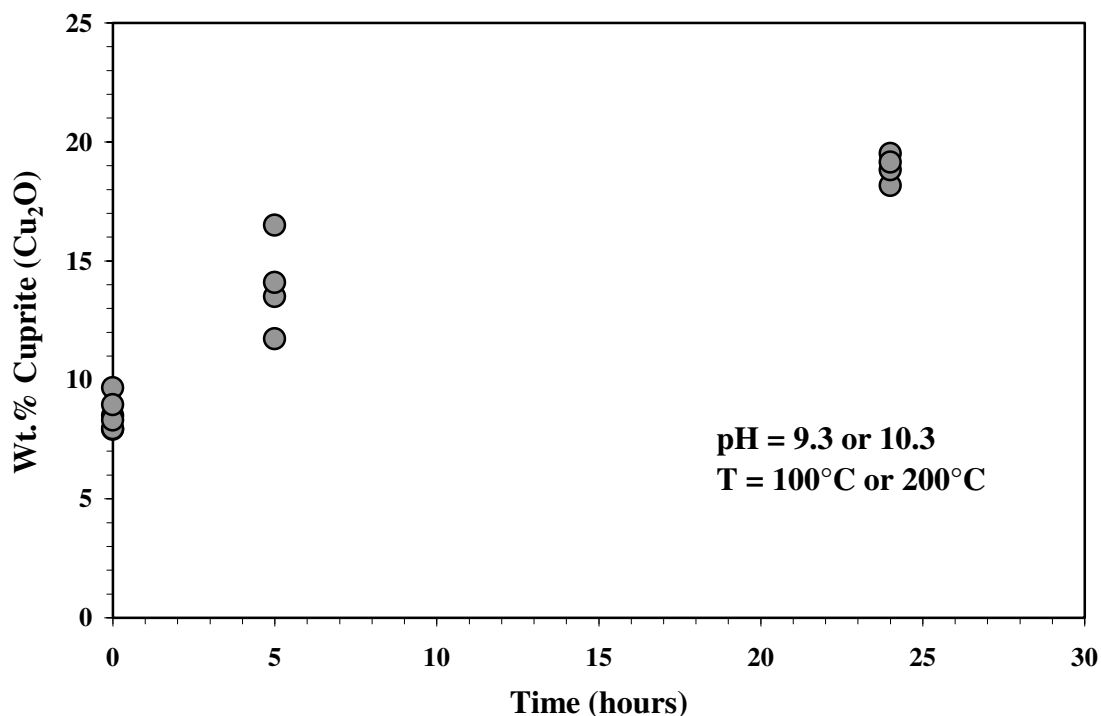


**Figure 5-25**  
High Temperature Oxidation of Copper Powder at 0.4 ppm Oxygen and 400 ppm Hydrazine

## Oxygen Stoichiometry

A stoichiometric analysis shows how much oxidation would be expected if all the dissolved oxygen were incorporated into the copper. A volume of 1.5 ml with 0.4 ppm oxygen is the equivalent of  $1.9 \times 10^{-8}$  moles of oxygen,

$$(1.5 \text{ ml}) \frac{0.4 \text{ } \mu\text{g O}_2}{\text{ml}} \frac{\text{mol O}_2}{32 \times 10^6 \text{ } \mu\text{g O}_2} = 1.9 \times 10^{-8} \text{ mol O}_2 \quad [5-5]$$

which would require only 4.8  $\mu\text{g}$  of copper to fully react with the oxygen to produce copper oxide ( $\text{Cu}_2\text{O}$ ),

$$(1.9 \times 10^{-8} \text{ mol O}_2) \frac{4 \text{ mol Cu}}{\text{mol O}_2} \frac{64 \text{ g}}{\text{mol Cu}} = 4.8 \text{ } \mu\text{g Cu} \quad [5-6]$$

## Possibility of Anaerobic Oxidation

However, this leads to a negligible increase in the fraction of the copper converted to copper oxide, indicating that either there was an air ingress during incubation or that an anaerobic reaction is taking place between water and copper (i.e., oxidation of copper by water to release hydrogen). The tubes were under pressure due to the increase in temperature above the temperature at which they were sealed. Since even at  $200^\circ\text{C}$ , there was no significant leakage of water vapor from the tube, it is reasonable to assume that there was no leakage of oxygen into the tube. There is some discussion of the controversial possibility of anaerobic oxidation of copper by water present in the literature [12, 13, 54, 55]. However, the reaction is generally considered to be thermodynamically unfavorable, and characterization of SG deposits usually shows the embedded copper to be almost exclusively in metallic form.

If the high pressure in the reaction tube was able to force out whatever hydrogen was formed (preferential leakage due to the small size of the hydrogen molecules), then the reaction might proceed. If the reaction were thus limited by the rate of hydrogen evolution, the insensitivity of the reaction rate to the temperature and the pH might be explained. Regardless of the mechanism, the increase in the oxide content is quite significant and orders of magnitude greater than that which would be produced if all the oxygen in the water reacted with the copper. The study of the reduction kinetics of copper oxides is thus complicated by the oxidation reactions that continue to occur even in the absence of oxygen.

## Stoichiometric Excess of Hydrazine with Respect to Cuprite

Two additional sets of experiments were run in order to further investigate the reduction of cuprite and the possible role of anaerobic reduction. In the first, the reaction tubes were dosed with hydrazine at twice the stoichiometric amount needed to reduce all of the copper oxide via Reaction 10 (dosed at a concentration of 0.4%). As shown in Figure 5-26, some oxidation was detected at 200°C, but in the tubes run at 100°C the overall effect was a reduction in the degree of oxidation. Since no significant differences due to temperature were observed in the absence of an excess of hydrazine, one can conclude that the differences in the presence of excess hydrazine were due to reaction rate differences in the autodecomposition of the hydrazine:



Thus, at the higher temperature, hydrazine decomposed more quickly, leaving less hydrazine to reduce the copper oxide.

The hypothesis that there is a competition for hydrazine between the autodecomposition reaction and the reduction reaction with copper oxide is further supported by the third set of experiments, which were conducted with a ten-fold stoichiometric dosing of hydrazine relative to the amount of copper oxide (2% hydrazine). The results from these experiments are shown in Figure 5-27. At this high level of hydrazine, there is considerably more reduction of copper, indicating that—even at hydrazine levels in excess of the stoichiometric amount—the hydrazine availability is the limiting factor in the reduction kinetics.

## Implications

The results from the reduction experiments have encouraging implications for SG corrosion. They may indicate that copper oxides formed during layup can be reduced back to metallic copper. However, more study of the competing hydrazine autodecomposition reaction is needed to determine the best conditions for executing this reduction. Based on the data collected to date, high levels of hydrazine at relatively moderate temperatures may produce the best results.

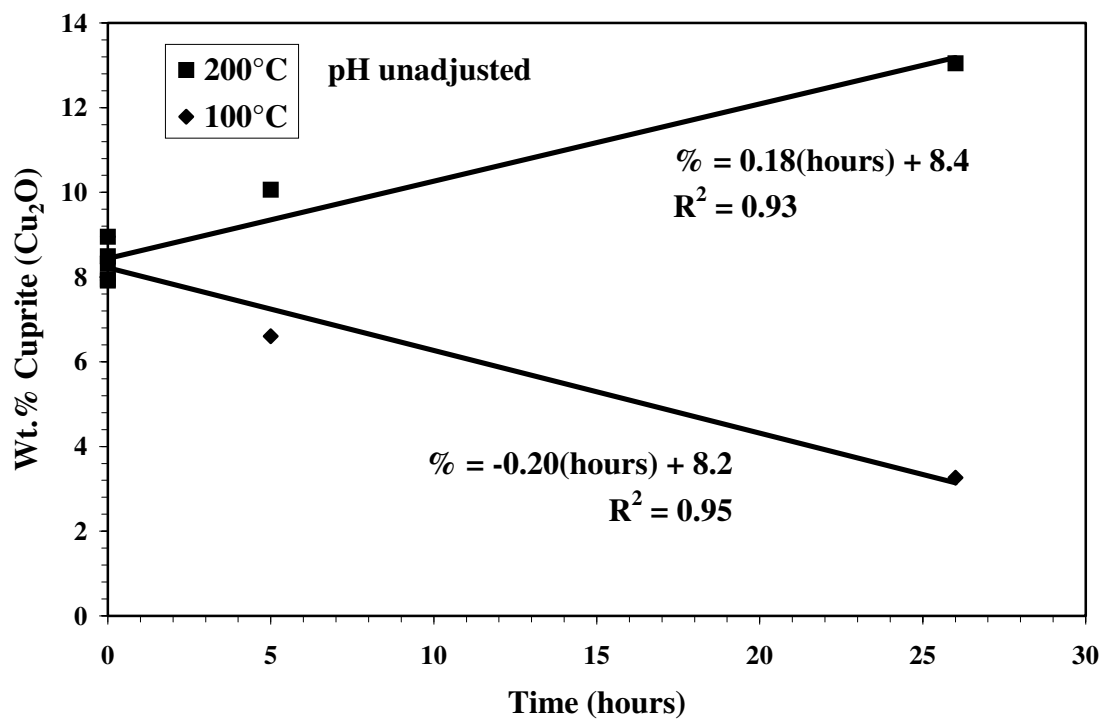


Figure 5-26  
Reaction of Copper Powder with 2x Stoichiometric Hydrazine with Respect to Cuprite

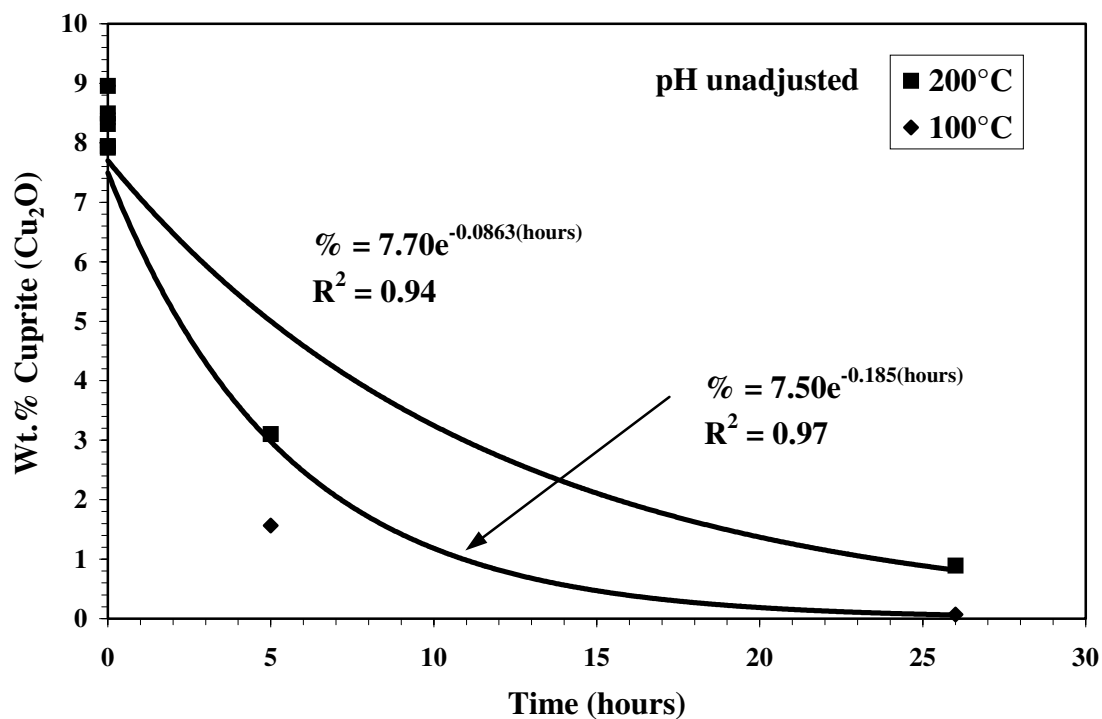


Figure 5-27  
Reaction of Copper Powder with 10x Stoichiometric Hydrazine with Respect to Cuprite

## Materials Used

Table 5-6 shows the suppliers and lot numbers of the materials used in the experiments discussed in Section 5. Table 5-7 shows the elemental composition of the steam generator deposit used in some of the aqueous oxidation experiments.

**Table 5-6**  
**Experimental Materials**

Chemical	Supplier	Catalog #	Lot #
Hydrazine	Acros	29681-5000	10938101
Metallic Copper	Aldrich	A44,750-1	11806TN
Cuprite	Fisher	C475	734685
Tenorite	Fisher	C472	755251
Magnetite	Fisher	I-119	986192
Hematite	Aldrich	I-1061	X9876

**Table 5-7**  
**Elemental Makeup of the Steam Generator Deposit Used (Plant C)**

Element	Wt.% as Oxide
Iron	85.84
Copper (metallic)	11.07
Zinc	1.68
Nickel	1.04
Silicon	0.000
Calcium	0.000
Manganese	0.254
Aluminum	0.000
Titanium	0.063
Chromium	0.045
Magnesium	0.017
Lead	0.0001

# 6

## REFERENCES

---

1. *Corrosion Evaluation of Thermally Treated Alloy 600 Tubing in Primary and Faulted Secondary Water Environments*, EPRI, Palo Alto, CA: 1996. NP-6721-SD.
2. *Characterization of PWR Steam Generator Deposits*, EPRI, Palo Alto, CA: 1996. TR-106048.
3. Hwang, I.S. and I.-G. Park, "Control of Alkaline Stress Corrosion Cracking in Pressurized-Water Reactor," *Corrosion*, **55:6**, 616, June 1999.
4. Sawicki, J.A., M.E. Brett and R.L. Tapping, "Corrosion-Product Transport, Oxidation State and Remedial Measures," Paper 30, 3<sup>rd</sup> Int. Steam Generator and Heat Exchanger Conference, Toronto, 1998.
5. Kishida, A., H. Takamatsu, H. Kitamura, S. Isobe, K. Onimura, K. Arioka, T. Hattori, T. Arai and M. Sato, "The Cause and Remedial Measures of Steam Generator Tube Intergranular Attack in Japanese PWR," 3<sup>rd</sup> International Symposium on Environmental Degradation of Materials in Nuclear Power Systems—Water Reactors, Traverse City, September 1987.
6. Pierson, E., J. Stubbe and G. Deny, "Stress Corrosion Cracking of Alloys 690, 800 and 600 in Acid Environments Containing Copper Oxides," Paper 119, Corrosion 96, 1996.
7. Cabrera, N. and N.F. Mott, "Theory of Oxidation of Metals," *Rep. Progress Physics*, **12**, 163, 1949.
8. Krishnamoorthy, P.K. and S.C. Sircar, "Influence of Oxygen Pressure on the Oxidation Kinetics of Copper in Dry Air at Room Temperature," *J. Electrochemical Society*, **116**, 724, 1969.
9. Lenglet, M., K. Kartouni and D. Delahaye, "Characterization of Copper Oxidation by Linear Potential Sweep Voltammetry and UV-Visible-NIR Diffuse Reflectance Spectroscopy," *J. Applied Electrochemistry*, **21**, 697, 1991.
10. Mrowec, S. and A. Stoklosa, "High Temperature Oxidation of Copper," *Bulletin de L'Académie Polonaise des Sciences: Série des Sciences Chimiques*, **18**, 531, 1970.
11. Manara, A., V. Sirtori and L. Mammarella, "Optical Ellipsometry and Electron Spectroscopy Studies of Copper Oxidation Related to Copper on Printed Circuit Boards," *Surface and Interface Analysis*, **18**, 32, 1992.

12. Hultquist, G., "Short Communication: Hydrogen Evolution in Corrosion of Copper in Pure Water," *Corrosion Science*, **26:2**, 173, 1986.
13. Simpson, J.P. and R. Schenk, "Short Communication: Hydrogen Evolution from Corrosion of Pure Copper," *Corrosion Science*, **27**, 1365, 1987.
14. Kubaschewski, O., E.L. Evans and C.B. Alcock, *Metallurgical Thermochemistry*, Pergamon, Oxford, 1967.
15. Bowers, D.H., D.M. Littrell and B.J. Tatarchuk, "Reduction Kinetics of Thin and Thick Cupric Oxide Films at Room Temperature by Hydrazine," *Thin Solid Films*, **169**, 143, 1989.
16. Hur, D.H., H.S. Chung and U.C. Kim, "Corrosion Behaviors During the Iron Removal Process for Chemical Cleaning of Nuclear Steam Generators," *Journal of Nuclear Materials*, **224**, 179, 1995.
17. Pierson, E. and C. Laire, "The Influence of Copper on the SCC of Alloy 600 and Alloy 690 Steam Generator Tubes," Fontevraud IV, 381, September 1998.
18. White, E.L., W.E. Berry and W.K. Boyd, "Effect of Copper Oxides on the Stress Corrosion Cracking of Inconel Alloy 600," International Copper Research Association Project #N33403, INCRA Res. Rep. 285, October 1977.
19. Burgmayer, P., "Where's All That Copper in Your Boiler Coming From?" *Materials Performance*, 28:9, 75, September 1989.
20. Millet, P.J. and J.M. Fenton, "High Temperature, Aqueous-phase Diffusion of NaCl through Simulated Deposits of Corrosion Products," *Corrosion*, **49:7**, 536, 1993.
21. Margulova, T.Kh. and Yu.M. Kostrikin, "On the Mechanism of Copper Deposit Formation," *Thermal Engineering*, **15**, 72, 1968.
22. Gorman, J.A., A.R. McIlree, T. Gaudreau, L. Björnkvist and P.-O. Andersson, "Influence of Startup Oxidizing Transients on IGA/SCC in PWR Steam Generators," 3<sup>rd</sup> International Steam Generator and Heat Exchanger Conference, Toronto, 1998.
23. *Proceedings: 1999 EPRI Workshop on Startup Oxidant Control*, Chattanooga Tennessee, January 19–20, 1999, EPRI, Palo Alto, CA: 1999. TR-112815.
24. Guan, R., H. Hashimoto and T. Yoshida, "Electron-Microscopic Study of the Structure of Metastable Oxides Formed in the Initial Stages of Copper Oxidation. I. Cu<sub>4</sub>O," *Acta Crystallographica*, **B40**, 109, 1984.
25. Mills, T. and U.R. Evans, "The Effects of Sulphur Dioxide on the Oxidation of Copper," *J. Chemical Society, London*, 2186, 1956.
26. Swanson, A.W. and H.H. Uhlig, "Effect of Gaseous Pretreatment on Oxidation of Iron," *J. Electrochemical Society*, **121**, 1551, 1974.



27. Allen, J.A., "Oxide Films on Electrolytically Polished Copper Surfaces," *Trans. Faraday Society*, **48**, 273, 1952.
28. Bradley, W.W. and H.H. Uhlig, "Effects of Heating Single Crystal Copper in H<sub>2</sub> and N<sub>2</sub> on Thin-Film Oxidation Kinetics," *J. Electrochemical Society*, **114**:7, 669, 1967.
29. Winterbottom, A.B., "Polarimetric Studies of Oxide Film Formation on Metals," *Nature*, 364, August 28, 1937.
30. Evans, U.R. and H.A. Miley, "Measurement of Oxide Films on Copper and Iron," *Nature*, 283, February 13, 1937.
31. Krishnamoorthy, P.K. and S.C. Sircar, "Effect of an Applied Electric Current on the Rate of Oxidation of Copper at Room Temperature," *Acta Metallurgica*, **16**, 1461, 1968.
32. Roy, S.K., P.K. Krishnamoorthy and S.C. Sircar, "Kinetics of Oxidation of Copper at Low Temperatures Under the Influence of Externally Induced Current Flow," *Acta Metallurgica*, **18**, 519, 1970.
33. Pinnel, M.R., H.G. Tompkins and D.E. Heath, "Oxidation of Copper in Controlled Clean Air and Standard Laboratory Air at 50° to 150°C," *Applied Surface Science*, **2**, 558, 1979.
34. Roy, S.K., S.K. Bose and S.C. Sircar, "Pressure Dependencies of Copper Oxidation for Low and High Temperature Parabolic Laws," *Oxidation of Metals*, **35**:1/2, 1, 1991.
35. Khoviv, A.M. and L.A. Malevskaya, "Kinetics of Low-Temperature Copper Oxidation in a Dry Oxygen Atmosphere," *Inorganic Materials*, **31**, 988, 1995.
36. Choi, W.K., W.Z. Oh and S.I. Woo, "Dissolution Behaviors of Copper Metal in Alkaline H<sub>2</sub>O<sub>2</sub>-EDTA Solutions," *Journal of Nuclear Science and Technology*, **30**, 549, 1993.
37. D'Elia, E., O.E. Barcia, O.R. Mattos, N. Pébère and B. Tribollet, "High-Rate Copper Dissolution in Hydrochloric Acid Solution," *J. Electrochemical Society*, **143**, 961, 1996.
38. Faita, G., G. Fiori and D. Salvatore, "Copper Behavior in Acid and Alkaline Brines—I: Kinetics of Anodic Dissolution in 0.5M NaCl and Free-Corrosion Rates in the Presence of Oxygen," *Corrosion Science*, **15**, 383, 1975.
39. Landolt, D., R.H. Muller and C.W. Tobias, "High Rate Anodic Dissolution of Copper," *J. Electrochemical Society*, **116**, 1384, 1969.
40. Charette, G.G. and S.N. Flengas, "Thermodynamic Properties of the Oxides of Fe, Ni, Pb, Cu and Mn by EMF Measurements," *J. Electrochemical Society*, **115**:8, 796, 1968.
41. Bidwell, L.R., "Free Energy of Formation of Cupric Oxide," *J. Electrochemical Society*, **114**:1, 30, 1967.
42. Levenspiel, O., *Chemical Reaction Engineering*, John Wiley & Sons, New York, 1972.

---

References

43. Perry, R.H. and D.W. Green, *Perry's Chemical Engineering Handbook*, Sixth Edition, McGraw-Hill Book Company, New York, 1984.
44. Bird, R.B., W.E. Stewart and E.N. Lightfoot, *Transport Phenomena*, John Wiley & Sons, New York, 1960.
45. Incropera, F.P. and D.P. DeWitt, *Fundamentals of Heat and Mass Transfer*, John Wiley & Sons, New York, 1990.
46. Stecher, P.G., *The Merck Index*, Eighth Edition, Merck & Co., Inc., Rahway, 1968.
47. Froment, G.F. and K.B. Bischoff, *Chemical Reactor Analysis and Design*, Second Edition, John Wiley & Sons, New York, p. 158, 1990.
48. Smith, D.K., "Introduction to Diffraction Methods," from *Metals Handbook Ninth Edition, Volume 10: Materials Characterization*, American Society for Metals, Metals Park, 1986.
49. ASTM D-5543-94, "Standard Test Methods for Low-Level Dissolved Oxygen in Water," from *1998 Annual Book of ASTM Standards, Section 11: Water and Environmental Technology*, ASTM, West Conshohocken, 1998.
50. Bohnsack, G., "Chemistry of Corrosion Inhibition and Surface Passivation of Mild Steel by Hydrazine in Power Plant Circuits," Paper 461, Corrosion 89, 1989.
51. Rhodin, Jr., T.N., "Low Temperature Oxidation of Copper. I. Physical Mechanism," *J. American Chemical Society*, **72**, 5102, 1950.
52. Lazarus, D., "Diffusion in Metals," *Solid State Physics*, **10**, 71, 1960.
53. Uhlig, H.H. and R.W. Revie, *Corrosion and Corrosion Control*, John Wiley & Sons, New York, 1985.
54. Hultquist, G., G.K. Chuah and K.L. Tan, "Comments on Hydrogen Evolution from the Corrosion of Pure Copper," *Corrosion Science*, **29:11/12**, 1371, 1989.
55. Eriksen, T.E., P. Ndalamba and I. Grenthe, "Short Communication on the Corrosion of Copper in Pure Water," *Corrosion Science*, **29:10**, 1241, 1989.
56. Bear, J., *Dynamics of Fluids in Porous Media*, Dover Publications, Inc., New York, 1972, p. 110.
57. *Source Book on Limiting Exposure to Startup Oxidants*, EPRI, Palo Alto, CA: 1999. TR-112967.
58. Millett, P.J. and J.M. Fenton, "Measurement of Effective Diffusion Coefficients for Chloride Salts in Nonprotective Magnetite," *Corrosion*, **46:9**, 710, 1990.

# A

## SUMMARIES OF THE LITERATURE REVIEWED

---

A literature search was conducted for information on the oxidation and reduction of copper in steam generator deposits and the effects of copper oxides on steam generator construction material corrosion rates. The literature search included consideration of EPRI technical reports as well as conference papers and articles from peer reviewed journals. A subject by subject survey of these references is given in the main body of the report. Below are individual summaries of each of the papers reviewed.

Authors: J.A. Allen [27]

Title: Oxide Films on Electrolytically Polished Copper Surfaces

Source: Trans. Faraday Society, 48, 273, 1952.

Summary: The authors investigated oxidation of copper films at room temperature in air using electrometric techniques. Before oxidation the films were cleaned in a phosphoric acid bath. It was determined that the oxide growth rate was significantly dependent on the nature of the cleaning process. Although the kinetic data given in the article are limited, they are significant because they point to the sensitivity of the oxidation process to surface preparation.

Authors: J. Bardeen, W.H. Brattain and W. Shockley

Title: Investigation of Oxidation of Copper by Use of Radioactive Cu Tracer

Source: J. Chemical Physics, 14:12, 714, 1946.

Summary: The authors investigated the physical mechanism of copper oxidation. A film of copper was electroplated with radioactive copper. At a high temperature (1000°C) the film was oxidized in air. Subsequently, the film was chemically stripped in stages to determine a profile of radioactivity verses depth. The observed profile was consistent with the theory of oxide formation by cation vacancy diffusion.

Authors: L.R. Bidwell [41]

Title: Free Energy of Formation of Cupric Oxide

Source: J. Electrochemical Society, 114:1, 30, 1967.

Summary: The author measured the electrochemical potential of a cuprous/cupric oxide cell in order to determine the change in free energy between the two copper oxides. Using literature data for the free energy of cuprous oxide, the free energy of formation of cupric oxide was determined at several temperatures. The results are presented as an empirical equation for the standard free energy of oxidation as a function of temperature.

Authors: G. Bohnsack [50]

Title: Chemistry of Corrosion Inhibition and Surface Passivation of Mild Steel by Hydrazine in Power Plant Circuits

Source: Paper 461, Corrosion 89, 1989.

Summary: The author reviews the current understanding of the mechanism of the interaction between hydrazine and iron. Hydrazine works as a passivation agent and not as a reductant. Hydrazine is known not to reduce hematite to magnetite. Hydrazine works by oxidizing soluble  $\text{Fe}(\text{OH})_2$  to insoluble  $\text{Fe}_3\text{O}_4$  to create a passivation layer.

Authors: D.H. Bowers, D.M. Littrell and B.J. Tatarchuk [15]

Title: Reduction Kinetics of Thin and Thick Cupric Oxide Films at Room Temperature by Hydrazine

Source: Thin Solid Films, 169, 143, 1989.

Summary: The authors investigated the kinetics of the reduction of copper oxide films by gaseous hydrazine using X-ray photospectroscopy and gravimetry. Film thicknesses were on the order of 5 to 20 nm. Temperatures ranged from 295K to 381K. Hydrazine pressures ranged from 1 to 1462 Pa. They found that for thin films ( $\leq 5$  nm) the reaction was first order in hydrazine, which combined with the observed Arrhenius factors led to the conclusion that the reaction was adsorption rate limited. For thicker films and high levels of hydrazine, there was a parabolic rate of reduction, which was insensitive to the hydrazine concentration, leading to the conclusion that the reaction was diffusion controlled. Times for complete reduction were on the order of one hour.

Authors: W.W. Bradley and H.H. Uhlig [28]

Title: Effect of Heating Single Crystal Copper in  $\text{H}_2$  and  $\text{N}_2$  on Thin-Film Oxidation Kinetics

Source: J. Electrochemical Society, 114:7, 669, 1967.

Summary: The authors investigated the kinetics of oxide film growth on a single crystal of copper in pure oxygen at 1 atm and 200°C. The relative rates of growth on the various faces of the crystals were measured. The effect of pretreatment at 450°C with hydrogen or nitrogen gas was also studied. Hydrogen treatment was found to retard the growth of the oxide film. Nitrogen treatment had no effect.

Authors: D.W. Bridges, J.P. Baur, G.S. Baur and W.M. Fassell, Jr.

Title: Oxidation of Copper to  $\text{Cu}_2\text{O}$  and  $\text{CuO}$

Source: J. Electrochemical Society, 103:9, 475, 1956 and 104, 749, 1957.

Summary: The authors investigated the kinetics of oxide film growth on copper at temperatures ranging from 600°C to 1000°C and oxygen pressures of 0.026 to 20.4 atm. The oxygen pressure was not found to have any effect on the rate of oxide growth. The ratio of  $\text{Cu}_2\text{O}$  to  $\text{CuO}$  was determined using X-ray diffraction and was found to be independent of the temperature and pressure. A modification of the parabolic growth rate law (such that the growth rate is finite at time zero) was found to fit the data well.

Authors: P. Burgmayer [19]

Title: Where's All That Copper in Your Boiler Coming From?

Source: Materials Performance, 28:9, 75, September 1989.

Summary: The author investigated the corrosion of copper tubing under various aqueous conditions. The parameters varied were temperature, pH, oxygen content, flow rate and amine concentration and type. The corrosion rate was unaffected by flow rate. There was a positive correlation between corrosion and temperature, oxygen concentration and amine concentration. There was a negative correlation between corrosion and pH.

Authors: N. Cabrera and N.F. Mott [7]

Title: Theory of the Oxidation of Metals

Source: Rep. Progress Physics, 12, 163, 1949.

Summary: The authors develop three models to predict the rate of growth of oxide films. For very thin films ( $x \ll 100 \text{ \AA}$ ) they predict a logarithmic growth rate,  $1/x = A - B \ln(t)$ , where  $A$  and  $B$  are experimentally determined. For thin films ( $x \leq 100 \text{ \AA}$ ) they predict a parabolic growth rate,  $x^2 = kt$ , where  $k$  is determined experimentally. For thick films ( $x > 100 \text{ \AA}$ ) they predict a parabolic growth rate,  $x^2 = kt$ , where  $k$  is determined experimentally and is different from the thin film rate constant.

Authors: W.E. Campbell and U.B. Thomas

Title: The Oxidation of Metals

Source: Transactions of the Electrochemical Society, 91, 623, 1947.

Summary: The authors present a considerable amount of data on the oxidation of copper and its alloys at temperatures from 100°C to 302°C. Among their significant findings is the determination that moisture lowers the oxidation rate of copper.

Authors: G.W. Castellan and W.J. Moore

Title: Diffusion of Radioactive Copper During Oxidation of Copper Foil

Source: J. Chemical Physics, 17:1, 41, 1949.

Summary: The authors use copper films electroplated with radioactive copper to investigate the physics of copper oxidation at high temperatures (800°C to 1000°C). The oxidized films were stripped with hydrochloric acid to develop a profile of radioactivity verses oxide depth. The resulting profile was consistent with copper ion diffusion through the oxide film to the oxide/oxygen interface. Values for the diffusion coefficient of copper ions in copper are given as a function of temperature.

Authors: G.G. Charette and S.N. Flengas [40]

Title: Thermodynamic Properties of the Oxides of Fe, Ni, Pb, Cu and Mn by EMF Measurements

Source: J. Electrochemical Society, 115:8, 796, 1968.

Summary: The authors use half cell potential measurements to determine the free energies and enthalpies of reaction for the oxidation of the titular metals. These properties are given as functions of temperature over the range of 500°C to 1200°C.

Authors: F. Chehab, W. Kirstein and F. Thieme  
Title: The Interaction of Hydrogen with Ni-Rich (111) Cu-Ni Surfaces  
Source: Surface Science, 152/153, 367, 1985.  
Summary: The authors studied the adsorption of hydrogen onto Cu-Ni alloys at low temperatures and pressures. The hydrogen was found to adsorb preferentially to nickel rich areas. The structure of the adsorbed hydrogen was found to be similar to the metal crystalline structure.

Authors: W.K. Choi, W.Z. Oh and S.I. Woo [36]  
Title: Dissolution Behaviors of Copper Metal in Alkaline H<sub>2</sub>O<sub>2</sub>-EDTA Solutions  
Source: Journal of Nuclear Science and Technology, 30, 549, 1993.  
Summary: The authors investigated the dissolution of copper in a solution of hydrogen peroxide and EDTA using dynamic polarization. They found that the copper dissolution rate increased linearly with hydrogen peroxide concentration due to a reaction between the hydrogen peroxide and the copper.

Authors: D.L. Cocke, G.K. Chuah, N. Kruse and J.H. Block  
Title: Copper Oxidation and Surface Copper Oxide Stability Investigated by Pulsed Field Desorption Mass Spectroscopy  
Source: Applied Surface Science, 84, 153, 1995.  
Summary: The authors used a specially shaped metal sample to investigate the nature of copper oxides by gradual ionization of the metal sample. They determined that the oxygen molecules present may be found in three thermodynamic states: surface adsorbed molecular oxygen, sub-surface dissolved molecular oxygen and reduced atomic oxygen. These findings indicate that the outer layer of the oxide has some dissolved oxygen present. These findings somewhat contradict the determinations made using radioactive tracers.

Authors: R.J. Day and M.A. Frisch  
Title: Chromium Chromate as an Inert Marker in Copper Oxidation  
Source: Surface and Interface Analysis, 8, 33, 1986.  
Summary: The authors investigated oxidation of copper coated with a thin film of chromium chromate. It was determined that the copper oxidized by diffusing through the chromium chromate and subsequently through the oxide film. These findings are in accord with those from radioactive tracer studies which indicate that copper oxidation proceeds through the vacancy diffusion of copper cations to the oxide/oxygen interface.

Authors: E. D'Elia, O.E. Barcia, O.R. Mattos, N. Pébère and B. Tribollet [37]  
Title: High-Rate Copper Dissolution in Hydrochloric Acid Solution  
Source: J. Electrochemical Society, 143, 961, 1996.  
Summary: The authors investigated the dissolution of copper in a solution of hydrochloric acid using dynamic polarization. They investigated a reaction regime with mixed kinetics that lies between the potential plateaus for this reaction (1 to 3 V/SCE).

- Authors: T.E. Eriksen, P. Ndalama and I. Grenthe [55]  
Title: Short Communication on the Corrosion of Copper in Pure Water  
Source: Corrosion Science, 29:10, 1241, 1989.  
Summary: The authors investigated the corrosion of copper foil in pure water. The reaction of copper with water, evolving hydrogen, was not found to occur. Although oxygen levels were low, they were not measured and the authors speculate that the significant oxidation observed was the result of residual oxygen levels. Films of 500 to 5000 Å were observed after exposure times of 61 days. No pretreatment of the copper was made. The film thickness was measured by cathodic reduction. Significant differences in the oxide film thickness were found due to differences in purity levels between the copper samples. Pure copper oxidized faster.
- Authors: U.R. Evans and H.A. Miley [30]  
Title: Measurement of Oxide Films on Copper and Iron  
Source: Nature, 283, February 13, 1937.  
Summary: The authors present data obtained from electrometric measurement of copper oxide films at room temperature (18°C and 62°C) in air. The data indicate a period of rapid oxidation (15 minutes) followed by a slower oxidation period.
- Authors: G. Faita, G. Fiori and D. Salvatore [38]  
Title: Copper Behavior in Acid and Alkaline Brines—I: Kinetics of Anodic Dissolution in 0.5M NaCl and Free-Corrosion Rates in the Presence of Oxygen  
Source: Corrosion Science, 15, 383, 1975.  
Summary: The authors investigated the dissolution of copper in a solution of sodium chloride using dynamic polarization. The pH of the solution was adjusted using NaHCO<sub>3</sub>, NaCO<sub>3</sub> and NaOH. At low pH (~3) pH changes did not have a marked effect and diffusion through the CuCl film was determined to be the rate limiting step. At higher pH (~8) increasing pH suppressed the dissolution of CuCl which became the rate controlling step.
- Authors: W.E. Garner, T.J. Gray and F.S. Stone  
Title: Oxidation and Reduction of Copper  
Source: Proceedings of the Royal Society, A197, 294, 1949.  
Summary: The authors investigated the effect of repetitive oxidation and reduction on the kinetics of copper reactions. Cycling the material was found to have an impact on the kinetics, but the data presented are sparse.
- Authors: W.E. Garner, F.S. Stone and P.F. Tiley  
Title: The Reaction between Carbon Monoxide and Oxygen on Cuprous Oxide at Room Temperature  
Source: Proceedings of the Royal Society, A211, 472, 1952.  
Summary: The catalytic action of cuprous oxide in the conversion of carbon monoxide to carbon dioxide is investigated.

- Authors: J.A. Gorman, A.R. McIlree, T. Gaudreau, L. Björnkvist and P.-O. Andersson [22]  
Title: Influence of Startup Oxidizing Transients on IGA/SCC in PWR Steam Generators  
Source: Third International Steam Generator and Heat Exchanger Conference, Toronto, ON, 1998.  
Summary: The authors hypothesize that IGA/SCC in PWR steam generators can be caused by oxidation during shutdown, layup and startup. They cite anecdotal evidence including the success of stringent SLS procedures at Kori 1, a study of Belgian plants showing a correlation between IGA/SCC and number of shutdowns and the success of Swedish stringent control of oxidants during SLS in reducing IGA/SCC. They recommend wider use of the stringent control of oxidants during SLS.
- Authors: M. Grüne, J. Radnik and K. Wandelt  
Title: Reaction of Nitrogen with fcc- and bcc-Iron Films on Copper (100)  
Source: Surface Science, 402, 236, 1998.  
Summary: The authors investigated the adsorption of nitrogen gas onto iron films at very low temperatures and pressures. By using thin films of iron on a copper base, the crystalline structure of the iron could be independently controlled. The crystalline structure of the adsorbed nitrogen depends on the structure of the underlying metal.
- Authors: G.R. Gruzalski, D.M. Zehner and J.F. Wendelken  
Title: An XPS Study of Oxygen Adsorption on Cu (110)  
Source: Surface Science, 159, 353, 1985.  
Summary: The authors studied the low pressure, low temperature adsorption of oxygen onto copper metal using XPS.
- Authors: R. Guan, H. Hashimoto and T. Yoshida [24]  
Title: Electron-Microscopic Study of the Structure of Metastable Oxides Formed in the Initial Stage of Copper Oxidation. I. Cu<sub>4</sub>O  
Source: Acta Crystallographica, B40, 109, 1984.  
Summary: The authors investigated the initial phases of copper oxidation using scanning electron microscopy. The formation of a metastable film of Cu<sub>4</sub>O was observed. Measurements of the crystalline structures of these films were made.
- Authors: R. Guan, H. Hashimoto and K.H. Kuo  
Title: Electron-Microscopic Study of the Structure of Metastable Oxides Formed in the Initial Stage of Copper Oxidation. III. Cu<sub>64</sub>O  
Source: Acta Crystallographica, B41, 219, 1985.  
Summary: The authors investigated the initial phases of copper oxidation using scanning electron microscopy. The formation of a metastable film of Cu<sub>64</sub>O was observed. Measurements of the crystalline structure of this film were made.
- Authors: R. Guan, H. Hashimoto, K.H. Kuo and T. Yoshida  
Title: Electron-Microscopic Study of the Structure of Metastable Oxides Formed in the Initial Stage of Copper Oxidation. IV. Cu<sub>4</sub>O-S<sub>1</sub> and Cu<sub>4</sub>O-S<sub>2</sub>  
Source: Acta Crystallographica, B43, 343, 1987.  
Summary: The authors investigated the initial phases of copper oxidation using scanning electron microscopy. The formation of two different metastable films of Cu<sub>4</sub>O was observed. Measurements of the crystalline structures of these films were made.



Authors: R. Guan, H. Hashimoto and K.H. Kuo

Title: Electron-Microscopic Study of the Structure of Metastable Oxides Formed in the Initial Stage of Copper Oxidation. V.  $\text{Cu}_4\text{O}_{0.75}$

Source: Acta Crystallographica, B46, 103, 1990.

Summary: The authors investigated the initial phases of copper oxidation using scanning electron microscopy. The formation of a metastable film of  $\text{Cu}_4\text{O}_{0.75}$  was observed. Measurements of the crystalline structure of this film were made.

Authors: A.T. Gwathmey and A.F. Benton

Title: The Reaction of Gasses on the Surface of a Single Crystal of Copper I. Oxygen

Source: J. Physical Chemistry, 46, 969, 1942.

Summary: The authors observed the formation of oxides on the several surfaces of a single crystal of copper. The temperature range considered was 200°C to 1000°C. The partial pressure of oxygen was varied from 0.3 mmHg to atmospheric. No quantitative kinetic data were taken, but the authors observed significant differences in reaction rates on the various surfaces.

Authors: M.G. Hapase, M.K. Gharpurey and A.B. Biswas

Title: The Oxidation of Vacuum Deposited Films of Copper

Source: Surface Science, 9, 87, 1968.

Summary: The authors investigated the oxidation of thin films of copper formed by vapor deposition. Before oxidation the films were annealed under hydrogen at 250°C. The oxidation studies were carried out at temperatures of 150°C to 400°C under 70 mmHg of oxygen.

Authors: W.W. Harris, F.L. Ball and A.T. Gwathmey

Title: The Structure of Oxide Films Formed on Smooth Faces of a Single Crystal of Copper

Source: Acta Metallurgica, 5, 574, 1957.

Summary: The authors examined the oxide films formed on the various surfaces of a single crystal of copper. The oxidation was conducted in air at 150°C after annealing in hydrogen at 550°C. The oxide film was electrochemically stripped from the copper base and examined by transmission electron microscopy. Different morphologies were observed to form on each face. Generally, there were three main types of morphology observed: small nucleation particles, larger polyhedron-shaped particles and films.

Authors: B. Hearn, M.R. Hunt and A. Hayward

Title: Solubility of Cupric Oxide in Pure Subcritical and Supercritical Water

Source: J. Chem. Eng. Data, 14:4, 442, 1969.

Summary: The authors present solubility data in the range 50~500°C and 3500~6000 psig for  $\text{CuO}$  at a pH of 7.5.

Authors: G. Hultquist [12]  
Title: Short Communication: Hydrogen Evolution in Corrosion of Copper in Pure Water  
Source: Corrosion Science, 26:2, 173, 1986.  
Summary: The author conducted copper oxidation experiments by measuring the weight gain of copper foil and the amount of hydrogen produced. The reaction under consideration is the oxidation of copper by water to produce copper oxide and hydrogen. The experiments were conducted without oxygen control at a temperature of 297 K for a period of 650 h. The weight gain by the copper foil was used to verify the reaction measurements made with the hydrogen probe. Over the course of 650 h an average reaction rate of 0.11 nm/h was observed.

Authors: G. Hultquist, G.K. Chuah and K.L. Tan [54]  
Title: Comments on Hydrogen Evolution from the Corrosion of Pure Copper  
Source: Corrosion Science, 29:11/12, 1371, 1989.  
Summary: The authors conducted qualitative experiments to determine the nature of copper oxidation in water. Semipermeable membranes were used to conduct experiments with constant atmospheric conditions, constant hydrogen conditions and sealed atmosphere. Several corrosion products were observed including CuH, CuO, CuOH, Cu<sub>2</sub>O and Cu<sub>2</sub>OH. In the cases conducted with limited oxygen present, the copper reacted with the oxygen first. After the oxygen had been consumed it started reacting with the water to evolve hydrogen. No kinetic data were taken.

Authors: G. Hultquist, M. Seo, T. Leitner, C. Leygraf and N. Sato  
Title: The Dissolution Behavior of Iron, Chromium, Molybdenum and Copper from Pure Metals and from Ferritic Stainless Steels  
Source: Corrosion Science, 27, 937, 1989.  
Summary: The authors investigated the dissolution of the titular materials in water, saltwater and acid. Some measurements of enrichment are made.

Authors: D.H. Hur, H.S. Chung and U.C. Kim [16]  
Title: Corrosion Behaviors During the Iron Removal Process for Chemical Cleaning of Nuclear Steam Generators  
Source: Journal of Nuclear Materials, 224, 179, 1995.  
Summary: The authors investigated the dissolution of several SG construction materials using dynamic polarization. The test solutions included variation of the levels of EDTA hydrazine, NH<sub>4</sub>OH and synthetic sludges (mixtures of iron and copper oxides). Among their significant findings was the observation that the presence of sludge could increase the corrosion rate by up to a factor of thirty.

Authors: I.S. Hwang and I.-G. Park [3]  
Title: Control of Alkaline Stress Corrosion Cracking in Pressurized-Water Reactor  
Source: Corrosion, 55:6, 616, June 1999.  
Summary: The authors present a case study on the effect of SLS conditions on IGA/SCC in a steam generator at South Korea's Kori 1. Due to the use of copper tubing in the condensers, copper content in SG sludge was very high, over fifty percent of solids. It was hypothesized that copper oxidation during SLS promoted IGA/SCC. Reduction measures were implemented during heat-up, and a significant decrease in IGA/SCC tube failure was observed.

- Authors: K. Inouye, K. Ichimura, K. Kaneko and T. Ishikawa  
Title: The Effect of Copper(II) on the Formation of  $\gamma$ -FeOOH  
Source: Corrosion Science, 16, 507, 1976.  
Summary: The authors studied the effect of various levels of copper on the oxides of iron formed. They concluded that copper may promote the conversion of  $\gamma$ -FeOOH to  $\text{Fe}_3\text{O}_4$ , implying that the presence of copper may result in better passivation.
- Authors: R.J. Jacko [1]  
Title: Corrosion Evaluation of Thermally Treated Alloy 600 Tubing in Primary and Faulted Secondary Water Environments  
Source: EPRI NP-6721-SD, 1990.  
Summary: The author investigated the differences between mill annealed and thermally treated Alloy 600. As part of this investigation he carried out experiments to determine the effect of deposits on the corrosion potential and the corrosion rate of Alloy 600 in caustic solutions. It was found that levels of CuO as low as 0.1% could raise the corrosion potential. 0.045% CuO was found to significantly raise the corrosion potential in the presence of other sludge constituents. CuO levels of 0.01% were found to have no significant influence on the corrosion potential.
- Authors: G.C. Jain, B.K. Das and R. Avtar  
Title: Kinetics of the Oxidation of  $\text{CuFeO}_2$  in Cu-Fe-O System  
Source: Bulletin of Materials Science, 1, 99, 1979.  
Summary: The authors investigated the dry, high temperature (500°C to 900°C) oxidation of  $\text{CuFeO}_2$ . A reaction model was developed and kinetic data were presented.
- Authors: A.M. Khoviv and L.A. Malevskaya [35]  
Title: Kinetics of Low-Temperature Copper Oxidation in a Dry Oxygen Atmosphere  
Source: Inorganic Materials, 31, 988, 1995.  
Summary: The authors reported on the kinetics of copper oxidation. Using ellipsometry, they measured the thickness of the oxide film formed on polished copper in an oxygen atmosphere. They found that the growth of the oxide film thickness can be modeled with a power law,  $x = kt^n$ , with  $k$  and  $n$  being fitted parameters. They measured the growth of oxide films at several temperatures between 150°C and 250°C.
- Authors: A. Kishida, H. Takamatsu, H. Kitamura, S. Isobe, K. Onimura, K. Arioka, T. Hattori, T. Arai and M. Sato [5]  
Title: The Causes and Remedial Measures of Steam Generator Tube Intergranular Attack in Japanese PWR  
Source: 3<sup>rd</sup> International Symposium on Environmental Degradation of Materials in Nuclear Power Systems—Water Reactors, Traverse City, September, 1987.  
Summary: The authors reviewed the IGA/SCC history of several Japanese plants and attempted to correlate these findings with plant operating conditions. One significant finding was that copper oxides were present in those plants that had the most extensive IGA. It was also determined that the presence of cuprite or tenorite will significantly raise the corrosion potential of Alloy 600 (by several hundred mV).

- Authors: P. Kofstad  
Title: Oxidation of Metals: Determination of Activation Energies  
Source: Nature, 179, 1362, 1957.  
Summary: The author presents a novel technique for determining the temperature dependency of reaction rate constants. During the course of the oxidation experiment the temperature is raised in a linear fashion. Using an *a priori* rate law, the transient reaction rate is measured. A parametric relationship between the reaction rate and the temperature is obtained. This technique is useful only when the rate law (e.g., parabolic, logarithmic, etc.) is known over the entire temperature range of interest.
- Authors: P.K. Krishnamoorthy and S.C. Sircar [31]  
Title: Effect of an Applied Electric Current on the Rate of Oxidation of Copper at Room Temperature  
Source: Acta Metallurgica, 16, 1461, 1968.  
Summary: The authors used electrometric measurement of oxide thickness to investigate the room temperature (30°C) oxidation of copper films. To determine the validity of the Cabrera-Mott theory of space charge influenced cation diffusivity an external electrical charge was imposed on the copper to be oxidized. The results were in agreement with the theory to be tested.
- Authors: P.K. Krishnamoorthy and S.C. Sircar  
Title: Oxidation Kinetics of Copper in the Thin Film Range  
Source: Acta Metallurgica, 17, 1009, 1969.  
Summary: The authors investigated the kinetics of the oxidation of copper in its earliest stages. The temperature range considered was 65°C to 120°C. However, the data presented were manipulated in an undescribed manner.
- Authors: P.K. Krishnamoorthy and S.C. Sircar [8]  
Title: Influence of Oxygen Pressure on the Oxidation Kinetics of Copper in Dry Air at Room Temperature  
Source: J. Electrochemical Society, 116, 734, 1969.  
Summary: The authors investigated the rate of oxidation of polished copper at room temperature in air under various pressures of oxygen (0.01 to 0.21 atm). They found that the growth of copper oxide could be modeled with the logarithmic growth law of Cabrera and Mott.
- Authors: O. Kubaschewski, E.L. Evans and C.B. Alcock [14]  
Title: Metallurgical Thermochemistry  
Source: Pergamon Press, Oxford, 1967.  
Summary: A standard textbook. Includes a discussion of dissociation pressures and useful tables of thermodynamic data.

- Authors: C. Laire, G. Platbrood and J. Stubbe  
Title: Characterization of the Secondary Side Deposits of Pulled Steam Generator Tubes  
Source: 7<sup>th</sup> International Symposium on Environmental Degradation of Materials in Nuclear Power Systems—Water Reactors, Breckenridge, August 7–10, 1995.  
Summary: The authors investigated tubes pulled from several Belgian plants. The deposits consisted mostly of iron with many other species present in minor quantities. Copper was more prevalent in the free span area. Most copper was present in metallic form, but some oxides were detected. Oils and carboxylates were present. There was a chromium oxide layer present at the metal/oxide interface.
- Authors: D. Landolt, R.H. Muller and C.W. Tobias [39]  
Title: High Rate Anodic Dissolution of Copper  
Source: J. Electrochemical Society, 116, 1384, 1969.  
Summary: The authors investigated the dissolution of copper in a solution of  $\text{KNO}_3$  and  $\text{K}_2\text{SO}_4$  using dynamic polarization in a flow cell. They found that the passivation of copper is impaired by the imposition of a high flow rate ( $\geq 400$  cm/s).
- Authors: M.A.H. Lanyon and B.M.W. Trapnell  
Title: The Interaction of Oxygen with Clean Metal Surfaces  
Source: Proceedings of the Royal Society, A227, 387, 1955.  
Summary: The authors investigated adsorption of oxygen onto metal surfaces. Among those studied was copper. However, the authors found that oxygen would not adsorb onto the metal, but would react with it to form an oxide.
- Authors: D. Lazarus [52]  
Title: Diffusion in Metals  
Source: Solid State Physics, 10, 71, 1960.  
Summary: The author reviewed the then current understanding of diffusion in metals including a discussion on vacancy diffusion and self diffusion. Various activation energies associated with diffusion constants were discussed.
- Authors: M. Lenglet, K. Kartouni and D. Delahaye [9]  
Title: Characterization of Copper Oxidation by Linear Potential Sweep Voltammetry and UV-Visible-NIR Diffuse Reflectance Spectroscopy  
Source: J. Applied Electrochemistry, 21, 697, 1991.  
Summary: The authors used the two titular analytical techniques to observe the oxidation of copper. It was observed that during the initial phases of oxidation copper first forms a compound  $\text{Cu}_x\text{O}$  with a similar crystalline structure to  $\text{Cu}_2\text{O}$  but in which Cu has a mixed valence between Cu(I) and Cu(0). As oxidation continues the oxide becomes  $\text{Cu}_2\text{O}$  with a high concentration of crystal defects. Finally, the oxide develops into  $\text{CuO}$ .

Authors: J.S. Lewis  
Title: The Reduction of Copper Oxide by Hydrogen  
Source: J. Chemical Society, 820, 1932.  
Summary: The author investigated the reduction of copper oxide by hydrogen gas. It was found that the water that forms during the reaction coats the oxide, protecting it from further reduction. This mechanism was not as significant at high temperatures. The author suggested that the water might form a complex with the oxide. Drying of the copper oxide before reduction sped the reaction.

Authors: A. Manara, V. Sirtori and L. Mammarella [11]  
Title: Optical Ellipsometry and Electron Spectroscopy Studies of Copper Oxidation Related to Copper on Printed Circuit Boards  
Source: Surface and Interface Analysis, 18, 32, 1992.  
Summary: The authors measured the rate of growth of oxides of polished copper using ellipsometry and electron spectroscopy. They found that the growth of the oxide thickness followed a parabolic rate law. During the initial stages of oxidation (first 5 minutes) they found that the oxide was  $\text{Cu}_2\text{O}$ . After the initial stages, the oxide was composed of two layers, a layer of  $\text{Cu}_2\text{O}$  in contact with the metal interface and a layer of  $\text{CuO}$  above that.

Authors: D.S. Mancey  
Title: Corrosion of Carbon Steel Support Structures at Their Intersection with Steam Generator Tubes During Crevice Cleaning  
Source: Water Chemistry of Nuclear Reactor Systems 7, BNES, 1996.  
Summary: The author investigated the acid dissolution of magnetite and postulated that the electron source for this reaction may be metallic iron. Hence the auto reduction of iron may lead to iron dissolution.

Authors: T.Kh. Margulova and Yu.M. Kostrikin [21]  
Title: On the Mechanism of Copper Deposit Formation  
Source: Thermal Engineering, 15, 72, 1968.  
Summary: The authors present the hypothesis that copper ammonia complexes are a transition state in the formation of copper inclusions in deposits. The ammonia dissolves copper ions and at the heat source is vaporized, leaving behind metallic copper inclusions near the tube wall.

Authors: G.N. Markos'yan and A.I. Molodov  
Title: Kinetics of Univalent Copper Oxidation by Oxygen  
Source: Russian J. of Electrochemistry, 31, 249, 1995.  
Summary: The authors investigated the oxidation of thin films of  $\text{CuCl}$  to  $\text{CuCl}_2$ . The reaction kinetics are presented.

Authors: J.T. Mason and J.G. Reagan  
Title: Cleaning Copper in Hydrogen Peroxide-Sulfuric Acid  
Source: Metal Finishing, 97, June 1986.  
Summary: The authors investigate the dissolution of copper oxide in the two titular solutions.

Authors: G.B. McGarvey and D.G. Owen

Title: Copper (II) Oxide as a Morphology Directing Agent in the Hydrothermal Crystallization of Magnetite.

Source: J. Materials Science, 31, 49, 1996.

Summary: The authors conducted an autoclave experiment on the conversion of hematite to magnetite in the presence of hydrazine at 150~175°C. The influence of the presence of several transition metals was observed. Only copper (CuO) was found to have a significant impact. CuO catalyzed the conversion of hematite to magnetite through reduction to copper metal and reoxidation. Some copper was also found to dissolve. The dissolution of copper was attributed in part to the presence of ammonia from the degradation of the hydrazine.

Authors: N.S. McIntyre, R.D. Davidson, T.L. Walzak, A.M. Brennenstuhl, F. Gonzalez and S. Corazza

Title: The Corrosion of Steam Generator Surfaces Under Typical Secondary Coolant Conditions: Effects of pH Excursions on the Alloy Surface Composition

Source: Corrosion Science, 37:7, 1059, 1995.

Summary: The authors investigated the effect of various time-pH profiles on the corrosion of several alloys. SEM with X-ray backscattering, X-ray photo-electron spectroscopy, optical microscopy and impedance measurements were used to characterize the oxide formed. Processing history was found to have a significant impact on the nature of the oxide formed.

Authors: N.S. McIntyre, T.E. Rummery, M.G. Cook and D. Owen

Title: X-ray Photoelectron Spectroscopy Study of the Aqueous Oxidation of Monel-400

Source: J. Electrochemical Society, 123, 1164, 1976.

Summary: The authors investigated the nature of the oxidation of the titular alloy. It was determined that a film of  $\text{Ni}(\text{OH})_2$  forms on the metal surface which subsequently converts to NiO. The conversion to NiO is faster at higher pH values.

Authors: W. McKewan and W.M. Fassel

Title: High Pressure Oxidation Rate of Metals—Copper in Oxygen

Source: J. of Metals, 1127, September, 1953.

Summary: The authors investigate the oxidation of copper at 600°C to 900°C under an oxygen pressure of 14.7 to 400 psi. The oxygen pressure was found to have no effect on the reaction kinetics.

Authors: S.P. Mehrotra

Title: Analysis of Kinetics of Oxidation/Reduction of Metal Sulfides Using the Concept of Distributed Reaction Rates

Source: Proceeding of the International Conference on Recent Advances in Chemical Engineering, 224, 1989.

Summary: The author presents a novel model to describe oxidation and reduction rates using a distribution of rate constants to account for surface inhomogeneities. However, since this distribution can only be measured in average it is not necessarily useful.

Authors: L.F. Melo and J.D. Pinheiro  
Title: Particle Transport in Fouling Caused by Kaolin-Water Suspensions on Copper Tubes  
Source: Canadian J. of Chemical Engineering, 66, 36, 1988.  
Summary: The authors investigated particle deposition on copper tubing. Their model was essentially a diffusion model in which deposition on the tube was a consumptive reaction.

Authors: H.A. Miley  
Title: Copper Oxide Films  
Source: J. American Chemical Society, 59, 2626, 1937.  
Summary: The author presents the details of electrometric measurement of oxide films and uses this technique to investigate the kinetics of copper oxidation at relatively moderate temperatures (94°C and higher).

Authors: P.J. Millett and J.M. Fenton [58]  
Title: Measurement of Effective Diffusion Coefficients for Chloride Salts in Nonprotective Magnetite  
Source: Corrosion, 46:9, 710, 1990.  
Summary: The authors conducted reverse denting experiments to measure the effective diffusivity of sodium and chloride ions through packed magnetite. The authors used literature values of the unrestricted diffusivity and measurements of the porosity of the magnetite to calculate a lithologic factor. The lithologic factor is equivalent to the tortuosity. The tortuosities reported ranged from 10 to 30.

Authors: P.J. Millett and J.M. Fenton [20]  
Title: High Temperature, Aqueous-phase Diffusion of NaCl through Simulated Deposits of Corrosion Products  
Source: Corrosion, 49:7, 536, 1993.  
Summary: The authors conducted membrane diffusion experiments using synthetic deposits packed between titanium screens. Three deposits were tested: sintered stainless steel, packed magnetite and packed carbon fibers. Literature values of the diffusivity were used to calculate a tortuosity factor from the measured effective diffusivity and the void fraction. For magnetite, over the range 25°C to 275°C the tortuosity ranged from 1 to 2, being slightly higher at higher temperatures.

Authors: T. Mills and U.R. Evans [25]  
Title: The Effect of Sulphur Dioxide on the Oxidation of Copper  
Source: J. Chemical Society, London, 2186, 1956.  
Summary: The authors investigate the oxidation of copper by oxygen in the presence and absence of sulfur dioxide. Prior to oxidation the copper samples were heated in hydrogen to reduce the surface. Electrometric measurements were used to measure the oxide film growth. A two region logarithmic growth law was observed to fit the data well for the case without sulfur dioxide. Changes in the oxygen pressure had no effect on the oxidation rate. The authors postulated that the change in the oxidation rate from one logarithmic relationship to another was due to a phase change in the copper oxide. Additional material was presented on the effects of the presence of sulfur dioxide.



- Authors: I. Milošev, M. Metikoš-Hukovic, M. Drogowska, H. Ménard and L. Brossard  
Title: Breakdown of Passive Film on Copper in Bicarbonate Solutions Containing Sulfate Ions.  
Source: Journal of Electrochemical Society, 139:9, 2409, 1992.  
Summary: The authors conducted a rotating electrode potentiodynamic corrosion study. Carbonate ions were found to suppress pitting but accelerate general corrosion. Carbonates suppressed the accelerative effect of sulfate ions.
- Authors: M. Moliere, Y. Verdier and C. Leymonie  
Title: Oxidation of Copper in High Purity Water at 70°C: Application to Electric Generator Operation  
Source: Corrosion Science, 30:2/3, 183, 1990.  
Summary: The authors examined the corrosion of copper foils in water. Three phases of corrosion were found: dissolution, particle shedding and oxide film growth. Low dissolved oxygen levels led to particle shedding while higher levels led to the formation of a passivating film. The protective film formed within about 200 h.
- Authors: W.J. Moore, Y. Ebisuzaki and J.A. Sluss  
Title: Exchange and Diffusion of Oxygen in Crystalline Cuprous Oxide  
Source: J. American Chemical Society, 62, 1438, 1958.  
Summary: The authors used radioactive oxygen gas to measure the diffusion of oxygen into cuprous oxide samples. Over the range of 1030°C to 1120°C at a partial oxygen pressure of 0.178 atm, the diffusion rate activation energy was 39.3 kcal/mol and the pre-exponential constant was 0.0065 cm<sup>2</sup>/s.
- Authors: W.J. Moore and B. Selikson  
Title: The Diffusion of Copper in Cuprous Oxide  
Source: J. Chemical Physics, 19:12, 1539, 1951.  
Summary: The authors used radioactive copper to measure the diffusion of copper ions through a cuprous oxide sample. A strip of cuprous oxide was immersed in an active cupric nitrate solution. After immersion, the oxide was electrolytically dissolved in stages and the activity concentration of each successively removed layer was measured. Over the temperature range from 800°C to 1050°C the activation energy for the diffusion constant was found to be 36.1 kcal/mol. The pre-exponential constant was 0.0436 cm<sup>2</sup>/s. These values were found to accord with a parabolic reaction rate constant of four times the diffusion coefficient.
- Authors: S. Mrowec and A. Stoklosa [10]  
Title: High Temperature Oxidation of Copper  
Source: Bulletin de L'Académie Polonaise des Sciences: Série des Sciences Chimiques, 18, 531, 1970.  
Title: Oxidation of Copper at High Temperatures  
Source: Oxidation of Metals, 3:3, 291, 1971.  
Summary: The authors reported on the kinetics of copper oxidation. Using gravimetry they measured the mass gains due to oxidation of clean copper exposed to varying pressures of oxygen (0 to 0.8 atm) at several temperatures (900°C to 1050°C). They found that the growth of the film followed a parabolic growth law,  $x^2 = kt$ , where  $k$  was found to depend on the oxygen pressure and the temperature.

Authors: J.R. Myers and A. Cohen  
Title: Pitting Corrosion of Copper in Cold Potable Water Systems  
Source: Materials Performance, 34:10, 60, 1995.  
Summary: The authors briefly reviewed the current understanding of pitting of copper tubing and discuss chemistry controls to avoid pitting. The cathodic depolarization of copper surfaces by carbon dioxide is mentioned.

Authors: R. Oliveira, L. Melo, M. Pinheiro and M.J. Vieira  
Title: Surface Interactions and Deposit Growth in Fouling of Heat Exchangers  
Source: Corrosion Reviews, 11, 55, 1993.  
Summary: The authors reviewed the current understanding of fouling due to particle deposition. Transport, adhesion and removal of particles were discussed.

Authors: R.J. Orth, R.S. Parikh and K.C. Liddell  
Title: Application of the Rotating Ring-Disk Electrode in Determining the Second-Order Rate Constant for the Reaction Between Cu(I) and Fe(III) in 1.0 mol/dm<sup>3</sup> HCl  
Source: J. Electrochemical Society, 136, 2924, 1989.  
Summary: The authors assumed that the reaction is in part diffusion controlled and used the kinematics of the fluid flow around the rotating disk to eliminate these effects and determine the true reaction rate constants.

Authors: R.N. Pease and H.S. Taylor  
Title: The Reduction of Copper Oxide by Hydrogen  
Source: J. American Chemical Society, 43, 2179, 1921.  
Summary: The authors investigated the reduction of copper oxide at 150°C to 200°C in a hydrogen atmosphere. At lower temperatures there was an incubation period before reduction started. Water was found to inhibit the reduction of the oxide. The reaction was determined to be autocatalytic, taking place at the copper metal/oxide boundary.

Authors: R.N. Pease and H.S. Taylor  
Title: The Catalytic Formation of Water Vapor from Hydrogen and Oxygen in the Presence of Copper and Copper Oxide  
Source: J. American Chemical Society, 44, 1637, 1922.  
Summary: The authors investigated catalytic properties of copper. Oxygen was found not to adsorb to any great extent on copper oxide. It was found that the reaction proceeded through the oxidation of copper metal by the oxygen followed by the reduction of the oxide by hydrogen. The kinetics are complicated by the simultaneous oxidation of copper and hydrogen which compete for the available oxygen. The reaction is highly temperature dependent proceeding rapidly to completion at 200°C and not proceeding at all at 100°C.

- Authors: E. Pierson and C. Laire [17]  
Title: The Influence of Copper on the SCC of Alloy 600 and Alloy 690 Steam Generator Tubes  
Source: Fontevraud IV, 381, September, 1998.  
Summary: The authors conducted capsule tests with acid solutions containing copper and copper oxide powders. Alloy 690 showed accelerated corrosion in the presence of copper and copper oxides. Hydrogen overpressures eliminated the acceleratory effect of the copper compounds. The authors concluded that the change in electrochemical potential was not sufficient to account for the acceleration and postulated a catalytic function for the copper.
- Authors: E. Pierson, J. Stubbe and G. Deny [6]  
Title: Stress Corrosion Cracking of Alloys 690, 800 and 600 in Acid Environments Containing Copper Oxides  
Source: Paper 119, Corrosion 96, 1996.  
Summary: The authors used capsule tests to investigate the formation of cracks in the titular alloys. In some environments, the presence of copper oxides was found to accelerate cracking. The presence of organic species was also found to significantly accelerate cracking. Hydrogen gas was determined to negate the effect of copper oxides.
- Authors: M.R. Pinnel, H.G. Tompkins and D.E. Heath [33]  
Title: Oxidation of Copper in Controlled Clean Air and Standard Laboratory Air at 50° to 150°C  
Source: Applied Surface Science, 2, 558, 1979.  
Summary: The authors investigated the oxidation of copper in air in the titular temperature range. The authors present data for film thickness as a function of time. The impurities present in normal laboratory air were found to significantly impact the kinetics of oxidation. A growth model was presented based on a parabolic law which ignored the initial stages of growth.
- Authors: G.M. Raynaud, W.A.T. Clark and R.A. Rapp  
Title: *In Situ* Observation of Copper Oxidation at High Temperatures  
Source: Metallurgical Transactions, 15A, 573, 1984.  
Summary: The authors observed the oxidation of copper on an ESEM hot stage. The reaction temperature was above 850°C. No kinetic data were taken. However, many microphotographs were shown which lead to insights about high temperature oxidation.
- Authors: T.N. Rhodin, Jr. [51]  
Title: Low Temperature Oxidation of Copper. I. Physical Mechanism  
Source: J. American Chemical Society, 72, 5102, 1950.  
Summary: The author investigated the kinetics of copper oxidation over the temperature range of 78K to 353K. Oxygen pressures ranging from 0.001 to 100 mmHg were investigated. Oxygen pressure had no effect over this range. Below 323K a logarithmic type growth law was found to agree well with the data. The experiments were carried out using single crystal, high purity copper that had been through a reduction process prior to oxidation.

Authors: T.N. Rhodin, Jr.

Title: The Anisotropy of Nitrogen Adsorption on Single Crystal Copper Surface

Source: J. American Chemical Society, 72, 5691, 1950.

Summary: The author observed the tendency of nitrogen to adsorb differently on different faces of a single crystal copper sample. It was suggested that these observations were linked to the previously observed differences in oxidation kinetics of the various faces.

Authors: A. Rönquist and H. Fischmeister

Title: The Oxidation of Copper—A Review of the Published Data

Source: J. Institute of Metals, 89, 65, 1960.

Summary: The authors reviewed the data available in the literature. A discussion of the various measurement techniques is included. The rate laws and their theoretical basis are reviewed. Discussion of other topics include: pre-oxidation preparation, single crystal anisotropy and oxide composition and structure.

Authors: S.K. Roy, S.K. Bose and S.C. Sircar [34]

Title: Pressure Dependencies of Copper Oxidation for Low and High Temperature Parabolic Laws

Source: Oxidation of Metals, 35:1/2, 1, 1991.

Summary: The authors investigate the growth of copper oxide films on polished copper. They used electrometric and gravimetric techniques to measure the growth rate. They studied growth at low temperature (383K to 398K) and high temperature (1123 K) under various oxygen pressures (0.278 to 21.27 kPa). They found that the growth of oxides could be modeled using a parabolic growth law,  $x^2 = kt$ , where  $k$  depended on both temperature and oxygen pressure.

Authors: S.K. Roy, P.K. Krishnamoorthy and S.C. Sircar [32]

Title: Kinetics of Oxidation of Copper at Low Temperatures Under the Influence of Externally Induced Current Flow

Source: Acta Metallurgica, 18, 519, 1970.

Summary: The authors investigated the kinetics of copper oxidation in dry air at 75°C, 90°C and 101°C using an externally applied current to accelerate or decelerate the reaction kinetics. 75°C was found to be the boundary between logarithmic and parabolic growth. The copper began oxidation with a 10 Å film of oxide already present.

Authors: S.K. Roy and S.C. Sircar

Title: A Critical Appraisal of the Logarithmic Rate Law in Thin-Film Formation During Oxidation of Copper and Its Alloys

Source: Oxidation of Metals, 15:1/2, 9, 1981.

Summary: The authors investigated the kinetics of copper oxidation at temperatures between 75°C and 100°C. A logarithmic rate law with temperature dependent rate constants was found to fit the data well. Data are presented as rate law constants.

- Authors: P. Saurin, M. Clinard, M. Organisa, J.M. Fiquet and J.P. Veysset  
Title: Copper Elimination During Secondary Side Chemical Cleaning  
Source: Paper 53, Water Chemistry of Nuclear Reactor Systems 6, BNES, 1992.  
Summary: The authors describe the chemical cleaning of steam generators using gluconic and citric acid.
- Authors: J.A. Sawicki, M.E. Brett and R.L. Tapping [4]  
Title: Corrosion-Product Transport, Oxidation State and Remedial Measures  
Source: Paper 30, 3<sup>rd</sup> Int. Steam Generator and Heat Exchanger Conference, Toronto, 1998.  
Summary: The authors discuss the formation and transport of oxides using observations made at Ontario Hydro plants. They review the chemistry of corrosion products, mechanisms for transportation within a water system and measures taken to monitor and reduce corrosion product formation and transport.
- Authors: M. Seo, J. Guo, G. Hultquist, C. Leygraf and N. Sato  
Title: The Effect of Copper Addition on Electrochemical Behavior and Surface Composition of Ferritic Stainless Steel in Sulfuric Acid Solution  
Source: 10<sup>th</sup> International Conference on Metal Corrosion, Paper 2.11, Madras, 1987.  
Summary: The authors investigated the influence of copper on the corrosion of steel through dynamic potentiometry. Although the copper slowed the corrosion rate of steel, it reduced the passivity.
- Authors: T. Shahrabi, R.C. Newman and K. Sieradzki  
Title: Stress-Corrosion Cracking of Alpha-Brass without Copper Oxidation  
Source: J. Electrochemical Society, 140, 348, 1993.  
Summary: The authors investigated the initiation and propagation of transgranular cracks in the presence and absence of Cu(I) and Cu(II).
- Authors: J.P. Simpson and R. Schenk [13]  
Title: Short Communication: Hydrogen Evolution from Corrosion of Pure Copper  
Source: Corrosion Science, 27, 1365, 1987.  
Summary: The authors studied the reactions of copper in chloride solution. No hydrogen evolution was observed. No oxygen was present in the experiment. The authors repudiated Hultquist's findings.
- Authors: M. Sotto, S. Gauthier, F. Pourmir, S. Rousset and J. Klein  
Title: LEED Study of Activated Nitrogen Adsorption on (100) and (h11) Faces of Copper  
Source: Surface Science, 371, 36, 1997.  
Summary: The authors use low energy electron dispersion to measure the adsorption of nitrogen onto copper at room temperature and low pressures ( $10^{-7}$ ~ $10^{-3}$  torr). They found that nitrogen saturates when covering ~1% of the surface.
- Authors: A. Spitzer and H. Lüth  
Title: An XPS Study of the Water Adsorption on Cu(110)  
Source: Surface Science, 160, 353, 1985.  
Summary: The authors investigated the adsorption of water vapor onto copper at very low temperatures and pressures.

- Authors: F.G. Straub  
Title: Comparison of the Reducing Power of Sodium Sulfite and Hydrazine in the Steam-Water Cycle of Steam Power Plants  
Source: Combustion, 34, January, 1957.  
Summary: The author investigated the ability of the titular reductants to reduce copper oxide in a flow through reactor with a residence time on the order of 3 to 5 minutes. CuO will completely oxidize hydrazine, but it is not clear if it is reduced in the process or only acts as a catalyst. The reduction of CuO goes to completion at 300°F but does not progress at all below 120°F. Fe<sub>2</sub>O<sub>3</sub> is completely reduced by hydrazine over 500°F but not reduced at all below 280°F. Hydrazine oxidation by oxygen is relatively slow. There is a slight, but statistically significant, pH effect.
- Authors: J. Stubbe, C. Laire, E. Pierson, G. Platbrood and P. Van Royen  
Title: Corrosion Secondaire des GV de Doel 4: Le Plomb et le Cuivre Sont-Ils Impliqués?  
Source: Fontevraud III, 1994.  
Summary: The authors present a case study on Doel 4. The effects of a recent chemical cleaning are addressed. Copper is indicated to have an adverse effect. Copper may also catalyze the formation of organic acids.
- Authors: A.W. Swanson and H.H. Uhlig  
Title: The Initial Oxidation Rates of Single-Crystal Copper and the Effects of Gaseous Pretreatment  
Source: Solid State Science, 118:8, 1325, 1971.  
Summary: The authors investigated the kinetics of copper oxidation on different faces of a single crystal. Oxidation was observed to proceed anisotropically. Kinetics data are presented and a two stage logarithmic growth law is proposed.
- Authors: A.W. Swanson and H.H. Uhlig [26]  
Title: Effect of Gaseous Pretreatment on Oxidation of Iron  
Source: J. Electrochemical Society, 121, 1551, 1974.  
Summary: The authors gathered data on the rate of oxidation of iron after various pretreatments. The logarithmic rate law was found to describe the data well. The rate constants were heavily dependent on the pretreatment used. The authors argue that pretreatment affects the crystal orientation of the oxide formed.
- Authors: H.G. Tompkins and M.R. Pinnel  
Title: On the Rate—Controlling Step of Copper Diffusion/Oxidation through Gold  
Source: J. Applied Physics, 50, 7243, 1979.  
Summary: The authors postulate a simple diffusion problem for determination of the limiting step in copper oxidation. A film of gold is laid over a copper surface. Copper diffuses through small pores in the gold film to reach the ambient air where it oxidizes. The authors use a parabolic growth law to model the reaction rate.

- Authors: D. Tromans and R.-H. Sun  
Title: Anodic Behavior of Copper in Weakly Alkaline Solutions  
Source: J. Electrochemical Society, 139:7, 1945, 1992.  
Summary: The authors investigated the effect of various environmental parameters on the dissolution rate of copper at 25°C. The solubility of CuO was found to have a minimum at a pH of ~8.8. Changes in the pH can disrupt the passivating film. In the presence of sulfates and chlorides, pH has an amplified impact. Formation of hydrogen ions on the surface can lower the local pH leading to higher rates of dissolution.
- Authors: R.F. Tylecote  
Title: Review of Published Information on the Oxidation and Scaling of Copper and Copper Based Alloys  
Source: J. Institute of Metals, 78, 25, 1950.  
Summary: The author reviews analytical methods for studying oxide formation. Various mechanisms for formation are discussed.
- Authors: R.F. Tylecote  
Title: The Oxidation of Copper in the Temperature Range 200°–800° C  
Source: J. Institute of Metals, 81, 681, 1952.  
Summary: The author investigated the oxidation of copper in the titular temperature range. The samples were pretreated by heating in nitrogen and hydrogen at 500°C. Moisture was found to have no effect on the oxidation rate. Oxidation in pure oxygen was slower than in filtered lab air.
- Authors: R.F. Tylecote and R. Eborall  
Title: The Adherence of Oxide Scales on Copper  
Source: J. Institute of Metals, 78, 301, 1950.  
Summary: The author investigates the morphologies of copper oxides formed at high temperatures.
- Authors: M.V. Vazquez, S.R. de Sanchez, E.J. Calvo and D.J. Schiffrin  
Title: The Electrochemical Reduction of Hydrogen Peroxide on Polycrystalline Copper in Borax Buffer  
Source: Journal of Electroanalytical Chemistry, 374, 179, 1994.  
Summary: The authors performed a potentiodynamic corrosion study on copper dissolution. A Cu<sub>2</sub>O/CuO conversion cycle was found to catalyze the decomposition of H<sub>2</sub>O<sub>2</sub>. Chloride ions were found to inhibit the catalysis by increasing the solubility of the copper.
- Authors: T.J. Wen, C.H. Liang, T.C. Huang, T.C. Cheng, H.C. Wang, R.F. Sheng and C.S. Huang  
Title: Feedwater Iron Crud Reduction for Chinshan Nuclear Power Station  
Source: Paper 26, Water Chemistry of Nuclear Reactor Systems 6, BNES, 1992.  
Summary: The authors describe dry layup procedures for a BWR.

- Authors: E.L. White and W.E. Berry  
Title: Effects of Copper and Nickel Compounds on the Corrosion of Pressurized Water Reactor Steam Generator Materials  
Source: Nuclear Technology, 55, 135, 1981.  
Summary: The authors conducted autoclave investigations into the corrosion of Alloy 600. Copper oxide was not found to have a significant effect.
- Authors: E.L. White, W.E. Berry and W.K. Boyd [18]  
Title: Effect of Copper Oxides on the Stress Corrosion Cracking of Inconel Alloy 600  
Source: International Copper Research Association Project #N33403-1, INCRA Res. Rep. 285, October 1977.  
Summary: The authors conducted strain testing in an autoclave. The experiments were conducted in a 50% NaOH solution at 550°F. High levels of copper oxide had a pronounced effect. Lower levels did not have a significant impact.
- Authors: A.B. Winterbottom [29]  
Title: Polarimetric Studies of Oxide Film Formation on Metals  
Source: Nature, 364, August 28, 1937.  
Summary: The author presents details on making polarimetric measurements of oxide film thickness. Data are presented for copper oxide film growth at low temperatures (14°C, 18°C and 95°C). The copper was pretreated by heating under hydrogen gas.
- Authors: A. Yanase, H. Matsui, K. Tanaka and H. Komiyama  
Title: Optical Observation of Oxidation and Reduction of Small Supported Copper Particles  
Source: Surface Science 219, L601, 1989.  
Summary: The authors observe the oxidation of small (4 to 10 nm) copper particles. They found that initially the copper oxidizes to an intermediate form  $\text{CuO}_x$ , with  $x = 0.67$  before converting to  $\text{CuO}$ .
- Authors: F.W. Young, Jr., J.V. Cathcart and A.T. Gwathmey  
Title: The Rates of Oxidation of Several Faces of a Single Crystal of Copper as Determined with Elliptically Polarized Light  
Source: Acta Metallurgica, 4, 145, 1956.  
Summary: The authors observed the oxidation rates on several faces of a single crystal copper sample. The copper was pretreated by annealing in hydrogen at 500°C. The specimen was oxidized in pure dried oxygen. Polarizing spectrophotometry was used to measure the film thickness. The temperature of the experiment ranged from 70°C to 178°C. Significant anisotropy was found.
- Authors: V.I. Zarembo, V.G. Kritskii, A.A. Slobodov and L.V. Puchkov  
Title: Behavior of Copper Corrosion Products in Water Loops of Heat-Exchange Units  
Source: Journal of Applied Chemistry of the USSR, 62:1, 63, January 1989.  
Summary: The authors calculate the free energy phase diagrams for copper and iron species in water. Other species included in the calculations are amines and hydrazine.



Authors: T.R. Zhao and H. Takei  
Title: Study of the Oxidation and Reduction Kinetics of Copper Iron Oxide [CuFeO<sub>2</sub>] in the Cu-Fe-O System  
Source: Materials Research Bulletin, 32:10, 1377, 1997.  
Summary: The authors investigated the oxidation of CuFeO<sub>2</sub> at high temperatures.

Authors: L. zur Nedden, J. Stubbe and E. Pierson  
Title: Effect of Simulated Outage Conditions in Acid Environment Containing Copper on Corrosion of Steam Generator Tubes  
Source: 8<sup>th</sup> International Symposium on Environmental Degradation of Materials in Nuclear Power Systems—Water Reactors, Amelia Island, August, 1997.  
Summary: The authors used capsule tests to investigate the influence of copper and copper oxides on steam generator tube corrosion. Metallic copper was found to be benign while copper oxides accelerated corrosion. Metallic copper that had been exposed to air was also detrimental.



# **B**

## **FILM THICKNESS AS A FUNCTION OF FRACTION OF OXIDE**

---

### **Purpose**

The purpose of this calculation is to provide a means to convert oxide weight fraction to film thickness for the formation of an oxide film on copper particles.

### **Summary of Results**

The calculation allows the prediction of oxide film thickness  $x$  as a linear function of the oxide weight content  $\eta$  (for  $\eta$  less than 0.5), given the initial radius of the particle  $r_o$ :

$$x \approx 0.545r_o\eta \quad \text{[B-1]}$$

### **Calculation Input Requirements**

- Specific surface area,  $a$
- Densities and molecular weights of Cu and Cu<sub>2</sub>O

### **References**

B.1 Stecher, P.G., *The Merck Index*, Eighth Edition, Merck & Co., Inc., Rahway, 1968.

### **Assumptions**

The powder is assumed to be monodispersed spherical copper particles although the actual dispersion and shape of the particles are unknown. The specific surface area is used to calculate an area-weighted average radius, which is the most appropriate for the determination of an area-related phenomenon. Therefore, the assumption of monodispersed sphericity is reasonable for the manipulations made here.

## Analysis

In order to calculate the oxide film thickness from an oxide fraction, it is first necessary to determine the radius of the particles. The first section of the analysis provides a method for determining an area-weighted average radius from a specific surface area measurement. The second section provides a method for calculating the thickness of an oxide layer when the oxide fraction is less than 50%. The third section provides a simpler approximation that is valid for oxide fractions of less than about 5%.

### Calculation of the Area-Weighted Average Radius

The specific surface area is defined as the surface area of a sample divided by its mass. If the sample is taken to be a set of uniformly sized spherical particles, then the formulae for the volume and area of a sphere can be substituted into this definition:

$$a = \frac{\text{area}}{\text{mass}} = \frac{4\pi r^2}{\rho_{Cu} \frac{4}{3}\pi r^3} = \frac{3}{\rho_{Cu} r} \quad [\text{B-2}]$$

This equation can be rearranged so that a radius can be calculated from a known specific surface area:

$$r = \frac{3}{\rho_{Cu} a} \quad [\text{B-3}]$$

### Spherical Approximation

At some time of interest, a copper metal core is surrounded by a crust of cuprite. Because the cuprite has a lower density than the copper metal, the particle radius,  $R$ , is somewhat larger than the initial radius,  $r_o$ . A copper balance indicates that the mass of copper before oxidation must equal the mass of copper at any subsequent time:

$$\rho_{Cu} r_o^3 = \rho_{Cu} r^3 + \rho_{Cu2O} \frac{MW_{2Cu}}{MW_{Cu2O}} (R^3 - r^3) \quad [\text{B-4}]$$

Note that the factor  $4\pi/3$  cancels out of this equation.

The mass fraction of oxide is defined as the mass of oxide divided by the sum of the mass of the oxide and the mass of the metallic copper core:

$$\eta = \frac{\rho_{Cu2O} (R^3 - r^3)}{\rho_{Cu2O} (R^3 - r^3) + \rho_{Cu} r^3} \quad [\text{B-5}]$$

Note that this definition is preferred to the fraction of copper mass converted from metal to cuprite because of the XRD technique used to measure oxide content. However, the distinction is not too important because oxygen makes up only 11.2% of the mass of cuprite.

This definition of  $\eta$  can be rearranged to give  $R^3$  in terms of  $r^3$ :

$$R^3 = r^3 \frac{1 + \eta \left( \frac{\rho_{Cu}}{\rho_{Cu2O}} - 1 \right)}{1 - \eta} \quad [B-6]$$

Substituting this expression into the equation for the copper balance yields:

$$\rho_{Cu} r_o^3 = \rho_{Cu} r^3 + \rho_{Cu2O} \frac{MW_{2Cu}}{MW_{Cu2O}} r^3 \left( \frac{\rho_{Cu2O} + \eta(\rho_{Cu} - \rho_{Cu2O})}{\rho_{Cu2O}(1 - \eta)} - 1 \right) \quad [B-7]$$

Rearranging this equation allows the calculation of the metal core radius,  $r$ , as a function of the initial radius and the oxide weight fraction:

$$r^3 = r_o^3 \frac{1 - \eta}{1 - \eta \left( 1 - \frac{MW_{2Cu}}{MW_{Cu2O}} \right)} \quad [B-8]$$

The oxide film thickness is then easily calculated as:

$$x = \sqrt[3]{R^3(r, \eta)} - \sqrt[3]{r^3(\eta)} \quad [B-9]$$

For oxide weight fractions,  $\eta$ , of less than 0.5, the oxide film thickness given by Equation B-9 can be approximated closely as a linear function of the oxide fraction (using a least squares fit ( $R^2 = 0.998$ ) and density and molecular weight values from Merck [B.1]):

$$x \approx 0.5445 r_o \eta \quad [B-10]$$

### Planar Approximation

If it is assumed that the oxide film is thin compared to the radius of the particle, then the mass of the oxide approximates the density of the oxide times the thickness of the film times the surface area of the film. The surface area of the film is the specific surface area times the mass of one particle. The total mass is equal to the mass of the oxide film plus the mass of the copper core, which may be approximated with the mass of the initial copper particle:

$$\eta = \frac{\rho_{Cu2O} x a \rho_{Cu} \frac{4}{3} \pi r_o^3}{\rho_{Cu2O} x a \rho_{Cu} \frac{4}{3} \pi r_o^3 + \rho_{Cu} \frac{4}{3} \pi r_o^3} = \frac{\rho_{Cu2O} x a}{1 + \rho_{Cu2O} x a} \quad [B-11]$$

which can be rearranged to solve for  $x$  in terms of the oxide weight fraction:

$$x = \frac{\eta}{\rho_{Cu_2O} a(1-\eta)} = \frac{\rho_{Cu}}{\rho_{Cu_2O}} \frac{r_o \eta}{3(1-\eta)} \approx \frac{\rho_{Cu}}{\rho_{Cu_2O}} \frac{r_o \eta}{3} = 0.49 r_o \eta \quad [B-12]$$

Note that, although the planar approximation gives a film thickness apparently independent of particle radius, Equation B-12 shows that the radius is implicitly included in the value of the specific surface area,  $a$ . Comparison of the planar approximation to the results of the spherical approximation indicates that the planar approximation is accurate up to oxide fractions of about 5%.

## Nomenclature

$a$	specific surface area
$MW_{Cu_2O}$	molecular weight of cuprite (143.09 g/mol)
$MW_{2Cu}$	molecular weight of the copper equivalent to cuprite (127.09 g/mol)
$r$	radius of the copper core
$r_o$	initial particle radius
$R$	time dependent particle radius
$x$	oxide film thickness
$\eta$	weight fraction of oxide
$\rho_{Cu}$	density of copper (8.9 g/cm <sup>3</sup> )
$\rho_{Cu_2O}$	density of cuprite (6.0 g/cm <sup>3</sup> [B.1])

# C

## X-RAY DIFFRACTION (XRD) PENETRATION DEPTH

---

### Purpose

The purpose of this calculation is to determine whether the quantitative XRD measurement of the fraction of oxides in a powder mixture is comparable to that in a partially oxidized powder. That is, can calibration measurements made by mixing known weights of copper metal powder and copper oxide powder be used to measure the degree of oxidation of a copper metal powder?

### Summary of Results

The penetration of X-rays into a mixture of copper powder and copper oxide powder is sufficient to give a valid measurement of the fraction of oxides in a powder mixture. Likewise, X-rays sufficiently penetrate an entire copper powder particle, ensuring a valid measurement of the fraction of oxide in a partially oxidized copper powder.

### Calculation Input Requirements

Powder particle specific surface areas (from BET specific surface area measurements performed by the authors):

$$\begin{aligned}a_{Cu} &= 1.09 \text{ m}^2/\text{g} \\ a_{Cu_2O} &= 0.67 \text{ m}^2/\text{g}\end{aligned}$$

Mass absorption coefficients for Cu-K $\alpha$  X-rays (Jenkins and de Vries [C.1]):

$$\begin{aligned}(\mu/\rho)_{Cu} &= 55 \text{ cm}^2/\text{g} \\ (\mu/\rho)_O &= 12 \text{ cm}^2/\text{g}\end{aligned}$$

Densities (Merck [C.2]):

$$\begin{aligned}\rho_{Cu} &= 8.9 \text{ g/cm}^3 \\ \rho_{Cu_2O} &= 6.0 \text{ g/cm}^3\end{aligned}$$

### References

- C.1 R.H. Jenkins and J.L. de Vries, *Worked Examples in X-Ray Analysis*, Springer-Verlag, New York, 1972.
- C.2 Stecher, P.G., *The Merck Index*, Eighth Edition, Merck & Co., Inc., Rahway, 1968.

## Assumptions

Each type of particles being mixed is assumed to be composed of monodispersed spheres. Consequently, specific surface area is used to calculate an area-weighted average radius. The use of this radius is assumed to be adequate for the calculation performed.

## Analysis

In order to evaluate the relative magnitudes of the particle radius and penetration depth, it is first required that the particle radius be determined. This is done by determining an area-weighted average radius from a measurement of the specific surface area. This is presented below and followed by the determination of the X-ray penetration depth.

### ***Calculation of the Area-Weighted Average Radius***

The specific surface area is defined as the surface area of a sample divided by its mass. If the sample is taken to be a set of uniformly sized spherical particles, then the formulae for the volume and area of a sphere can be substituted into this definition:

$$a = \frac{\text{area}}{\text{mass}} = \frac{4\pi r^2}{\rho \frac{4}{3}\pi r^3} = \frac{3}{\rho r} \quad [\text{C-1}]$$

This equation can be rearranged so that a radius can be calculated from a known specific surface area:

$$r = \frac{3}{\rho a} \quad [\text{C-2}]$$

Specifically:

$$r_{\text{Cu}} = \frac{3}{\rho_{\text{Cu}} a_{\text{Cu}}} = 3 \frac{\text{cm}^3}{8.9 \text{ g}} \frac{\text{g}}{1.09 \text{ m}^2} \frac{\text{m}^2}{10^4 \text{ cm}^2} \frac{10^4 \mu\text{m}}{\text{cm}} = 0.31 \mu\text{m} \quad [\text{C-3}]$$

$$r_{\text{Cu}_2\text{O}} = \frac{3}{\rho_{\text{Cu}_2\text{O}} a_{\text{Cu}_2\text{O}}} = 3 \frac{\text{cm}^3}{6.0 \text{ g}} \frac{\text{g}}{0.67 \text{ m}^2} \frac{\text{m}^2}{10^4 \text{ cm}^2} \frac{10^4 \mu\text{m}}{\text{cm}} = 0.75 \mu\text{m} \quad [\text{C-4}]$$



### Determination of Penetration Depth

The intensity,  $I$ , of the X-rays which have penetrated to a given depth,  $d$ , is a function of the pre-penetration strength,  $I_o$ :

$$I = I_o e^{-\frac{\mu}{\rho} \rho d} \quad [\text{C-5}]$$

The mass adsorption coefficient for oxygen is sufficiently smaller than that for copper that the penetration intensity can be reasonably approximated by assuming that the X-rays are penetrating copper only. Thus, the relative intensity of the incident X-rays is given by:

$$\frac{I}{I_o} = e^{-\left. \frac{\mu}{\rho} \right|_{\text{Cu}} \rho_{\text{Cu}} d} = \exp \left( -55 \frac{\text{cm}^2}{\text{g}} \times 8.9 \frac{\text{g}}{\text{cm}^3} \times d \right) \quad [\text{C-6}]$$

Figure C-1 shows the fall in relative intensity as a function of depth. Since the relative intensity does not drop below one half even upon penetration of 13 times the radius of the larger particle, the quantitative measurement of oxide content in mixed powders is valid. In addition, the air in the spaces between particles does not significantly absorb X-rays. Similarly, the X-rays are expected to penetrate an entire copper particle, thus giving an accurate measurement of the degree of oxidation of copper particles with a growing oxide film.

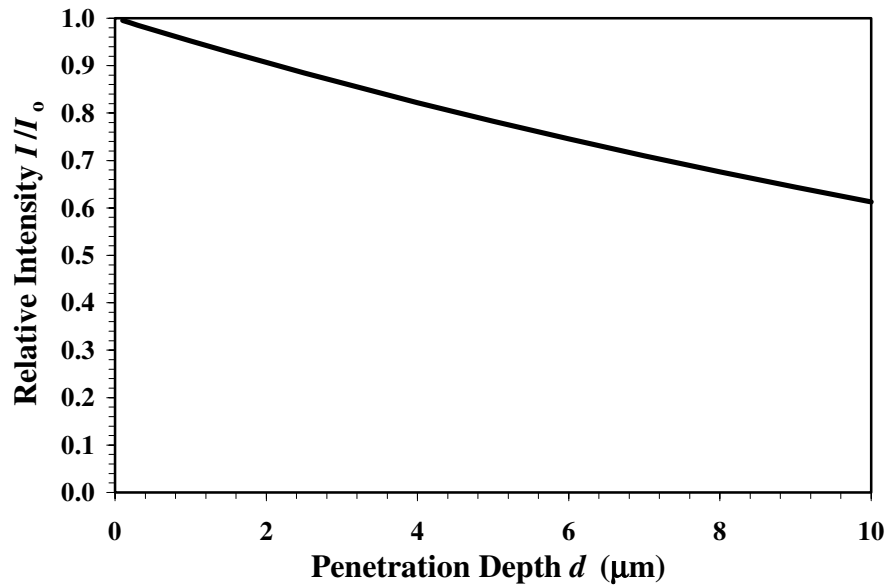


**Figure C-1**  
Penetration of X-Rays into a Copper Sample



*Targets:*

Steam Generator Project


Nuclear Power

**About EPRI**

EPRI creates science and technology solutions for the global energy and energy services industry. U.S. electric utilities established the Electric Power Research Institute in 1973 as a nonprofit research consortium for the benefit of utility members, their customers, and society. Now known simply as EPRI, the company provides a wide range of innovative products and services to more than 1000 energy-related organizations in 40 countries. EPRI's multidisciplinary team of scientists and engineers draws on a worldwide network of technical and business expertise to help solve today's toughest energy and environmental problems.

EPRI. Electrify the World

© 2001 Electric Power Research Institute (EPRI), Inc. All rights reserved. Electric Power Research Institute and EPRI are registered service marks of the Electric Power Research Institute, Inc. EPRI. ELECTRIFY THE WORLD is a service mark of the Electric Power Research Institute, Inc.

 Printed on recycled paper in the United States of America

I001204